

gas annular blast at the lower end of the melt crucible as it emerges through a hole into a reduced pressure area containing the substrate to be coated (Dunstan et al 1985). The droplets undergo in-flight cooling at 10^3 to 10^5 deg.C/second followed by a very fast deposition cooling and slow subsequent cooling. By controlling these stages a very thin liquid film is maintained on the surface of the coated substrate. Dendrites form in flight and shatter on impact, giving many nucleation sites and a fine equiaxed structure. One of the authors (M.G.H.) has seen this Osprey process and strongly recommends it for development and application.

6.7. COATING BY WELDING

6.7.1. GENERAL:

Surfacing by welding is one of the most widely practised bulk coating techniques. Cladding methods form the other group. Fig. 6-19 gives a comparative idea of the properties of major hardfacing alloys. The major welding processes currently used for surfacing are:

Gas, Powder, Manual Metal Arc (MMA), Metal- Inert Gas (MIG), Tungsten-Inert Gas (TIG) (which includes Plasma-Arc), Submerged Arc and Friction Welding.

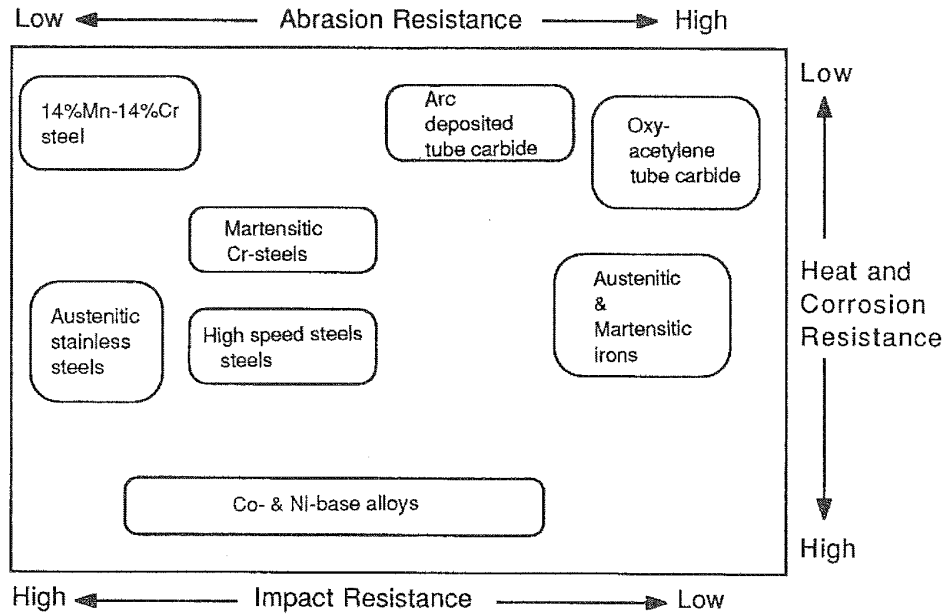


Fig.6-19: Position profiles of the major types of hardfacing alloys

The term 'surfacing' is generally used where coatings are thicker than 1 mm on the substrate, to greater than 8 mm. Several layers can be applied by welding techniques, the thickness restricted only by the mechanical and physical limitations specified for the application of the product material i.e. the coated substrate.

Bulk coating methods use coating material in the form of powder, sheet, strip, rod or paste, applied usually close to or above the melting point of the substrate-coating configuration. Amongst the bulk coating methods, welding, diffusion bonding and HIP methods result in an in situ diffusion bond unlike that obtained from overlay and other deposition methods. Bonding in overlay and other methods can occur by mechanical keying or over a period of time, by metallurgical bonding via thermal heat treatments, while bulk coating is wholly a metallurgical 'bond' formed during the liquid state with a good fraction of it containing the substrate material. Bulk coatings are applied to counter heavy wear and for use under conditions which impose mechanical and thermal shock. They have to be tough so as not to break under these conditions, apart from being metallurgically and chemically compatible to the substrate and resistant to the working environment. The thickness is a compromise for the wear and tear demanded during service and the utility not too dependent on significant dimensional variations as the coating wears. It is essential to achieve an optimised coating for the design service life, in view of the cost and bulk involved.

6.7.2. WELD SURFACING

A classification formulated by the British Steel Corporation may be considered representative of surfacing alloys normally used for coating by welding (Gregory 1980). The selection of the surfacing alloy involves three parameters at the outset, namely, the hardness, the purpose, and abrasion and/or oxidation resistance. Compatibility in characteristics with the substrate metal is the next important factor as only this ensures the integrity of form and performance of the finished component. In general, ferrous alloys are employed for abrasion resistance, nickel and cobalt alloys for oxidation and corrosion resistance, copper alloys for bearings, and, WC, chromium boride and similar compounds for wear resistance.

The process is known severally as hardfacing, weld-cladding, overlaying and by other proprietary names. Welding is particularly suited for local repair work of damaged bulk-coated components. It essentially involves melting the coating material with or without a flux and inert gas, on the substrate to be covered.

6.7.3. WELD SURFACING PARAMETERS

The foremost aspect is the dilution which results on welding. When molten weld metal contacts the substrate the substrate surface also melts and the resulting mixture is contained in the weld pool or the weld bead (Fig.6-20). Dilution is defined as $100A/(A+B)$, where A is the amount of weld metal and B is the substrate metal in the weld pool. On solidification there will be a zone in between the weld and the substrate which has

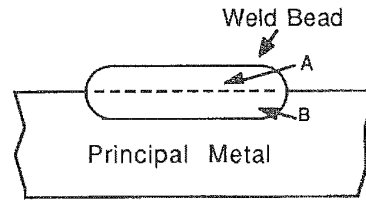
a composition different from both the weld metal and the substrate. There will be an effective reduction in the original substrate thickness, but the total surfaced material will be thicker with the modified welded material bonded to the substrate. Dilution can vary from 10-40% and can be reduced to even 5% depending on the welding method used.

The second parameter is the rate of deposition. The relative mass of coating dealt with in bulk surfacing far exceeds the normal rates of deposition. The latter are usually expressed in mg or g $\text{cm}^{-2} \text{hr}^{-1}$ while surfacing is defined in kilograms per hour.

6.7.4. WELD SURFACING METHODS

Table 6:12 and Fig. 6-21 give some of the features of seven welding processes commonly used. Several variations on these basic themes are in practice. Oxy-acetylene methods are the slowest of all the methods causing also the minimum of dilution, as the flame temperature is much less than arc temperatures. The feed material is a rod or powder and lands on the substrate in a small pool or as molten droplets respectively, which causes restrained fusion and hence there is very little or virtually no loss of the substrate into the weld zone. A precise control and on-site welding is possible but the methods are unsuitable for large scale operations.

Very high temperatures are encountered in arc welding but TIG welding using a non-consumable W electrode is similar in scope to gas-welding in precision and operation, but somewhat higher in dilution and deposition rate. The plasma arc method improves on TIG-welding by employing two arc routes, the major arc current being the non-transferred arc passed between the W electrode and a water-cooled copper annulus around it, while the transferred arc passes between the electrode and the workpiece via the hot plasma issuing from the torch. Unlike TIG, plasma arc can cover large areas with precision and requires minimum finish. But it cannot lay down a coating more than about 1.5 mm thick.



$$\% \text{ Dilution} = (A \times 100)/(A + B)$$

Fig.6-20: Dilution in a Weld Bead

TABLE 6 : 12

WELD-CLADDING

Process:	Oxy-acetylene	Powder	TIG	Plasma arc	MMA	MIG	Submerged arc
Also-known as:	Gas-welding		Tungsten-Inert-Gas; Gas-W-Arc; Argon arc	Variation of TIG	Shielded metal arc; Stick-; Electric-arc	Metal-Inert-Gas; Gas-shielded-metal-arc; CO ₂	
Weld-on-site:	Yes, portable	Yes, portable	Non-portable	Non-portable	Yes; versatile	portable	Non-portable
Type:	Wholly manual	Manual or mechanisable	Manual	Mechanisable	Manual	Manual or semi-mechanisable	Fully mechanised
Weld-material-form:	Rod	Powder	Rod	Rod or powder	Flux-covered rod electrode; tubular rod electrode containing flux	Continuous wire electrode	Continuous wire fed after a prior flux deposit
Dilution, %:	1-5	Virtually nil	4-10	5	10-30	10-30	10-40
Deposition rate kg/h:	1	0.5	2	3.5	1-7	1-10	30
Deposition thickness mm:	<1	0.05-3	2-4	<1.5	≥2.5	>3	>4
Procedure:	Flame from gas source to provide heat. Welder co-ordinates rod-feed-rate into flame as weld-pool advances.	Powder fed via a hopper by gravity into the torch. Molten droplets contact substrate	Non-consumable W electrode Rod fed into the arc. Argon or similar inert gas (N ₂ , He) shields weld-pool	2-arc process	Very sturdy; vertical or overhead welding possible	CO ₂ or argon shield. Flux cored wire, also flexible used as feed wire; can increase rate to 12 Kg/h without shielding gas.	Very good deposit achieved requiring little surface finish.

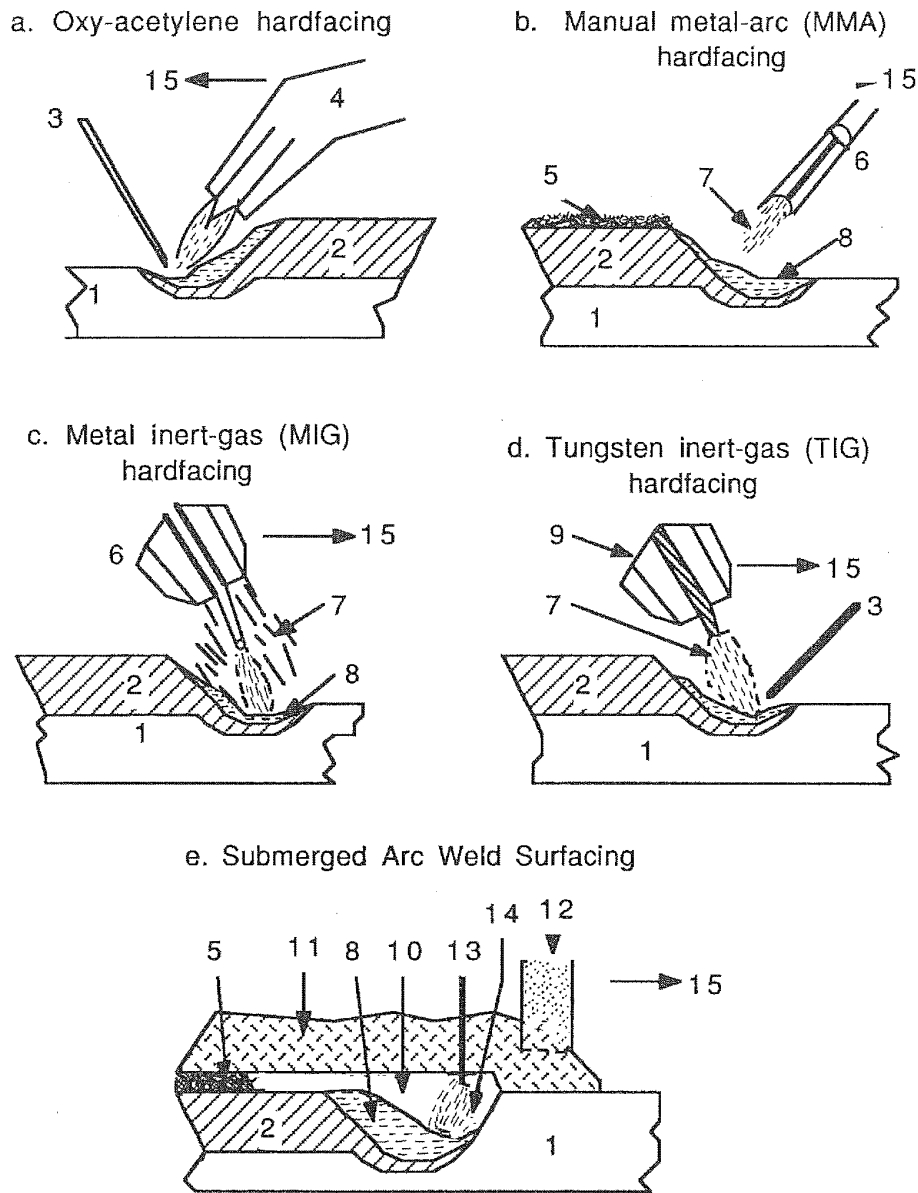


Fig.6-21: Weld Surfacing Techniques

Weld Surfacing Techniques : a: Oxy-acetylene; b: Manual Metal Arc (MMA); c: Metal Inert-gas (MIG); d: Tungsten Inert-gas(TIG); e: Submerged arc

a. 1.Parent metal, 2. Weld metal, 3. Filler rod, 4. Blowpipe nozzle (introducing oxy-acetylene gas mixture, 15. Welding direction

b. 1,2 ,15 - as in a; 5. Slag, 6. Consumable electrode (core wire with a flux cover), 7. Gas shield, 8. weld pool

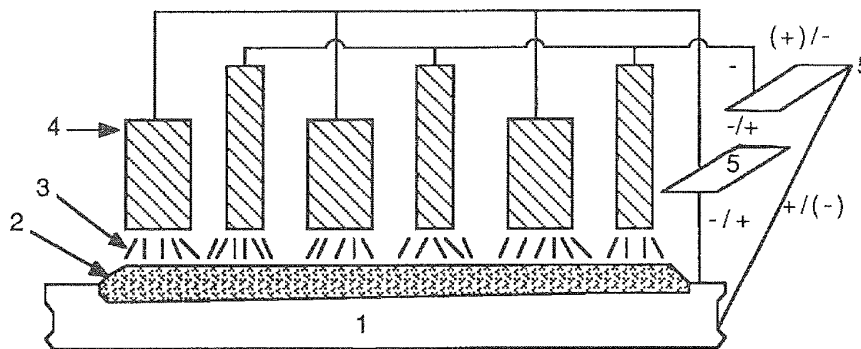
c. 1,2,6,7,8,15 as in a,b above; the consumable electrode is fed through a contact tube which also carries the protective shielding gas supply

d. 1,2,3,7,8,15 - as in a,b, above; 9. Non-consumable electrode with a supply of shielding gas in a co-axial tube. 13. see 'e' below.

e. 1,2,5,8,15 - as in a, b above; 10. Excess weld metal, 11. Granular Flux, 12. Flux Tube feed, 13. Gas shield, 14. Arc submerged in the excess weld pool

MMA and MIG methods are more versatile and sturdy, capable of very high deposition rates. Vertical or overhead runs are possible and on-site operations. The flux-cored arc welding method can give thicker deposits and higher deposition rates using flexible feed wire packed with its flux and additives. A fully mechanised but strictly workshop method is submerged-arc welding. Granular flux is deposited ahead of a continuous wire and the arc submerges, under the flux resulting in a weld surface requiring minimum finish. Friction welding or surfacing is performed by pressing a rotating metal rod with its axis at right angles to a laterally moving substrate.

A multiple strip weld surfacing schematic is shown in Fig. 6-22.



1. Parent metal 2. weld overlay 3. arc 4. strip sheet electrodes passed through feed rollers 5. arc current source

Fig.6-22. Schematic of multiple strip weld surfacing

6.7.5. WELD COATED FINISH

Weld coated surfaces are usually wavy and slightly convoluted ending with a surface roughness of up to 2 mm difference between the maximum and minimum thickness. The wave nature is due to the electrode of a limited width having to pass to and fro on the work surface. Surface tension of the weld pool settling on the substrate which subsequently solidifies as the electrode passes on, causes an unevenness in the weld-coated surface. This surface roughness requires to be smoothed out by machining, grinding, polishing, or light abrading. For components like bulldozer blades or rock crushers this may not be necessary, but it is essential for gear wheels or valve seats.

Shrinkage effects during cooling can distort the coated component as stresses are created. Bending for instance, can be countered by offering the work pre-bent in the opposite direction along the same axis. Where thick layers or heavily restrained coatings are involved cracking is a possible or inevitable hazard. This can be compensated by applying an intermediate coat of soft-metal (ductile) and by intermittent applications with pre-heating of components especially when hard and brittle alloys are deposited.

6.8. CLAD SURFACING

Cladding is a broad term used which includes methods such as explosive impact and magnetic impact bonding, or hot isostatic pressing (HIP) or cladding (HIC), or mechanical bonding such as extrusion. This would introduce an overlapping between cladding and diffusion bonding when the above methods have to be categorized.

Cladding methods can be classified on the basis of the speed with which substrate to coating material bonding can be achieved. Table 6:13 shows the three groups with the bonding they achieve and other details (Bucklow 1983). In general, the substrate is referred to as the backing plate and the coating material is called the flyer plate. Ferrous materials form the most handled clad components, with Ni-based alloys coming second. Other cladding alloys like Co alloys on steel are less used, chiefly in view of cost and availability. More detailed information may be had from the references appended (Bucklow 1983; Edmonds 1978; Bahrani 1978; Bahrani 1967).

Amongst the cladding methods listed, rolling and extrusion processes are perhaps the most widely applied. Explosive bonding was accidentally discovered in 1957; hot isostatic pressing (HIP) and electromagnetic impact bonding (EMIB) are comparatively new; diffusion bonding process spans the early 20th century ferrous technology to date on Ni-base and other high temperature alloys for special applications. Some of the outstanding features of the above processes will be given in the following sections.

6.8.1. ROLLING & EXTRUSION

This is the most economical of all cladding methods and the restriction in rolling and extrusion to sizes of components is only shop-capacity dependent. Both rolling and extrusion methods are practised for ferrous alloys with a wide variety of compositions and applications and for a number of Ni-based alloy/ferrous alloy combinations, Al-alloys and others have also been developed to meet increasing requirements for corrosion and oxidation resistance for ambient and high temperature applications in a variety of sulphur and chloride containing environments, and for high temperature uses ranging over energy, aviation and nuclear industries. Type 310 steel coextruded with 50Cr-50Ni alloy has been reported to have very good service under hot corrosion conditions in boiler systems (Meadowcroft 1987). Both rolled and extruded composite materials are only demand-limited, with the normal metallurgical limitations. Cladding materials are usually strip form, but powders can be employed quite effectively (Sugano et al 1968).

TABLE 6:13 (L.H.S.)

CLADDING PROCESSES

Group A
Ultra-rapid cladding

Process	(i) Explosive Cladding	(ii) Electromagnetic Impact-Bonding (a) Hot (b) Cold
	Time-factor	Micro-seconds
Pressure developed	not given	350 MPa
Substrate shape	Simple; sheets	Simple; tubes or rings only
Substrate size	15 m ² ; max 35 m ²	<300 mm ²
General requirement	Thickness >10 mm; and at least 2X cladding sheet thickness; sufficiently ductile	Sufficient strength to withstand magnetic discharge impact
Cladding material	Sheet; reasonably ductile	Sheet or pre-sintered powder spray
Bonding	Solid state, mechanical keying by shear flow, impact & scouring action, atomic contact & bonding	Components heated to recrystallisation temperature; high speed hot pressure diffusion bonding As in explosive cladding - atomic keying as a result of a shock wave
Limitations	Comparatively large area - substrate/clad sheets as they are easy to handle; Explosive hazard; Some material deformation needs correction	Bulky equipment, expensive; small shapes restriction; components must have good electrical conductivity
Advantages	Very fast; very strong & continuous bonds; unlimited combinations; very little surface preparation required	Safer than explosive cladding very fast

TABLE 6-13 (R.H.S.)

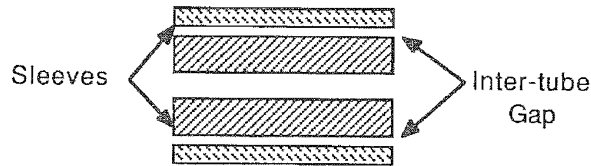
CLADDING PROCESSES

Group B Medium-time cladding		Group C Slow cladding	
Rolling	(ii) Extrusion	(i) Diffusion-bonding	(ii) Hot Isostatic Pressing (HIP)
1-2 minutes	1-2 minutes	10 minutes to >10 hours	
		variable; 10-100 N/mm ²	100-200 MPa
Sheets	Tube; rods	Simple or complex	
Shop-capacity	Shop-capacity	Furnace-size-dependent	Reasonably small
Creep-resistant	Creep-resistant		
Sheet sheet	Tube or ductile	Sheet or powder	Sheet or powder
Mechanical	Mechanical	Metallurgical	Metallurgical
Several passes required to ensure sound bonding. Clad materials must be malleable	Shape restriction; only ductile coating materials can be handled	Expensive equipment and time consuming; uneconomical for large components; high technology components are usually considered for these two cladding methods	
Least expensive; several pairs can be rolled in a pack; also allows composite rolling	Economical	Well suited for very complex shapes and high technology components requiring close metallurgical control. HIP can be used for metal-ceramic bonding	

=====

1. Quality check of the two component tube materials
2. Preparation of a 'sleeve' length of each component
3. Special cleaning of the tube inter-contact surfaces necessary for a faultless metallurgical bond.
Accurate surface machining and a thorough removal of contamination are vital steps.
4. Inter-tube Gap controlled within tight limits

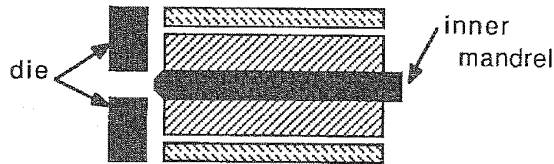
5.



The sleeves are end-welded to prevent contamination during further processing

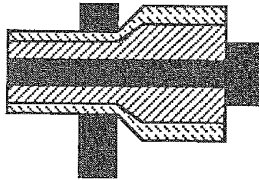
6. The composite billet enters a furnace to bring it to extrusion temperature.
7. Powdered glass is applied on the billet. At the extrusion temperature the molten glass acts as a lubricant.

8.



An inner mandrel concentric with an outer die are aligned as the composite billet bearing the lubricant enters the extrusion press (3000 tons)

9. The billet undergoes a reduction as well as an elongation in the extrusion press.



10. The extruded, clad tube is then cooled, and trimmed
Further reductions can be carried out by reducing either cold or cooler temperatures.

Fig.6-23: Co-Extrusion Process Steps

Some of the special features in rolling and or extrusion are:

(i) A thin primary layer of electrodeposit usually ensures a better bond between the substrate creep resisting steel and the overlay clad material.

(ii) Cladding can be given with the substrate as a sandwich.

(iii) With a parting agent, usually Cr_2O_3 , several composite pairs or trios can be packed together in a single thin container or "can" of steel and then rolled together. The can is sometimes evacuated or back-filled with N_2 .

(iv) The exposed edges of the clad/substrate configuration are sealed by welding to prevent relaxation stresses from wrenching apart the rolled or extruded product.

Co-extrusion of clad tube is shown in Fig.6-23.

6.8.2. EXPLOSIVE CLADDING

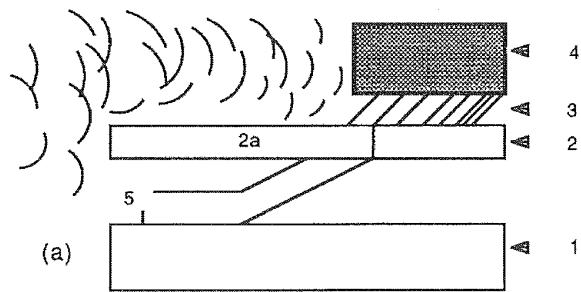
This technique is also called explosive-welding. An accidental discovery in 1957 when a sheet metal got stuck to its die while an explosive experiment was carried out led to this method. An earlier report on the technique and its mechanism is available (Bahrani 1967; Bahrani 1978), and another has appeared in 1987 (Hardwicke 1987). The phenomenon seems to have been noted much earlier than 1957 in military circles when shells and metal fragments were seen to bond with metallic surfaces when impacted at certain angles.

Fig.6-24a,b illustrate schematically one of the modes of the process operation (Bucklow 1983). Bonding can be achieved by an oblique, or parallel high velocity collision between two plates to be joined. Shear and plastic flow are the instantaneous reactions as the shock wave speeds over the clad plate either at supersonic or sub-sonic velocities.

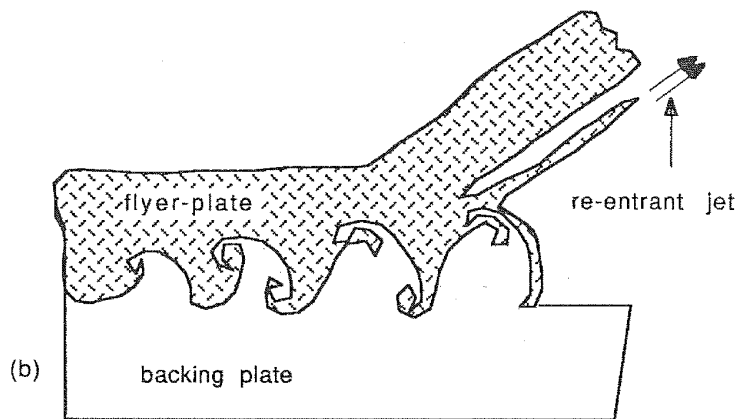
The Method of Explosive Cladding (Bahrani 1967; Hardwicke 1987):

The substrate plate is called the backing plate and the flyer plate is the cladding material. The backing plate must be at least twice the thickness of the flyer plate, preferably not less than 10 microns. Three basic requirements are as follows:

1. The flyer plate is spaced at a 'stand-off gap' parallel to the plate at a distance greater than its own thickness, or touching its edge to the substrate at an oblique angle. When explosion occurs the components must be brought together over this gap to collide progressively over the surface area. A collision front traverses this surface area.



1. Backing plate 2. Flyer-plate 2a. Starting position of flyer plate - parallel to backing plate 3. Buffer 4. Explosive 5. Flyer-plate after deformation by detonated explosive. The two plates are inter-locked during the instant of contact.



Melt flow and interlocking configuration at the impact region

Fig.6-24 a,b: Schematic diagram of Explosive Cladding

2. A protective (buffer) sheet is placed on the flyer plate (usually rubber) and the explosive is spread on it as a slurry or a sheet. The quantity of the explosive must be controlled to result in an optimum detonation velocity of, e.g. 2000 m/s for a thick plate. Slow explosions fail to secure a good bond and larger magnitude could shatter, distort, spall or melt the cladding. The velocity of the collision front must be below sonic velocity in the metals being joined. Shock waves travel through the materials at the velocity of sound. The subsonic velocity level of the collision front ensures that the shock wave precedes the bond being formed at the collision front. Failing this produces non-bonding or immature bonding in the composite. The explosion initiates this progressive shock wave which shear impacts the flyer plate to the backing plate. At such a high speed and pressure, the surfaces also get heated up and squirt out in a scouring action as if they are liquid. The surfaces of both contacting faces are pushed out along with any contaminants, e.g. oxide layers and atomically clean surfaces lock into each other.

3. The interfacial pressure at the collision front must significantly exceed the material yield strength to enable plastic deformation.

The collision angle of the flyer and backing plates determines the interface wave vortex morphology of the resulting composite. The volume of entrapped melt at the interface and the associated bond strength depend on the collision angle. A low collision angle results in an interlocking with a large vortex and a high degree of entrapped material as if it is a frozen melt. If the angle is very low the vortices link up and become continuous, instead of being discretely isolated, and the resulting bond is highly undesirable, since, effectively there are three layers of uncertain bond strength. The higher the collision angle, the more undulated the wave form will be with reduced vortices and entrapped melt. A very steep angle could result in a completely flat surface with little or no entrapped melt. The steep angle detonation configuration was thought commercially non-viable but has been achieved and patented (Szecket et al 1985; Inal et al 1985).

It seems that this process is only suitable for large masses of metal, but in principle ought to be applicable to any metal-metal bond as long as they are not very brittle, and have simple shapes such as sheets, tubes, and low convex-concave radius components - crucibles etc. Direct cladding of large areas, for instance 30 sq.m., have been produced and thin sheet composite cladders fusion welded together from 2 metre wide strips. Double sided clads, with the cladders bonded simultaneously have also been reported. Cup forgings and tube forgings have been streamlined. A better understanding of the process has enabled bonding of many metals and alloys. Laminar composites of alternating material layers of widely divergent mechanical properties have unique resistance to fatigue failure. Transition composite joints can be produced in tubular or flat form with two dissimilar metals. bonding of strictly identical materials (for multi-layer lami-

nates) which are almost impossible to diffusion bond, e.g. Al-Li alloys, are very successfully explosion bonded. Imploded Zr-alloy to outer steel tubes have proved their worth in drilling tube service in sour gas oil wells.

The method has been found especially useful to bond normally 'mismatched' alloy bi-, tri- and quad-laminates, e.g. a V-20Ti bonded to Mo or Nb which itself was bonded to Cu (Kaminsky 1980); Pt, V, or Mo bonded to Ni-Cr-Fe-, or Fe-22Cr- alloys for high temperature use. Most of the clad materials listed by Gregory (1980) can be explosively bonded. A number of alloy combinations have emerged. Conversion rolling, formerly strictly reserved for stainless steel are now common for copper-nickel, all of Ti-base alloys, Hastelloys, many nickel alloys and Zr-clads. Zr-alloys which used Ti as interlayer, now are clad without it. Aerospace transition joints of Ti6Al4V to stainless steel, Al-alloys to Ti-alloys, multi-layer laminates of Al-Li alloys rank amongst the advances made by explosive cladding (Hardwicke 1987). Particular mention may be made of the straight waveless interface of Al to steel and Ti6Al4V to mild steel (Szecket et al 1985; Inal et al 1985).

6.9. DIFFUSION BONDING

A majority of coating processes include heat treatment as an intermediate or an ultimate step to ensure a sound substrate to deposit bond. Thus, almost all "non-overlay" deposition can be termed as diffusion bonds. This section discusses diffusion bonding employed as a primary process unlike its secondary role in other deposition techniques.

Diffusion bonding is a solid state method where component parts are pressed together and heated to form a bond by interdiffusion. Diffusion bonding requires high temperature data of all the components used in metallurgical technology for the concerned substrate-coating complex. Yet, the least characterized of all metallurgical parameters seems to be in the diffusion reaction area, e.g. diffusion constants for elements in multi-component alloys. Often, simplified or estimated values are extrapolated. This is perhaps, one of the important areas where further fundamental research is needed.

Diffusion bonding is a slow process because a metallurgical bond by elements is achieved between two surfaces in contact by a solid-state diffusion process giving rise to a three-zone composite. Composition, microstructure, physical, chemical and mechanical properties are affected and controlled by the duration of heat treatment, the temperature and the pressure at which the process is carried out and the rate and type of cooling given subsequently. The physical, chemical and mechanical properties for the composite, such as hardness, stress/strain, oxidation, corrosion effects, microstructure etc., help in material selec-

tion and use. These are the parameters which decide diffusion bonding as a cladding process. Elliott and Wallach (1981) consider five main process parameters to be time, temperature, pressure, surface condition and environment. Unless otherwise stated diffusion bonding is carried out under vacuum in order to prevent inclusions and oxidation.

Diffusion bonding is also termed as solid-state welding. A few useful sources of information are appended: Tylecote 1968; Bartle 1969; Gerken & Owczarski 1965; Bartle 1978; Ohashi & Hashimoto 1976; Fielding 1978. Drewett (1969a,b) discusses diffusion coatings on steel on a wider context; Derby and Wallach (1982) present a theoretical model for solid-state diffusion bonding. Diffusion bonding is a suitable technique for joining materials which are difficult to join by conventional welding methods (e.g. Ti and its alloys) and to achieve bonding on a more commonly used material, e.g. steel.

6.9.1. PRIMARY CHARACTERISTICS OF DIFFUSION BONDING

Two material layers can be bonded when brought into elemental contact with an applied interfacial pressure at high temperature in the region $0.5-0.8 T_m$ where T_m is the melting point in degrees Kelvin, of the material being bonded. Often additional layers in the form of coatings of a few microns, or loose shims are interposed to facilitate bonding or to act as diffusion barriers to specific elements.

The advantages of diffusion bonding are (Derby & Wallach 1982):

- (i) Large areas can be joined.
- (ii) Metal joining is possible under unconventional situations, e.g. space environment, or as part of a superplastic and bonding sequence.
- (iii) Bonding is possible with minimum deformation.
- (iv) Minimum microstructural damage and stress results while keeping a thin diffusion zone and smaller thermal gradients occur than in processes like fusion welding.

The disadvantages are:

- (i) Poor adherence over large areas due to impurities such as oxides or grit at the interface.
- (ii) Poor bonding due to interface separation via vacancy concentration and void formation during diffusion.
- (iii) Unknown thermal effects on the properties of the bonding elements.

6.9.2. BONDING MECHANISM

Derby and Wallach summarise earlier approaches in their 1982 review in their model. The presence of an oxide film on the substrate is considered an inhibitor but not as rate determining to bonding since except for metals with insoluble oxides, e.g. Al, the oxide dissolves rapidly in the parent metal as bonding proceeds. The diffusion layer formed at the interface could be a solid-state bonding, purely mechanical, or a phase reaction in a solid-state exchange or a eutectic substrate-coating phase transformed to a solid microstructure on cooling. Surface roughness requires data specific to the material considered and generalization is not possible. The authors propose a broader based mechanism by considering diffusion bonding analogous to pressure sintering. The proposed six mechanisms of mass transfer are:

1. Surface diffusion from surface sources to a neck.
2. Volume diffusion from surface sources to a neck.
3. Diffusion along the bond interface from interfacial sources to a neck.
4. Volume diffusion from interfacial sources to a neck.
5. Power law creep deforming the ridge.
6. Plastic yielding deforming the ridge.

1 and 2 above are surface source related, driven by surface curvature differences across the surface of an interfacial void. 3 and 4 consider chemical potential along the bond line as driving force while 5 and 6 are gross deformation mechanisms driven by applied pressure with some surface tension effects. Five process parameters have been interwoven to apply the above six mechanisms, namely, temperature, pressure, initial surface roughness, initial surface aspect ratio and time.

Computer mapping yields the theoretical data which ironically offer limited verification for lack of adequate high temperature diffusion and creep data. Almond et al (1983) envisage a pressure-sinter mechanism in the diffusion bond of hard metal joints, lending partial support to the Derby-Wallach model. They consider an evaporation-condensation mechanism in the case of WC-Co wear resistant bonds. Further experimental work in high temperature creep, diffusion and most other physico-mechanical properties is needed.

6.9.3. ROLE OF INTERLAYERS IN DIFFUSION BONDING

The practical side of diffusion bonding has side-stepped technical difficulties in straight metal-to-metal bonding by using intermediate layers.

1. Applied as coatings, these prevent oxidation of the substrate prior to bonding (Crane 1967; Kammer et al 1969),

2. They assist micro-deformation and establish contact between faying surfaces (Bartle 1978; Hauser et al 1967),
3. They obviate bonding inhibition caused by contaminant films by increasing the rate of their dissolution,
4. They enhance the diffusion rates (Kharchenko 1969; Davis & Stephenson 1962; Lehrer & Schwartzbart 1961) and,
5. They can minimise Kirkendall void formation and prevent or reduce intermetallic phases at the interface (Crane 1967).

The above five causes have been inferred in the context of different diffusion bond pairs. Much more work is required to associate any of these with a proven mechanism (Elliott & Wallach 1981).

6.9.4. DIFFUSION BONDED MATERIALS

Aluminium on steels has been an industrial diffusion bond technique for nearly four decades. Aluminizing and chromizing on steels over forty years and later on Ni- base alloys over the last twenty years have been, consequently, the most investigated of all diffusion bond systems. High temperature and/or corrosion resistant materials such as Co-, Ti-, Mo-, and W- alloys have been investigated more recently. Materials listed by Gregory (1980) provide a reasonable cross section. Table 6:14 gives a list of elements which may or may not form good diffusion coatings on steel (Gregory 1980).

6.9.4.1. Aluminium on Steel:

The two impeding factors for good bonding in the Al- steel system are, (i) the oxide film which forms readily on Al- surface and (ii) brittle intermetallics, e.g. $FeAl_3$, Fe_2Al_5 which develop during the diffusion process at the interface. A number of circumventing parameters have been tried from pressure welding at one extreme which attempts to "squeeze" or break up the oxide film and affect plastic deformation, creep etc., to the other end where the oxide layer can be dissolved and the microstructure changed in situ by interposition.

Comprehensive sources of reference are available (Drewett 1969b; Elliott & Wallach 1981). Pressure bonding, wedge bonding, butt-joint forming by twisting, force fitting tapered joints are a few of the mechanical deformation methods tried. Additions of Mg(0.3-2%), Si(1-6%) and Cu(3%) to Al have improved bonding, Si being the best, Mg being detrimental. Presence of 0.08% O_2 and N_2 in Fe is found to be beneficial, the probable effect being that a ceramic oxy-nitride barrier inhibits intermetallic formation.

TABLE 6:14

A SURVEY OF ELEMENT COMPATIBILITY TO FORM DIFFUSION COATING
ON IRON

Elements Readily Compatible (good solubility)		Elements Incompatible (insoluble)		Elements of Unknown Ability or Untried	
Element	Size-factor	Element	Size-factor	Element	Size-factor
Al	1.15	Ag	1.16	Ce	1.47
Au	1.16	Ba	1.75	Ga	0.98
As	1.01	Bi	1.25	Ge	0.98
Be	0.91	Ca	1.58	Hf	1.27
Co	1.01	Cd	1.20	In	1.31
Cr	1.01	Cs	2.10	Ir	1.09
Cu	1.03	Hg	1.21	Os	1.09
Mn	0.95	K	1.86	Pd	1.11
Mo	1.09	Li	1.23	Pt	1.12
Nb	1.15	Mg	1.29	Ru	1.07
Ni	1.00	Na	1.50	Sc	1.22
Re	1.08	Pb	1.41	U	1.12
Sb	1.17	Rb	1.96	Y	1.46
Sn	1.13	Sr	1.73	Zr	1.26
Ta	1.15	Tl	1.45		
Ti	1.18				
V	1.05				
W	1.10				
Zn	1.17				

Several intermediate layers have been tried for Al- steel diffusion bonding. Ag (260-320°C), Cu(575°C and eutectic), Ag-Be (0.5-2%Be), Ni(0.2 mm) 625°C, Ni-Ag (6 micron electroplate - 5 micron foil) may be quoted as a few examples. Cu is a poor candidate layer because of its tendency to rapid oxidation at the diffusion bonding temperature. Ag and Ni have proved to be good, providing good bond strength.

6.9.4.2. Other Diffusion Bonded Materials:

Diffusion bonded WC-Co has been interlayered with Co, Ni, tool steel or mild steel at 1300°C (Almond et al 1983). Co and steel interlayers are found to be sensitive to the differential carbon contents encountered in the hardface-interlayer pair. At 1300°C a vapour phase evaporation/condensation mechanism is considered to play a vital role in diffusion bonding with creep and diffusion complementing it. The undesirable brittle eta-phase can be developed at low carbon contents at the interlayer/hardface metal junction. Choosing a high carbon content Fe, or Co or Ni interlayer prevents eta-phase formation.

6.9.5. HOT ISOSTATIC PRESS BONDING - (HIP) CLADDING

This is a relatively new method developed over the last decade and is particularly advantageous for complex shapes. Beltran and Schilling (1980) discuss the innovation in cladding at the General Electric Company for gas turbine components. A metal-ceramic HIP cladding method is reported by Allen and Borbidge (1983). Useful related literature can be found in these two sources. Patent literature (1980) and the powder HIP process (Nederveen et al 1980; Anon. 1982) have been mentioned by Bucklow (1983).

Ni-base and Co-base gas turbine alloys, MCrAlY-series, Ti- and Zr-alloys form some of the metal-metal HIP- processed components. It can also be applied to metal- ceramic pairs, e.g. Pt, Pd, Au, Ag or Fe, Co, Ni, Cu to Al_2O_3 , ZrO_2 , MgO, SiO_2 and BeO (Allen & Borbidge 1983). The process uses high temperature-high pressure equipment. The coating material is applied to the substrate by spot welding or local brazing a sheet, or by powder spraying. The substrate-coating pair is surrounded with a pressure-transmitting medium, e.g. glass chips later molten, in a deformable container and heated. Isostatic pressure is applied for various lengths of time; pressure, time and temperature are work-dependent. Sprayed deposits are consolidated and diffusion bonded, sheet material is forced by the pressure contact and diffusion bonded. The glass is then removed.

Powder ingots of Fe25Cr4Al1Y and Co25Cr3Al10Ni5Ta0.2Y alloys have been formed by HIP, with subsequent improved fabricability. Both the alloys contain intermetallic precipitates and dispersions and in cast or wrought form have low ductility. The components were argon-atomized, prealloyed powdered, and HIP-densified with a 20% improved tensile strength powder ingots (Beltran & Schilling 1980). The cladding process involves a preliminary substrate cleaning, a 12 micron Ni electroplate and then cladding, with the sheet (250 microns) fabricated from the powder ingot, and finally HIP diffusion bonding. The Ni interlayer prevents TaC formation at the interface due to interdiffusion between Ta in the clad material and C from the substrate. HIP temperatures and pressures ranged over 1093-1150°C and 6.9-103 MPa.

Two HIP-techniques are reported. The first where the work is totally immersed in a low viscosity ($<10^{-6}$ centipoise) soda-lime glass cullet in an outgassed, evacuated steel container, and heated to 1000°C in an argon pressurized autoclave. The second method side steps the difficult task of removing solidified glass at the post-process stage from cooling holes, crevices etc. This is achieved by a first step controlled vacuum brazing cycle to seal the substrate-cladding seams, e.g. a braze alloy Ni45Cr10Si is used to seal IN738/coating seams at 1150°C for 10 minutes, the temperature being slightly above the braze alloy solidus temperature of 1135°C. Direct pressure transfer occurs in the autoclave, between the substrate and cladding as the annular space will have been evacuated before seam sealing.

A metal-ceramic HIP process with Al_2O_3 -Pt- Al_2O_3 sealing has been carried out using temperatures of 1100 - 1800°C , time 12 minutes to 10 hrs and pressures 0.13 to 10MPa. The standard operating conditions used were 1450°C , 0.8MPa, 4h. For maximum bond strength the conditions were 1700°C , >10h at 2MPa contact pressure. Note the low contact pressure contrasting the 100MPa used in the metal-metal HIP process. The authors do not consider mechanical keying as the bond mechanism since the bond strength does not continue to increase with increase in pressure. The bond is found to be very strong even at very high temperatures, with a 25% loss in strength at 1100°C from that at ambient temperature. It is inferred that a HIP bond in metal-ceramic is a solid-state reaction bonding (Allen & Borbidge 1983).

Particle size and its distribution have been shown via an analytical deformation model, to influence the powder morphological changes and the kinetics of densification (Kissinger et al 1984). Samples of Rene 95 superalloy, graded on three particle sizes, viz. monosize 75-90, bi-modal 75-90 and 3-35, and commercial 100 microns, were canned and given the HIP treatment at 1120°C over a time range 5-180 minutes at 10.3 or 103 MPa. It was found that component densification was achieved almost entirely by time independent plastic deformation of powder particles, that of smaller particles being the greater. The variations of HIP temperature and pressure, the effect of creep and superplastic flow etc., are yet to be investigated to clarify the role of the dominating plastic deformation behaviour.

HIP consolidation and the kinetics of densification of powder compacts need to take into consideration, the particle size, its distribution and powder morphological changes.

Cladding of Al onto steel requires $14 \times 10^4 \text{ kN/m}^2$ at 400°C or $21 \times 10^4 \text{ kN/m}^2$ at 345°C . Subsequent annealing doubles the bond strength. Equipment for HIP is commercially available (Anon. 1985).

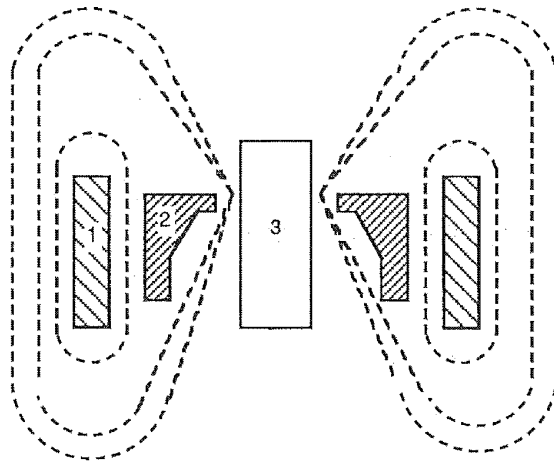
Hot isodynamic compression (HIC) may be mentioned in this section as a technique claiming an advantage over HIP in being more cost-effective while also providing improved metallurgical bonding. Both processes are new and quick conclusions of the advantage of one over the other may prove to be misleading. The HIC process has been applied to a low alloy steel substrate arc plasma sprayed with rapidly solidified platelet-powder mixtures of 57.5Ni23.5Mo9.0Fe10.0B prepared by spin-cast techniques. Particle size distribution (wt.%) was 65 of 100-270 mesh, 15 each of 80-100 and 270-325 mesh and 5 of >325 mesh. The spray coated steel was subjected to transformation treatments at two temperatures using hot forging techniques with a composite die as the transfer medium. This is described as the HIC treatment carried out at 827 MPa pressure over 0.5 seconds dwell time at 1010 - 1066°C and subsequently normalized. Results based on EDS, microstructure, hardness and statistical evaluations have been used to show that HIC technique provides a better bond and very low porosity in the

arc plasma sprayed coating than the HIP technique (Hays & Harris 1987).

6.9.6. ELECTRO-MAGNETIC IMPACT BONDING (EMIB)

EMIB employs magnetic energy to produce the impact which explosive cladding achieves by chemical combustion, but unlike it, EMIB cannot handle very large or thick components (not greater than 300 mm²). It also requires the components to have a reasonable electrical conductivity, and only simple shapes such as rings, tubes, which are circumferentially continuous are acceptable. EMIB can act on heated or cold components. Hot EMI- bonded components have a diffusion zone at the interface while cold EMIB is achieved by mechanical keying. The substrate-cladding pair is introduced into the EMIB equipment, to be surrounded by a coil. A sudden surge of current through the coil produces an intense magnetic field which translates its force as a pressure on the work piece. In a few microseconds a pressure of 300 MPa can develop which impact seals the cladding onto the substrate (Fig.6-25). Gas turbine blades have been sealed by this method (Obrzut 1972).

EMIB is expensive to install and its use is limited. But it is safe, quick and clean to operate within its materials limitations.



1. Compression coil 2. Field Sharper 3. Workpiece

Fig. 6-25: Electromagnetic Impact Bonding

CHAPTER 7

Physical and mechanical properties of coatings

7.1. INTRODUCTION

The brief survey made in this chapter is in three categories: (i) the physical aspects of coatings, viz. microstructure and temperature-related properties, namely, thermal-expansion, thermal cycling, thermal conductivity and interdiffusion, (ii) physico-mechanical properties such as adhesion, stresses, strength, ductility, creep and hardness, and (iii) mechanical properties such as wear and erosion. Physical and mechanical properties are very inter-related and are strongly influenced by each other, and in turn also affect the chemical properties as will be evident in the following chapter.

There will be an inevitable overlapping of Chapters 7 and 8 with the mid-section of Chapter 9 which deals with characterization of coatings. The divisions of the three chapters are more for convenience rather than any validity for segregation of topics. Much of the information dealt with in this chapter should be useful for the assessment of coatings, dealt in Chapter 9.

7.2. EVOLUTION & MICROSTRUCTURE OF COATINGS

7.2.1. GENERAL

Coatings and thin films often exhibit different microstructure and properties from the bulk processed materials because many of the coatings processes can produce deposits in metastable states and non-equilibrium phases.

Factors which influence the formation of coatings are:

1. The substrate on which the deposit arrives,
2. The temperature of the substrate, and the temperature of the process,
3. The medium of deposition,
4. The rate of arrival and mass transfer, and,
4. The substrate/coating compatibility.

Coatings processes discussed in this book broadly divide into those which deposit from a vapour and/or charged medium, and those which arrive at the substrate as droplets, or attach to it in bulk. The routes by which they finally appear as coatings are thus vastly different. The deposit which arrives in a macroform of the material it will eventually be, needs mechanical keying to the substrate and interlinking to the arriving mass. But the deposit which arrives as a particle in a charged state, or as a vapour, needs to be neutralized, seek nucleation sites, then build up from an atom to unit cell and then onto a crystalline morphology or be amorphous as the conditions influence. The development of microstructures of the two types of deposition are different as are their modes of growth. There are further differences between those processes which deposit through a 'vapour' medium, e.g. PVD, CVD, pack etc., and those which use an electrolyte or a gel or plasma.

7.2.2. THE ROLE OF THE SUBSTRATE

7.2.2.1. Nature of the Substrate:

The evolution of a deposit can start either by the formation of 3-dimensional nuclei on favoured sites on the substrate followed by lateral growth and thickness, or as a continuous film formed from the start with no island growth. The first mode occurs where there is poor interaction or bonding between the coating and substrate and the outward growth proceeds to produce in many cases a "columnar" structure. The second mode occurs under conditions where no oxide films are present or any other impedance, and good bonding between the coating and substrate metal occurs. The geometrical shape of the substrate significantly affects the coverage of the deposit in some of the processes, and coating discontinuity due to 'shadowing' is a common defect on contoured substrates for which adequate precautions must be taken. The types of bonding obtained between a superalloy IN 718 and a glass-ceramic is deeply graded with three zones of morphology (Madden 1987).

7.2.2.2. The Substrate Temperature:

Blocher (1974) & Bunshah (1981) have discussed the effect of temperature on deposit manifestation and mode of growth. Table

7:1 shows the pattern and influence of temperature and supersaturation on deposit structure.

TABLE 7:1

THE INFLUENCE OF TEMPERATURE & SUPERSATURATION ON THE SUBSTRATE OF CONDENSED MATERIALS
(Blocher 1974)

Effect of Increased Supersaturation	↓ Epitaxial Growth Platelets Whiskers Dendrites Polycrystals Fine Grained Polycrystals Amorphous Deposits Gas Phase Nucleated "Snow" ↓	↑ Effect of Increased Temperature
-------------------------------------------	-------------------------------------------------------------------------------------------------------------------------------------------------------------------	--------------------------------------------

Increasing substrate temperature has the effect of increasing the mobility of the coating atoms on the surface thus promoting diffusion (Sherman et al 1974). The kinetic energy of the incoming atoms can be increased by partially ionizing the vapour flux and this can lead to epitaxial growth (Boone et al 1974). In this case, the effective surface temperature of the growing film is much higher due to ion bombardment. Movchan and Demchischin (1974, 1969) studied the variation of microstructure with deposition temperature for Ni, Ti, W, Al₂O₃ and ZrO₂ and proposed a 3 zone model of structures as shown in Fig.7-1.

At low temperatures, the coating atoms have limited mobility and the structure is columnar, with tapered outgrowths and weak open boundaries. Such a structure has also been called "botyroidal" and corresponds to Zone 1. If the substrate temperature (T_l) is increased above 0.3 of the melting point (T_m) (in °K) of the coating material, then although the structure (Zone 2) remains columnar, the columns tend to be finer, with parallel boundaries, normal to the substrate surface. T_l is 0.3T_m for metals and 0.22-0.26T_m for oxides. These boundaries are stronger than in the Zone 1 structure and contain no porosity. At a substrate temperature (T_l) above 0.45 of the melting point (T_m) of the coating material, the structure (Zone 3) shows an equiaxed grain morphology. The transition from one zone to the next is not abrupt but smooth. Zone 2 structures have been associated with enhanced surface diffusion and Zone 3 structures with bulk diffusion. Zone 3 is not seen very often in materials with high melting points.

Formation of thick coatings by atomistic deposition processes often gives a very columnar morphology of low density. In electrodeposition this morphology can be prevented by levelling or brightening agents which continually re-nucleate the growing film

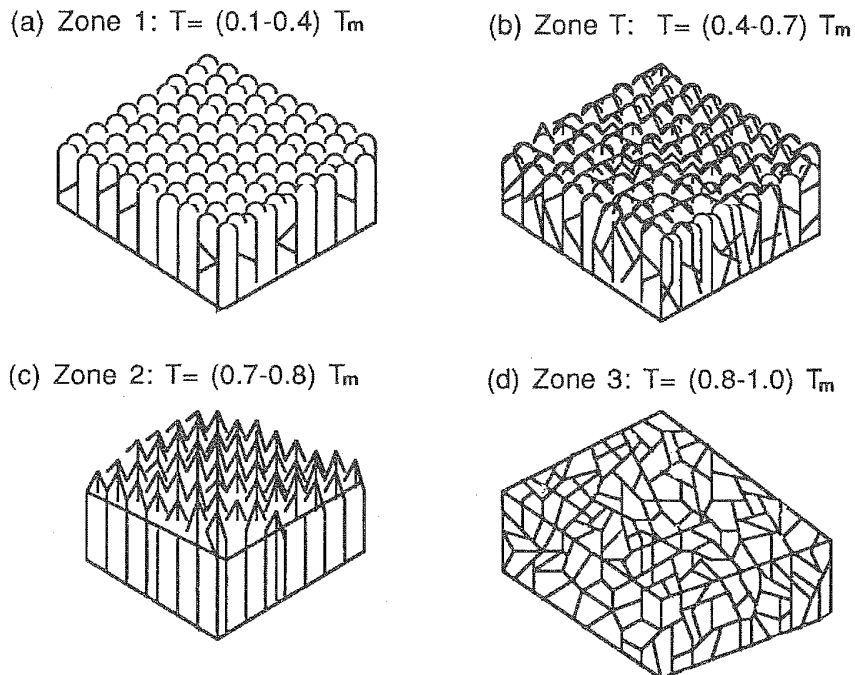


Fig.7-1: Structural Zones in Vacuum Condensates

(Movchan & Demchischin categorization; Zone T - Tucker Model)

(Bockris & Reddy 1970). In CVD (Holman & Huegel 1967) and electrodeposition the columnar structure can be prevented by mechanically disturbing the surface during coating (Kennedy 1968). Ion bombardment during coating alters the density, appearance and growth of thick metallic coatings produced by CVD (Culbertson & Mattox 1966), sputtering (Bland et al 1974; Mattox & Kominiak 1972) and vacuum evaporation (Mattox & Kominiak 1972; Bunshah & Juntz 1972) including electron beam evaporation (Bland et al 1974; Mattox & Kominiak 1972; Mattox 1973). High internal stresses and defect concentrations can sometimes cause unexpected structures (Patten et al 1971).

Low rate low temperature PVD produces fine columnar grains of 250 Angstroms diameter (Nb and Sn), on a substrate at 570°C. Grain boundary grooves (cavities) occupy about 15 volume% of the structure. Low rate, high temperature deposition (750°C) increases the grain size about 10 times and gives no grain boundary cavities, but the structure is still columnar. At a five times higher rate, and high temperature deposition at 750°C, crystal grains are twice as small and more uniform (Jacobson 1981).

Coatings of mirrors for solar energy heliostats by Ag vapour deposition on glasses show strong preferred structural orientation effects, which are absent on chemically deposited films

which have much smaller crystallite sizes. Heat treatment of chemically deposited films to 350°C increases their crystallite size to that of vapour deposited films. Vapour deposited films are more uniform and defect-free (Shelby 1980).

Post coating mechanical peening densifies the surface and then a heat treatment promotes some interdiffusion for bonding. Methods of simultaneous spraying and peening have been investigated (Singer 1984). Heat treatment is usually at the solution temperature and does not disrupt the mechanical properties of the substrate.

7.2.2.3. Surface Roughness & Angle of Incidence of the Vapour Stream:

Since evaporation is primarily a line-of-sight process, the effect of any asperity or projection on the surface will be increased when the vapour stream is at a low angle to the substrate surface. Leaders are columnar defects which are poorly bonded to the rest of the coating and result from localized rapid growth due to shadowing effects caused by surface protrusions. Decreased initial specimen surface roughness can significantly reduce the number and size (width) of open columnar defects although they do still occur. Exposing surface height irregularities to varying angles of incoming vapour by compound specimen rotation results in improved as-deposited coating quality.

7.2.3. GAS PRESSURE

High gas pressure during deposition inhibits surface mobility and hence can be the cause of columnar structures even at elevated temperature.

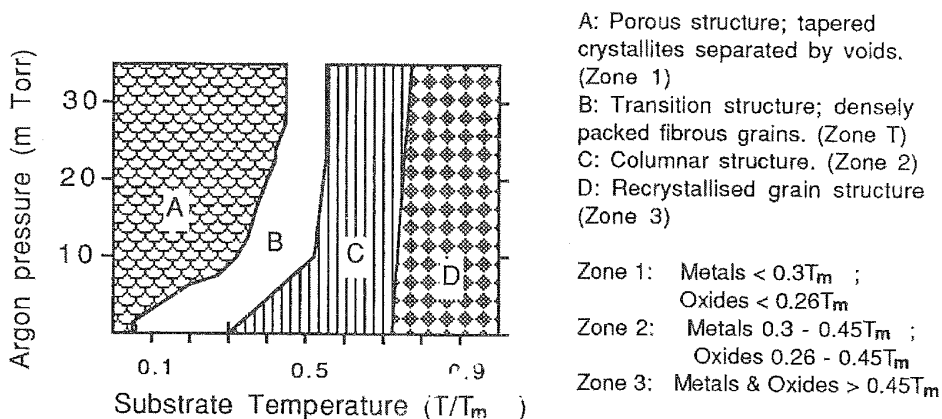


Fig.7-2: Influence of Substrate Temperature & Argon Pressure on Condensate Structure

COATINGS: PHYSICAL & MECHANICAL PROPERTIES

The model proposed by Movchan and Demchischin (Fig. 7-1) was extended by adding an additional axis to account for the effect of gas and was subsequently modified by Thornton (1975,1981) to account for an additional transition zone (Zone T, Fig.7-1,b). This was identified between Zones 1 and 2. Zone T is a columnar Zone 1 structure with small crystal sizes that appear fibrous and with boundaries that are sufficiently dense to yield good mechanical properties. Fig.7-2 shows the gradation of structure as related to argon pressure and substrate temperature. Coatings produced for laboratory scale studies and for industrial applications have been reviewed (Bunshah 1981).

7.2.4. CVD DEPOSIT MICROSTRUCTURE

In CVD processes the structure/property/process inter-linking is complex and specific to the deposit-substrate-process-purpose configuration chosen. Thus a successful CVD coating of carbon on particles is governed by a set of control parameters totally different from that required to achieve a carbon rocket nozzle by CVD. A good cross section of available information may be had in references cited : (Blocher 1974; Takahashi & Itoh 1977; Proc. International CVD Conf. 1976, 1978, 1980, 1981, 1983,1985,1987). It would be out of scope to deal with them here.

The main tools required for determining the desired structure are two-fold, viz. those which can provide the analyses of the reaction and those which can characterize the substrate/deposit configuration.

In general, a columnar deposit is weaker both mechanically and in environmental resistance when deposited in bulk on a broad substrate. But a preferred orientation may be desirable in particular cases, e.g. carbon with random a-b-growth but preferred orientation in the c-direction for increased thermal conductivity in rocket nozzles and re-entry vehicles and as a bowl liner in smokers' pipes. A preferred orientation for W increases its emitter efficiency to a maximum.

Davis (1980) discusses the formation of deposits by CVD, in particular, epitaxial films. A sustained growth of a heterogeneous film, energetically favourable requires a critical size for the nucleated, coalesced clusters of the deposit. Those which are smaller will decay or re-vaporize. In CVD processes supersaturation produces high yielding cluster radii of one or two atoms. Surface free energy and other classical thermodynamics parameters cannot be appropriate (being based on large statistical assemblies). An atomistic concept (Walton 1962) combining statistical mechanics and chemical bonding can be fitted. Surface sites with strong bonds are the more favoured nucleation sites. Since CVD is also a diffusion-limited process, stable clusters endeavoring to capture atoms in a 2-dimensional field have a much longer range than a corresponding 3-dimensional

nucleation (Lewis & Campbell 1967).

Low temperatures, high atom arrival rates, and atoms with covalent or ionic bonds favour amorphous growth, e.g. the group IV elements of C, Si, Ge, SiC, and oxides of Si, Zr and Ti. Blocher's review (1974) discusses microstructural aspects of CVD in considerable detail. Useful sources for literature on the morphological aspects of CVD deposits are: (Davis 1980; Kern & Ban 1978; Walton 1962; Lewis & Campbell 1967)

7.2.5. PACK & PLASMA SPRAY DEPOSIT MICROSTRUCTURE

As a "close-up CVD" process, pack-coating poses numerous experimental problems. This is probably the cause for poor characterization of the evolution of coating structures. The substrate must be thoroughly clean and free of oxide films or any other impurity, in order to ensure uniform deposition, bonding and diffusion on its entire surface. Elaborate cleaning procedures are normal as the flow sheets indicate. All operating conditions are worked out specifically for a substrate. Because the pack surrounds the substrate adequate coverage is ensured, enhanced further by vacuum slip pack and other methods. The nucleation and deposit growth aspects are left 'unseen'.

Deposit arrival in a greater mass and its subsequent consolidation on the substrate is encountered in bulk coating methods. The microstructure of both plasma and flame sprayed coatings is a series of overlapping lamellae caused by the splat solidification of droplets. Gamma alumina forms at large substrate-to-torch distances, low currents and high gas pressures; otherwise, delta and alpha alumina form. Gamma alumina has inferior properties but may be transformed to alpha alumina by heating above 1100°C, although the lower density of alpha causes an increase in coating porosity. The proportion of alpha in flame sprayed coatings increases linearly with substrate temperature reaching 85% at 800°C, but this does not apply to plasma sprayed coatings. However, pure alpha coatings are obtained if the substrate is held above 1100°C, but for low porosity it must be at 1450°C (McPherson 1980). The effect of substrate temperature on porosity is discussed (Smyth 1973).

Metastable structures and amorphous solid solutions are frequently observed, particularly in ceramic bulk materials. These are frozen in up to temperatures of $0.3T_m$. Thus materials with T_m of 2500-3300°C can be used over 700-1000°C. Predicting the constitution of a multi-component coating requires phase diagram and thermodynamic data. Deposition at low temperatures resulting in a less ordered structure followed by monitored heat treatment is an area open to further investigations. The system Ti-Al-N would be of interest in this context. Free energy calculations show that 0-60 mol.% AlN is a cubic mixed nitride when deposited at low temperatures and the metastable (Ti,Al)N solid solution does not

COATINGS: PHYSICAL & MECHANICAL PROPERTIES

decompose up to 800-1000°C. Similar studies on other systems have shown that:

TiC-TiB₂ form amorphous solutions with good adherence to substrate but lower strength than its crystallized state; the system also develops a multiphase layer when TiC and TiB₂ are deposited simultaneously, and crystallize slowly from 800-1000°C; TiC can form a multilayer deposit when sequentially sputtered with TiN, and WC with TiC and TiN can form gradient coatings Holleck & Schulze 1987).

Many hardfacing processes yield dendritic deposits; their size was found to decrease in the order of processes - oxyacetylene, TIG, PTA (Plasma Transfer Arc) and laser deposits (Monson & Steen 1986). The process by which discrete molten particles impact at random points within a surface area has been simulated using the Monte Carlo method and a computation model presented (Knotek & Elsing 1987).

A mathematical viscosity analysis of the impact of droplets on a cold substrate is given by McPherson (1980). The analysis shows that flattening and solidification are separate events for lamellae < 1 micron thick; thicker lamellae are thickness controlled by the solidification kinetics. Most alumina droplets reach 2500°C but freezing occurs at 1600°C due to undercooling. The viscosity is between 0.15 poise (2500°C) and 5 poise (1600°C). Cooling rates are found by direct measurements or indirectly from dendrite arm spacing. The gun technique (D-gun) where a droplet at high velocity hits a cold substrate, gives splat cooling rates of 10⁶ to 10⁸ degrees/second. Heat transfer theory shows, for thin lamellae, that the cooling rate depends on the nature of the interface and not on the substrate conductivity, the heat transfer coefficient being about 10⁵ watts/m² degree. The lamellae undercool and crystal nuclei grow at the limiting rate, liberating heat of fusion which suppresses further nucleation. It can be shown that this leads to a columnar microstructure.

If the heat transfer rate (to the substrate) were such that the temperature decreased after the initial nucleation, then the nucleation rate should increase due to the extreme undercooling. Hence the solidification rate would be controlled by the nucleation rate, resulting in a very fine equiaxed microstructure (McPherson 1980). The (undesirable) columnar microstructure of plasma sprayed alumina suggests that the heat removal rate is less than the heat generation rate. Heat transfer to particles in a plasma has been discussed (Vardelle and Fauchais 1983). For cold substrates, lamella thickness increase gives proportionately longer solidification times, but at high substrate temperatures the reduced heat transfer reduces the degree of undercooling and solidification becomes controlled by the heat removal rate.

The fraction of partially melted particles rises rapidly with particle size and explains the occurrence of some alpha alumina in cold substrate coatings. It is suggested that transformation

COATINGS: PHYSICAL & MECHANICAL PROPERTIES

to alpha is significant at lamellae thicknesses >20 microns for cold substrates and >10 microns for 1000°C substrates. For lamellae thicknesses resulting from <5 micron powder feeds, formation of alpha cannot be expected even for substrates heated to several hundred degrees. Flame sprayed alumina has more alpha content as lamellae are thick (about 10 microns) because the feed rod end must melt before it can be detached and so large particles are sprayed. The relation between alpha, gamma and delta alumina is discussed in detail by McPherson (1980).

7.3. THERMAL EXPANSION, THERMAL CYCLING

Thermal expansion is the commonest source of mismatch strains, especially important for ceramic coatings. The thermal expansion coefficient of ceramics is about $8 \times 10^{-6} \text{K}^{-1}$ and steel is about $14 \times 10^{-6} \text{K}^{-1}$ and a thin intermediate layer of oxide and metal can be used to reduce interface mismatch strains. Transformation strains depend inversely on the degree of stabilization in ceramics like ZrO_2 and may counteract some of the thermal expansion strain. Microcracking due to a phase transition or porosity may relieve thermal mismatch strains (Kvernes 1983). Ion plated coatings have excellent adhesion and resistance to thermal shock and vibration (Teer 1983).

Data on thermal expansion, especially on coatings of all categories are yet to be well documented. A useful source for non-metallic solids may be cited here (Toulonkian & Ho 1987). Table 7:2 lists selected data on oxide and nitride coatings (Richerson 1982; Hancock 1987).

TABLE 7:2

THERMAL EXPANSION COEFFICIENTS OF OXIDE & NITRIDE COATING MATERIALS

Coating Material	$\alpha \times 10^6 / ^\circ\text{C}$
Al_2O_3	8-9
CoO	15
Cr_2O_3	7-7.8; 9.6
MgO	12.9-13.9
MgO- Al_2O_3 spinel	9.1
NiO	14-17.1
SiO_2	3
ZrO_2	8-10
$\text{ZrO}_2 + \text{MgO}$	10-12.2
SiAlON	3-3.2
Si_3N_4 (hot pressed)	3
Si_3N_4 (reaction bonded)	3
SiC	3.7-4.8

COATINGS: PHYSICAL & MECHANICAL PROPERTIES

Thermal expansion coefficient values ($\alpha \times 10^6 / ^\circ\text{C}$) for typical substrate alloys are in the range 9.7-19.2 for Ni-base superalloys, 16.5-20.0 for stainless steel (25Cr 20Ni wt.%), 14.8 - 19.0 for stainless steel (18Cr 8Ni) and 12-14 for carbon steel. Thermal stability and thermal shock characteristics of carbides and nitrides are important in view of their barrier layer role on substrates of a wide variety, viz. on semi-conductors, graphite and refractory superalloys. AlN was found to be a suitable encapsulant for GaAs up to 1000°C in air and 1400°C in vacuum. It forms gamma-AlOOH at steam temperatures but is inert at room temperature (Abid et al 1986). Electron-beam thermal shocks imparted to TiC on graphite substrates were monitored to assess its application in fusion reactors (Brunet et al 1985). More work in this area is needed.

The possibility of adopting materials with negative thermal expansion has been explored, and the best way to achieve very low coefficients of thermal expansion seemed to be through composites. Many oxides have negative coefficient of expansion at low temperatures but few materials show negative values of this parameter at room temperature or above! During this study the authors found that although thermal expansion is an inherent thermo-physical property of a material, the observed values depended on the routes for sample preparation, and this has been attributed to errors creeping in via microcracking, grain boundary separation, plastic deformation and retardation in phase stabilization (Chu et al 1987).

Thermal cycling techniques and some results are discussed by Nicoll (1983). A few results on coated stainless steel and superalloys are shown in Fig.7-3. It is clear from the histogram (qualitative) that the superalloy substrate with stabilized zirconia coating where the substrate alloy was maintained at 20°C or heated to 316°C is far superior in thermal cycling conditions than the others shown in the diagram. Other substrate/coating systems tested for thermal cycling showed that superalloy substrates - Hastelloy, IN 738 with CoCrAlX (X = Y, Ce) and directionally solidified NiNbCrAl with Pt undercoat and NiCrAlY topcoat withstood thermal cycling very well, while steel substrates with a selection of coatings, e.g. Cr, WC12Co, 75CrC-25(80Ni20Cr), and silica and ceria 2-4 microns, were mediocre, and Al-alloys with cemented carbide, CrC-NiCr, NbC and AlN coatings were very poor as was Nb with Mo- and Nb- silicides.

Thermal barrier coatings have performed creditably in thermal cycle tests. Coating failure by thermal cycles depends on the applied stress on it (thermal and/or mechanical) and the strength of the substrate adhesion and interlinking to the coating. In a Rolls-Royce thermal cycling rig test on several coating systems (1125°C for 1 min. and forced cooling to 250°C for 1 min), argon shrouded LPPS coated 8% yttria stabilized zirconia and CaOTiO₂, with MCrAlY bond coat proved to be the two superior systems with 7000 and >6100 cycles respectively. Coatings of magnesia and yttria stabilized zirconia with Ni/Cr alloy bond coat failed in

Thermal Cycling at Various Temperatures

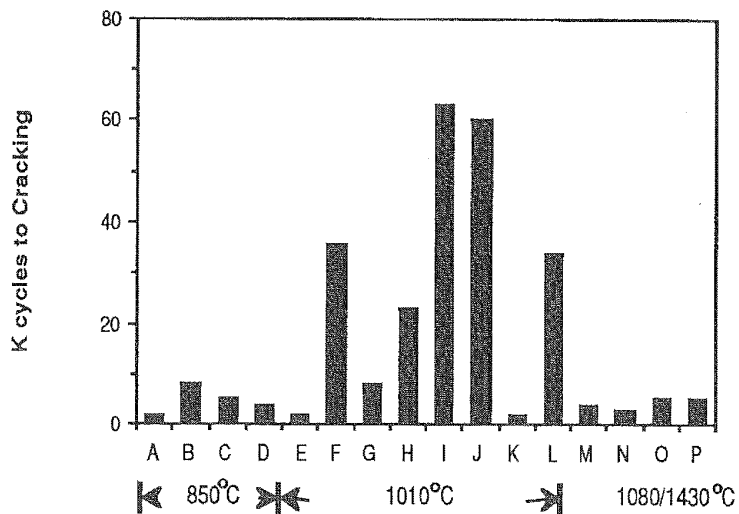


Fig.7-3

Legend	Substrate	Coating
A	IN738LC	none
B	IN738LC	NiCrSi
C	IN738LC	SiB
D	IN738LC	TiSi
E	Superalloy1	ZrO ₂ 20%Y ₂ O ₃ (plasma sprayed)
F	As in E	As above but columnar
G	As in E	As in E, but electron beam coated
H-K	As in E but heated substrate	
H	at -34 °C	As in E
I	at 20 °C	As in E
J	at 316 °C	As in E
K	at 649 °C	As in E
L	As in E	As in E, but with 21%MgO (microcracked)
M	As in E	ZrO ₂ .12%Y ₂ O ₃ /Ni16Cr6Al0.6Y Duplex coat
N	As in M	As in M
O	CrNiNb-st. steel	CeO ₂ - by Sol-gel process
P	As in O	SiO ₂ - by CVD

COATINGS: PHYSICAL & MECHANICAL PROPERTIES

<1000 cycles; PVD coated 20% yttria stabilized zirconia fared better with 4000 cycles (Bennett et al 1987).

Thermal fatigue cracking depends on the coating-substrate thermal expansion mismatch (Strangman et al 1977). To minimise the sharp transition from metal bond coat (expansion $17 \times 10^{-6}/\text{deg.C}$) to ceramic ($10 \times 10^{-6}/\text{deg.C}$), cermets with intermediate expansion have been used. But oxidation of the metallic particles in the cermet can cause strain and spalling and hence a two-layer coating system is preferred. But some type of monophase interlayer with the correct expansion and anti-strain features is desirable. With recent MCrAlY systems (M=Ni, Co), DBTT of 200°C and strain rates of 0.1%/second are achievable at low loads above 850°C . So at high temperatures such bond coats can deform to match the substrate and ceramic thermal barrier overcoat, so providing effective strain isolation for the latter. Oxidation, corrosion and ageing, in the bond coat may slowly increase its rigidity and so reduce its strain isolation potential.

Care must be taken to ensure that the values of coefficients of thermal expansion used are those for the phases actually present in the coating. Because of their lamellar microstructure, the thermal conductivity of D-gun and flame sprayed coatings is lower than that of solid, fully dense materials of the same composition. Their absorption characteristics may be very different as well because of their surface topology and in some cases slight shifts in composition (non-stoichiometry). One of the most common uses of coatings employing their thermal properties is for oxide thermal barriers. 500 cycles to 1000°C in air (9 minutes heating, 6 minutes cooling) cracks Ti-Si pack coatings on IN 738LC (Allen 1968). The thin trailing edge of a gas turbine blade heats and cools faster than the bulk and different expansion coefficients can cause cracking and hence corrosive attack and failure.

A successful coating in diesel engines for thermal shock resistance is $\text{MgO} + \text{ZrO}_2$ on a NiCrAlY bond coating (Kvernes 1983). MgO.ZrO_2 has good resistance to wear and flexural fatigue also. Ceramic thermal barrier coatings reduce substrate temperatures by 120 to 150°C . Control of porosity, segmentation, microcracking and residual stress, has given great increases in the number of cycles to failure compared with 1977 values (Spicer 1980).

Sol-gel and CVD silica and ceria coatings on 20Cr25Ni-Nb stainless steel (for gas cooled nuclear reactors) showed no effect on 825° to 625°C cycling for 860 days but some deterioration of the sol-gel silica coatings occurred after 9000 hours. The sol-gel ceria and CVD silica coatings were still effective after 15000 hours (Bennett 1983, 1981), no deterioration being caused by daily thermal cycling nor mechanical loads. No thermal fatigue or loading caused deterioration in 15K hours of CeO_2 (sol-gel coating) or SiO_2 (CVD), on 20Cr25NiNb stabilized stainless steel (Bennett & Price 1981).

CVD pyrolytic graphite is highly anisotropic and its thermal conductivity anisotropy is 300 (comparing radial and circumferential directions). Its accompanying thermal expansion anisotropy limits the ratio of thickness to bend radius in a curved section, beyond which delamination occurs on thermal cycling. Co-deposition with other materials to form 'alloys' modifies these effects and is an area for further research.

Self-healing plasma coatings are used in casting metal moulds which are subject to thermal cycling, doubling the life to 2000 castings and giving advantageous slower cooling rates (to avoid unwanted tempering). These coatings are also used on a 2-stroke diesel piston head, subject to thermal shock and sulphur corrosion from the oil. The piston showed no damage after 28000 hours and 230 million thermal shocks. Self-sealing coatings are also good on burners, combustion chambers and cracking reaction vessels, e.g. a cracking reactor of AISI-321 steel had a hot surface temperature of 2300°C (ZrO₂ surface) but only 510°C at the underside of the ZrO₂. Self-sealing coatings have an outer layer, e.g. ZrO₂, an intermediate layer, e.g. Cr + ZrO₂ whose porosity is reduced by its oxidation (which also causes mechanical and chemical bonding to the outer ZrO₂), and an inner layer, e.g. Cu-Ni. Recommendations are given (Perugini et al 1973).

The major factors affecting thermal cycling and high temperature resistance of plasma sprayed ceramic coatings are: thermal expansion mismatch between the coating and the alloy substrate, behaviour of the bond coating, interfacial phenomena during thermal treatment, phase transformations and composition changes (Herman & Shankar 1987).

Thermal fatigue degradation occurs due to phase transformations in FeAl coatings on Fe-Mn-Al steel (Guan et al 1981). Cr coatings on steel show spalling on high temperature thermal cycling, due to thermal expansion (Drewett 1969). Mo coatings on 304 stainless steel prepared by a CVD method have been subjected to two types of thermal cycling tests (Nicoll 1983). For uniform heating and cooling between 500 and 900°C, the coatings survived well up to 400 cycles whereas above 950°C intergranular microcracking was observed and failure occurred as maximum cycle temperature was increased. Results of electron pulse heating tests indicated that the coatings were still intact until maximum surface temperature reached the melting point of the substrate. It is suggested that cracking in the coatings is very closely related to melting of the substrate (Yamaneka et al 1982).

7.4. THERMAL CONDUCTIVITY, THERMAL BARRIER COATINGS

A high thermal conductivity increases resistance to thermal shock, while a low value allows higher engine temperatures and adiabatic designs. Unspecified refractory coatings are claimed to greatly improve the emissivity of furnace walls, roofs and

COATINGS: PHYSICAL & MECHANICAL PROPERTIES

hearths, which gives fuel savings by re-radiation of heat back into the furnace (Anon. 1981). A very fine grain structure decreases the porosity of the walls which affects conduction and re-radiation. Coatings are applied by air spray gun. Refractory dusting and spalling is reduced. The emissivity of steel is modified by Al or Si coatings (Pikashov et al 1980).

Thermal and electrical conductivity of plasma sprayed and D-gun coatings deposited in an inert atmosphere is much higher than for conventional coatings, due to very little oxide formation during coating. The lamellar microstructure of D-gun coatings gives a lower thermal conduction than of the fully dense solid.

The thermal conductivity of Al_2O_3 , Zr_2SiO_4 and $\text{Al}_2\text{O}_3\text{-MgO}$ coatings on metals has been measured. Tensile stress in AlN coatings is due mainly to differential thermal contraction on cooling but the net stress is compressive (Zirinsky & Irene 1978) and increases with deposition temperature. Adding Si_3N_4 sharply reduces the net stress and puts it into the tensile region. High temperature radiative coatings of TiO_2 and ZrO_2 can be plasma sprayed (Goward 1970) onto refractory metals and resist thermal shock. Holding MgO-stabilized ZrO_2 above 1000°C allows MgO to precipitate out, causing ZrO_2 instability and its increasing thermal conductivity can rise to three times its previous value. This causes the hottest areas to degrade fastest and needs further research.

7.4.1. THERMAL BARRIER COATINGS (TBC)

Ceramic coatings were first tried in the late 1940s and 1950s, and in the 1960s rocket nozzles and gas turbine sheet metal combustor components were candidate substrates; much wider test performances on turbine section components were made in the 1970s and now they are in regular service high temperature components, in a variety of gas turbines and diesel engines (Miller 1987b).

Thermal barrier coatings (TBC) as they are known today are composite coatings with a minimum 2-layer configuration of a metallic bond coat on the substrate with a ceramic top coat. The service performance, endurance and life time of TBC thus depend on the survivability of both the top- and bond-coats.

A coating graded in Al from 0% at the interface to 12% at the surface was produced by using a dual source of evaporation (Boone 1979). A dual target sputtering method has also been reported (Prater et al 1982; Patten et al 1979). A multi-source electron beam ion plating system designed specifically for graded coating production is another development for TBC (Nicholls & Hancock 1987). The equipment features EB sources, two rod-fed and four multi-hearth crucibles, which allow mixing of a coating in the vapour phase. Sputter cleaned components (using rf glow discharge) are given a strike layer of either the substrate alloy itself or a suitable underlay using one of the multihearth sources and the rod sources take over to produce a graded interface.

COATINGS: PHYSICAL & MECHANICAL PROPERTIES

Vacuum and power control allow more variations and rare earth element additions and other modifications are also reported to be possible.

Thermal barrier coatings fall into 2 types, thin (<0.05 cm) and thick (up to 0.625 cm). The thin barriers are used in gas turbine engines and diesel and petrol engine piston heads and valves. They are Ni-Cr, Ni-Al or MCrAlY with, e.g. ZrO_2 or $MgZrO_3$ as a thermal barrier on top. In earlier studies a continuous gradation from metal to oxide was considered for gaining on better thermal shock resistance. The metal part of the coating must resist oxidation (since the oxide layer is porous). This continuous gradation is more necessary with thick thermal barrier coatings. Thermal and mechanical properties of plasma and D-gun coatings are reviewed by Tucker (1981). As-sprayed coatings can have very low thermal conduction but on heating this can increase greatly due to sintering shrinkage. The performance and technology of TBC have been reviewed (Strangman 1985; Miller 1987a).

Cracks in a thermal barrier coating are stopped on reaching a more ductile NiCrAlY layer, for example, but this can lead to bad hot corrosion (Nicoll 1983). Yttria stabilized zirconia coatings have a high microcrack density next to their bond coat and were found inferior to MgO stabilized zirconia in thermal cycling. A martensitic transformation can occur and if the sprayed ceramic powder is a phase mixture the same nominal composition can give 2 orders of magnitude differences in rig test life. To get a single phase (homogeneous) powder for spraying, the sol-gel process is used and greatly increased performance results (Bennett et al 1984). Thermal cycling tests conducted on RB211-22B nozzle guide vanes have proved yttria stabilized zirconia coatings to be superior to the magnesia stabilized type (Bennett et al 1987). However, the latter appears to have had no bond coat as the former had. The results are, therefore, not conclusive.

Thermal barrier coatings have currently advanced to a point where they are in service in the turbine section of advance gas turbine engines. Fig.7-4a gives a schematic of the temperature profile across a metal substrate/bond coat/TBC (Bratton & Lau 1981). With an assumed hot spot gas temperature at $2280^{\circ}C$, an inlet pressure of 3.85 MPa, the coolant temperature and pressure at $538^{\circ}C$ and 40.4 MPa, the calculated surface temperature of an uncoated blade at the suction side is $1055^{\circ}C$. A ceramic layer 0.0127 cm thickness decreased the metal temperature by $189^{\circ}C$ and the thermal gradient across the ceramic was almost $400^{\circ}C$. A 50% reduction in the cooling air flow still held the gradient at $133^{\circ}C$ (Miller 1987b). The profile will be considerably modified when TBC configurations as envisaged on a multiple layer, Fig.7-4b (Prater & Courtright 1987) or different coating methods, e.g. PAPVD and EBPVD, to combine the advantages of both, with PAPVD improving the adhesion first followed by the more rapid EBPVD deposition (James et al 1987), are implemented. Whatever the coating method may be, one of the vital aspects is the surface state of substrate and the bond coat to ensure sound adhesion. The bondcoat

COATINGS: PHYSICAL & MECHANICAL PROPERTIES

has to be sufficiently rough to key the ceramic coat (Tucker et al 1976).

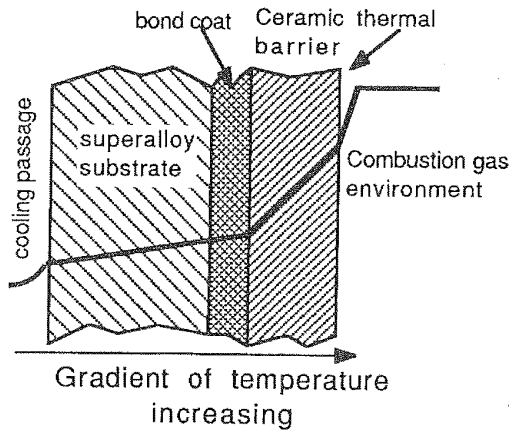


Fig.7-4a

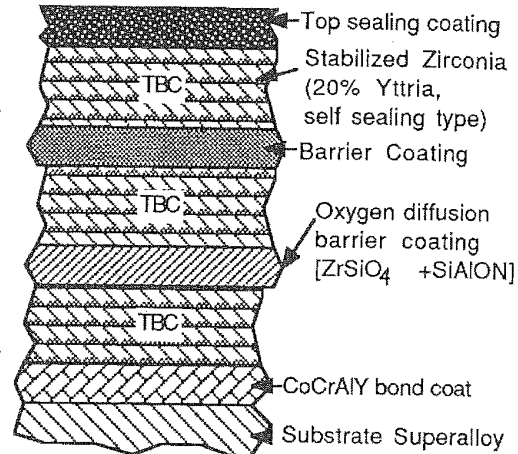


Fig.7-4b

- a: shows the temperature insulation offered by TBC;
- b: shows the multiple sealant, diffusion barrier and bond coats alternated with ceramic layers with controlled porosity to accommodate thermal shocks.

Schematic Single & Multi-Layer Thermal Barrier Coating
Fig.7-4a,b

Typical bondcoat compositions are shown in Table 7:3 (Dahman et al 1980):

Table 7:3

THERMAL BARRIER COATINGS - BOND COAT & CERAMIC COAT COMPOSITIONS

Designation	Bondcoat Composition					Ceramic Composition		
	Co	Ni	Cr	Al	Y	ZrO ₂	MgO	Y ₂ O ₃
LTB 4	23	48	17	12	0.3	75	25	
LTB 5	22	48	20	9	0.5	75	25	
LTB 6	23	48	17	12	0.3	88		12
LTB 7	22	48	20	9	0.5	88		12
LTB 8	39	32	21	7.5	0.5	75	25	
LTB 12	39	32	21	7.5	0.5	93		6.5
LTB 13	39	32	21	7.5	0.5	93		6.5

Notes: 1. Bondcoat thickness is normally 180 microns (0.007") and ceramic is normally 250-300 microns (0.01-0.012").
2. LTB 13 is processed to produce a controlled micro-crack density.

COATINGS: PHYSICAL & MECHANICAL PROPERTIES

Application of TBC together with a bond coat is established, the survival of which is a major long-term stability factor for the coating unit as a whole. Many temperature-dependent factors have not been yet rationalized, e.g. bond coat DBTT, ceramic creep and ratchetting, sintering and phase transformations. Residence time at high temperatures and the frequency of temperature cycles, the coating thickness and quality are also to be made available for long-term utility and planning. TBC are known to tolerate very high heat fluxes as shown with a plasma torch test, which indicates that the thermal gradient prevalent in a gas turbine is not a major contributor to TBC failure. However, failure occurs through cracking of the TBC, regardless of the origin of the stresses. This area of improving bond coat properties and its compatibility to TBC is still unexplored. Ceramic microstructure and composition control, bondcoat property control, surface sealing and stress accommodation capacity, improvement in both oxidation and mechanical properties, and alternatives to plasma coatings and design aspects, are all to be looked at critically for a better optimization of TBC (Miller 1987b).

7.5. INTERDIFFUSION

Many surface treatment methods depend on diffusion of an alloying element into the surface of the material, e.g. surface hardening by carburizing, nitriding or boronizing of steel. C and N diffuse fast interstitially and nitriding can be done as low as 500°C in ferritic steel. Diffusion of Al and Cr is slower and needs higher temperatures. 1% Al and 11% Cr keeps steel in its ferritic phase (fast diffusion phase) at all temperatures. Phase diagrams of refractory metals with Ni, Co and Cr show many intermetallic phases of low melting point and rapid interdiffusion prevents use of Ni and Co-base coatings on refractory metals. Interdiffusion between LPPS Ni₂₃Co₂₀Cr_{8.5}Al_{10.6}Y₄Ta on two Ni-base superalloys CMSX-2 (5Co₈Cr₆Al₆Ta₁Ti₁Mo₈W) and CoTaC 784 (10Co₄Cr_{6.5}Al₄Mo₄W₄Nb₄Re_{0.4}C) was found to be very limited at 850°C but quite significant at 1100°C but with different effects. In CMSX-2 W-rich gamma-prime phases, 40 microns thick, formed along with Ta-enrichment at the substrate-coating interface with outward diffusion of Ni, Cr and Co. But in Cotac 784, a gamma-prime depleted zone resulted above a coalesced gamma-prime zone which contained precipitates enriched with W, Re, Mo and Cr, and the diffusion reaction was found to be that of Ni diffusion outwards as in CMSX-2 but inward diffusion of Co and Cr (Veys & Mevrel 1987). The study indicates the relevance of interdiffusion data in specific coating/substrate systems at their operating conditions. Interdiffusion references have been listed, but more data are needed (Natl.Acad.Sci. 1970).

Coatings of Al, CrAl, SiAl and PtCrAl on IN738LC showed a needle phase extending into the IN738LC at 750°C but NiCoCrAlY showed no such interdiffusion. This did not affect creep strength (Strang 1979). Two main processes occur with aluminide coatings:

COATINGS: PHYSICAL & MECHANICAL PROPERTIES

(i) Outward Ni and inward Al diffusion, which increases coating thickness but decreases its outer Al content, (ii) Loss of Al due to alumina scale formation and spalling. These cause the beta-NiAl to become the less oxidation resistant gamma prime Ni₃Al and fingers of this phase finally penetrate through the coating causing rapid failure. As a basis for controlling the pack aluminizing process and the subsequent degradation of the coating, interdiffusivity measurements are needed. There is a strong dependence of D on composition in binary Fe-Al alloys. Good coating structure photographs and interdiffusivity values have been given. An equi-volume mixture of nitric, sulphuric and phosphoric acids is recommended as an etchant for the Fe-Al system (Akuezue & Whittle 1983). There is microstructural evidence of some interdiffusion of W, Mo and exothermically reacting NiAl coatings sprayed on steel, Ni or chromized Al (Coates et al 1968). The bond strength of ceramic coatings is generally attributed to interlocking, but some spinel formation is reported for Al₂O₃ on steel (Kofstad 1966) and Al₂O₃/TiO₂ on Al (Wagner 1965). But oxides on substrate surfaces or oxidation during plasma spraying, decrease bond strength (Perkins 1978). Diffusion bonding to fix WC tips onto machine tools has been studied (Almond et al 1983). Anomalous diffusion may accompany ion implantation due to vacancies and interstitialcies created by ionising radiation, which far exceed those produced thermally (Dearnaley 1973).

Interdiffusion in Si coatings on Ni produces several phases (Subrahmanyam 1982). In binary Fe-Al alloys interdiffusion shows strong dependence on composition (Akuezue & Whittle 1983). Interposing a diffusion barrier layer is unsuccessful. A high surface Al concentration is needed to form protective alumina films but this increases interdiffusion (Akuezue & Whittle 1983; Sivakumar & Rao 1982; Jackson & Rairden 1977; Glitz et al 1982). Pt acts not as a diffusion barrier but as a diffusion medium which allows Al to form a subsurface nickel aluminide (on Ni alloys) and a Pt₂Al₃ intermetallic outer layer which prevents outward Ni diffusion and thus allows unrestricted alumina formation (Wing & McGill 1981). W and Mo (solid solution strengtheners) are also prevented from escaping from the alloy; their escape would have an adverse hot corrosion effect. Pt₂Al₃ is preferred over PtAl₂ as its volume change is much less on forming PtAl (caused by alumina formation).

Inward Si diffusion, reacting with the interlayer, decreased the strength of NiSi₂, CrSi₂ and NiCrSi coatings on Fe, IN738, IN 100, Nimonic 90 and IN601 (Fitzer et al 1979). Considerable inward diffusion of a Ti-Si pack coating on IN 738LC occurs after only 500 cycles to 1000°C in air. 1000 cycles to 1000°C for CoCrAlY on IN738LC formed AlN and TiN under the coating (Nicoll 1983). Such brittle phases reduce alloy strength. The loss of Pt by its inward diffusion into the substrate can be estimated from $x^2 = 2Dt$, where x^2 is the mean square unidirectional displacement of solute atoms in a solvent in time t. For a Pt layer on steel at 900°C with $D = 10^{-10}$ cm²/sec, t is some tens of hours for a 25 micron thick Pt layer and thousands of hours for a 250

COATINGS: PHYSICAL & MECHANICAL PROPERTIES

micron Pt layer. Usually D is smaller the more refractory the substrate, and coating life on steel is much greater than on Mo, so Pt coatings on refractory metals last much longer. Loss of Pt also occurs at 900°C as volatile PtO₂ and 25 microns would last a few hundred hours and 250 microns for several thousand hours. For a 30Pt63Pd7Au alloy, the Pt life is 6 times longer (Kubaschewski 1971). Other reactions of Pt, with refractory oxides, are reviewed; metals can be brazed to refractory oxides using a Pt-containing brazing alloy (Exner 1982).

A 1 micron Al film reacts rapidly at 635°C with a thick Ti substrate forming TiAl₃, confining the Al to the surface region. At 900°C, Ti₃Al forms with little loss of Al into alpha Ti. But subsequent annealing at 900°C decomposes the Ti₃Al and releases Al into the alpha-Ti (Rao & Houska 1983). Considerable interdiffusion of Ti and Cr from a Nb-base alloy occurs into a Ni-base alloy at 1050°C in 30 minutes (Samsonov 1973), but Nb diffuses little. Ni diffuses considerably into the Nb alloy. Data for MSi₂ layer consumption, i.e. coating life, are given along with alumina and beryllide coating life. No Al diffuses into W at 1950°C, making W a good diffusion barrier. N embrittles Cr alloys; alumina coatings prevent this but substitute interdiffusion and a barrier is needed to immobilise the Al. C from Nb-alloy substrates diffuses into Ti-rich coatings and lowers the Nb alloy strength in hours at 1200°C (Natl.Acad.Sci.1970).

TiC coated molybdenum or graphite is considered as a promising material as diffusion barrier for application to fusion reactor first wall components. Thermal stabilities of TiC coatings on molybdenum and graphite prepared by ion-plating, magnetron sputtering, and chemical vapour deposition have been examined with particular reference to the interaction between the TiC layer and the substrate. A TiC coating was found to be markedly stabilized at elevated temperatures when it was deposited on the graphite substrate. This may be due to the diffusion behaviour of carbon from the graphite substrate. In contrast a TiC layer on Mo showed a large degree of weight loss above 1800°C on account of the Ti vaporization from the coating. This may be partly due to the formation of Mo₂C in the film-substrate interface. This tendency to lose weight at elevated temperatures was comparatively strong for the coatings prepared at low deposition temperatures by ion-plating and magnetron sputtering (Fukutomi et al 1982).

Sputtered yttria coatings 0.1 microns thick much reduce the reaction between metals and Si-base ceramics. Reaction bonded Si-SiC ceramics above 950°C react with Ni coatings by forming Ni-Si eutectics. Yttria coatings on SiC survive 26 thermal cycles between 1100°C to 25°C but yttria on Ni spalls after 4 cycles. But if yttria coated SiC and Ni were separately cycled and the spalled yttria cleaned off, then on assembly together and heating 100 hours at 1000°C the residual yttria gave considerable interdiffusion protection (although it could not be seen in the microscope). The barrier may be Y₂SiO₅ (Mehan et al 1983).

Bonding via interdiffusion is a developing technology. Bonding of Si_3N_4 to ZrO_2 without use of pressure but due to a solid state reaction and the presence of CaSiO_3 has been reported (Becher & Halen 1979). Reaction bonded ceramics have been known to give better performance than their hot pressed counterpart under certain hot corrosion conditions (Godfrey 1983). Pyrolytic deposition of Si_3N_4 avoids undesirable siliceous second phase but gives either coarse columnar or 'amorphous' textures. A sputtered interlayer of yttria is necessary to prevent reaction of a Si_3N_4 coating with a superalloy substrate. A post-coating heat treatment is necessary to improve the Si_3N_4 properties, by causing outward grain boundary diffusion of undesirable grain boundary second phases to an external silica sink (Lang 1983). Oxidation at 1350°C thereby increases the strength (Kreher & Pompe 1981; Evans & Heuer 1980). Additions of oxides such as CaO , SrO , Y_2O_3 and MgAl_2O_4 migrate to the grain boundaries, causing a loss of strength, forming silicates and causing weakness due to crystobalite formation. Less additives are possible if densifying is done by HIP. Further work is needed in this area.

Diffusion barrier layers are often required on carbon/carbon composites. Reviews on refractory coatings for graphite are available (Chown et al 1962; Criscione 1964; Schulz et al 1964; Samsonov & Epik 1966). Ir on graphite is reviewed (Criscione 1965a, 1965b; Criscione 1967). Ir is almost impervious to oxygen diffusion up to 2100°C and forms no carbide nor inter-diffusion. The expansion of Ir needs a graphite of high expansion. Coating methods include slurry and sintering, cladding, vapour deposition and electroplating (Natl.Acad.Sci. 1970). Two multiple layer systems have been described for providing compensations for thermal expansion and as barrier for oxygen and inter-diffusion:

(i) on the carbon/carbon substrate, CVD SiC is deposited which accommodates thermal expansion cracking, and this is top coated with CVD Si and B containing glassy coatings as a barrier to oxygen and carbon diffusion while also serving as crack sealers for the SiC undercoat;

(ii) The second type comprises of three layers, with a pyrolytic carbon coat on the carbon/carbon composite substrate, and CVD SiC is deposited on this, and in turn is coated with CVD Al_2O_3 (Stinton et al 1988).

7.6. ADHESION

7.6.1. GENERAL

The aim of any coating process is that the resultant workpiece functions as one component with superior properties for the environment for which it is designed. A coated material fails when the surface layer exposed to the environment separates completely or partially from the surface it is put upon. This can

COATINGS: PHYSICAL & MECHANICAL PROPERTIES

occur either due to an unsound contact between the substrate and the coating, or to an in-service breakdown arising from a surface environment reaction. This section is concerned with the first cause, and examines briefly, factors affecting bonding and adhesion.

Poor adhesion can arise at any of the three major stages in a coating process:

1. a. The substrate condition.
b. The purity of the coating chemicals.
c. The cleanliness of the equipment used.
2. The bonding between the substrate and the initial deposit; deposit growth.
3. The final compatibility of the substrate to the coating under the performing environment and temperature conditions.

Surface preparation of the substrate, its purity and that of the reactants, and their composition are the first-front influencing factors. Surface finish of the substrate is the last step prior to coating. All processes have this in common. Bulk coating processes, where the coating is itself a sheet, e.g. explosive cladding, need to surface treat two solid interfaces which interlock into each other.

Important parameters for adhesion and bonding are: substrate surface roughness, activation energies for surface and bulk diffusion and coating atom surface bonding energy. The last two properties are related and proportional to the m.p. and provide a basis for the Movchan and Demchischin structure zone model (fig. 7-1). A columnar structure (zone 1, low T/T_m ratio) is due to condensing a coating from a vapour arriving from one direction and with little subsequent surface diffusion. Inter-columnar voids become larger as the angle of vapour incidence increases. The three zones are well discussed by Thornton (1975, 1981). As T/T_m is increased, the columnar structure disappears but severe surface irregularities, e.g. debris can cause zone 1 (columnar) structures to persist into the Zone 2 and 3 regions (called columnar or linear defects). A smooth homogeneous substrate is essential. The use of ion bombardment (and its disadvantages) to suppress columnar zone 1 structures is also discussed by Thornton (1981). The adhesion of sputtered coatings is found to be better than those obtained by simple evaporation and condensation.

Coating adhesion depends on the bonding strength to the substrate and on the interface microstructure. The bonding can be chemical, Van der Waals and/or electrostatic. Chemical bonds are strongest (several eV), van der Waals arise from polarization (0.1 to 0.4eV) and electrostatic bonds are due to a double layer (0.1 to 0.4 eV). An 0.2eV bond should resist a high stress of $5 \times 10^8 \text{ N/m}^2$ (72 kpsi) but adhesion failures often occur due to internal stresses in coatings exceeding this value and to microstructural

flaws (Thornton 1981). Theories of adhesion are briefly discussed by Brewis (1982).

The thermodynamics of wetting of surfaces and its relevance to bonding is reviewed by Rance (1982). Three types of attractive forces operate at interfaces: primary bonding (covalent, electrostatic or metallic bonds, with binding energies of 40 to 400 kJ/mole), secondary bonding (Van der Waals forces, with energies of 4 to 8 kJ/mole) and hydrogen bond forces with energies of 8-35 kJ/mole. If intimate molecular contact between two materials were possible, then Van der Waals forces, even though they are the weakest of the bonding forces, would give adhesion far exceeding that observed (Tabor 1951). Attraction between two materials in molecular contact (about 0.5nm) is greater by a factor of about 10^4 than the attraction across a (typical) 10nm gap. 'Wetting' results in molecular contact. Metals have high surface energy, about 1 J/m^2 but all high energy surfaces readily adsorb contaminants (Rance 1982).

Wetting of steel is needed to obtain quality in coatings such as Zn and Al. Steels containing small amounts of strong oxide forming elements, e.g. Al, Si, have erratic adherence problems. Surface preparation methods may promote internal oxide formation. If the surface is hot pre-oxidised to form mainly a surface iron oxide which is then easily reduced before entering the liquid metal (Al or Zn), the surface is then readily wetted and a good coating results. If the surface is merely hot reduced before coating, adherence is poor because reducing conditions will favour alumina formation (Arnold et al 1977).

Interfaces are classed as: abrupt, compound-forming, e.g. inter-metallics), diffusion (needs considerable solubility), pseudo-diffusion, e.g. co-deposition to form graded interfaces, or irregular, e.g. due to grit blasting or etching (Mattox 1978). Compound interfaces may be brittle and so should be kept thin. For diffusion, an intermediate layer soluble in substrate and coating can be used. Abrupt interfaces are liable to act as 'contamination' layers which weaken Van der Waals bonds. If the nucleation density is low, lateral growth gives interfacial voids with poor adhesion due to the reduced contact area and easy crack propagation. Sputter cleaning forms surface defects which enhance the nucleation density and minimises void formation; it also promotes diffusion via these surface defects. Sputter cleaning is necessary (but sometimes difficult) when using cylindrical magnetrons (Thornton 1981; 1978). The substrate is negatively biased and plasma ions then sputter material and contamination from the surface: 1 to 5 mA/cm^2 , 100 to 1000 V , 5 to 20 minutes, removes 200 to 1000 A.U. ; an rf bias is needed for insulator substrates. Irregular interfaces resist cracking since an interface crack would have to change direction or propagate through a stronger material (Mattox 1978). Plastic deformation due to the roughening operation is another factor that must be taken into account (Tucker 1974).

Oxygen-active metals often adhere well to glass and ceramics and no sputter cleaning is needed (Thornton 1981). Thus Ti, Cr, Nb, Ta and W are used as intermediate layers for depositing Cu, Ag and Au on glass or ceramic (Hollar et al 1970). The effect of oxides on bond strength is reviewed by Tucker (Tucker 1981). Sometimes an abrupt interface gives more adhesion than a co-deposited, graded interface, e.g. alumina on Hf (Vossen et al 1977). Usually adhesion is good at temperatures $>0.3T_m$ if inter-diffusion is allowed by solubility (Natl.Acad.Sci. 1970). Hollow cathode ion plating of Ag onto stainless steel and Be gives excellent adhesion and a ductile fracture mode (Mah et al 1974). Fracture occurred in the Be, the Ag/Be interface being stronger. Adhesion of CVD coatings can be poor if the gases used attack the substrate (Bryant & Meier 1974). Adhesion test methods have been reviewed (Werber 1987; Tucker 1974; Davis & Whittaker 1967; Apps 1974).

The maximum thickness of a given coating is often limited by the increase in residual stress with coating thickness. Residual stress in a coating may change the apparent bond strength. Compressive stresses induced during rf magnetron sputtering of Al_2O_3 film have been closely correlated to its adhesion, the magnitude of the stress depending on the film thickness, deposition pressure and sputtering power (Roth et al 1987). Arc deposited TiN on high speed steel substrates showed increase in adhesion by a factor of two when the substrate bias was changed from 0 to 100 V, and deposits were dense and very adherent when the substrate temperature was $200^\circ C$, and registered higher critical loads ($>90N$) when heated further up to $450^\circ C$ (Erturk & Heuvel 1987). Highly ductile and adhesive Ti coatings have been obtained by vacuum plasma spray, with the process yielding deposits of low porosity. Substrate pre-treatment by sputtering and pre-heating resulted in very good adhesion on different substrates such as carbon and austenitic steels and Ti-alloys. Marginal variations were observed between as-deposited and annealed coatings (Lugscheider et al 1987).

A similar improvement in adhesion has been observed in TiN coatings by reactive magnetron sputtering on high speed steels. Adhesion increases with temperature reaching a maximum between $400-500^\circ C$, and is attributed to formation of FeO at the substrate interface, decomposing Fe_2O_3 and Fe_3O_4 as the substrate temperature is raised. Ti as an interlayer increases adhesion but only up to substrate temperature $400^\circ C$. Above that TiC formation lowers adhesion. Carbide distribution in steel influences likewise. Carbide as VC with lattice structure similar to that of FeO with only a slight mismatch, favours adhesion. In general, lowering of interfacial energy increased adhesion (Helmersson et al 1985).

Adhesion mechanisms have been reviewed as due to mechanical interlocking, alloying with the substrate, van der Waals forces, epitaxy, etc. (Tucker 1974; Van Vlack 1964; Malting & Steffens 1963). Other suggestions observed during corrosion studies such

as oxide pegging (Choi & Stringer 1987) will not apply in this context unless a heat treated interlayer containing Y as a constituent is considered. For Ti as a thin film on oxide substrates, chemical interactions are needed in addition to Van der Waal's forces and electrostatic forces, as the metal has a high negative free energy of oxidation. However, the adhesion strength has been found to depend on the mechanical strength of the substrate as indicated by 'peel' data decreasing in the order - sapphire, MgO, quartz, and fused silica substrates (Kim et al 1987).

Most plasma deposited coatings need a roughened surface to get significant bonding (Grisaffe 1965). Plastic deformation due to the roughening operation may be more significant than the actual roughness, e.g. NiCr on steel (Epik et al 1966). Bond strength and recrystallization of a worked surface layer are correlated (Malting & Steffens 1963; Allsop et al 1961). For spray coatings where oxygen was present, spinels or 'oxide cementation' may be important (Epik et al 1966; Ingham & Shepard 1965). But oxide films on impinging particles would reduce adherence. Bond and mechanical strength achieved for Al and Ti are not possible for steel (McNamara & Ahearn 1987). Between CVD TiC and TiN on cemented carbides, the latter shows superior adhesion because it is less brittle; TiC shows interfacial fractures and considerable work hardening of the interface (Laugier 1986).

The ideal requirements of an adhesion test are that the test should yield results which are quantitative, applicable to a range of thicknesses and materials, economical with minimal machining, reproducible, sensitive, and suitable for routine use. A test based on indentation fracture is described and fracture mechanics analysis gives a quantitative measure of the interface toughness (Chiang et al 1980).

7.6.2. SUBSTRATE CLEANLINESS vs ADHESION & BONDING:

The extent and thoroughness of substrate cleaning are tailored to the initial state of the substrate and the needs of the coating process. Treatment given to a steel sheet with grease and mill scale is drastically different to that given to a wafer-thin or brittle or precision substrate, e.g. Si, or a gas turbine blade, a vapofilm or an electronic component. There are several standard publications on the subject which should be consulted. Only a brief discussion is given here. Table 7:4 outlines broadly the type of surface and the various macro-cleaning/treating procedures adoptable. Cleaning by heating, sputtering, physical and chemical etching, vapour treatment and ultrasonics are methods adopted flexibly for substrates of all nature, shapes, and sizes (see section 7.8. for impact treatment of substrate).

TABLE 7 : 4

SUBSTRATE CLEANING OPTIONS

a. Pre-Coating Step

Surface Type	Treatment
Dust-covered	Suction
Solid dirt, loosely adherent	Brush (soft or wire); & suction
Solid dirt, firmly adherent	Abrasion or blasting with right size grit, or impact treatment with sand, metal shots, glass beads or ceramic granules.
Organic:grease, oil	Organic solvents wash
Inorganic:scales of known composition; viz rust	Abrasion; suitable acid and/or alkali cleaning with intermittent washing; Electro-cleaning, cathodic (or anodic)
Substrates which can be wetted	Washing with clean/or de-ionized water
Light scale	Acid/alkali etch/wash
Fine particle or debris	Ultrasonic cleaning
Final degreasing step	Vapour cleaning with organic solvents incorporating safety precautions; Solvents:Trichloroethylene, xylene, etc.,
Roughness a pre-requisite	Suitable peening.
Specific: metallurgically incompatible surface	Heat treatment to alter phase composition and/or microstructure or Inter-layer application to act as a diffusion barrier by suitable deposition techniques, viz. electrodeposition, spray, pack or vapour deposition.

b. Post-Coating Step

Electroplated finish	Soft-polishing to enhance reflectance or alter surface finish/light impact
Consolidation or extra step	Ion-implantation, Laser treatment; Sealing processes:- auxiliary sealing by CVD, PVD or amorphous material transformation - metallic or non-metallic.

=====

COATINGS: PHYSICAL & MECHANICAL PROPERTIES

It is necessary to remove millscale completely from steel before coating using hot H_2SO_4 or cold HCl causing H_2 evolution knocking it off mechanically while chemically etching the surface. Inhibitors (pickling restrainers) are added to reduce attack on the metal. Grit blasting is the most efficient mechanical method, using chilled iron or abrasive grit (but not shot, which embeds itself). Rust removal by phosphoric acid leaves a thin Fe_3PO_4 layer which gives some protection. Grit blasting is again the best mechanical method. A clean, grease-free surface will not show water droplets on it, when wetted. Guidelines for cleaning metals are available (Sykes 1982; Brit.Std. CP3012 1972; Moloney 1982).

Surface preparation can be a critical parameter for bond strength of sprayed aluminium coatings on grit blasted steel substrates. The type and condition of grit and the blasting angle influence bond strength markedly but blasting pressure or speed and nozzle-substrate distance has little effect. Blunted grit and low blasting angles reduce bond strength. The steel/sprayed Al bond is of a mechanical type ; alumina grit increases bond strength and moves the failure location from the interface to within the spray coat (Apps 1974).

An adhesive mechanism is proposed to account for the bonding of plasma sprayed Ni, Cr, Mo, Ta and W on aluminium and mild steel substrate. Part of the substrate gets molten giving rise to a boundary layer of an intermetallic compound and this bridges and links the substrate to the plasma coat (Kitahara & Hasui 1974). A similar adhesion mechanism is suggested for wire-explosion spraying which seems likely as both plasma and wire explosion can result in a high temperature small particle, high impact contact area of the substrate with the coating material (Suhara et al 1974).

7.7. BONDING

7.7.1. GENERAL

It is difficult to differentiate between bonding and adhesion except that the former implies substrate-coat linking on the micro-crystal, atomic, ionic scale while adhesion is a macro-term referring to a larger area-to-area bonding. Factors affecting bonding may be identified in the following areas:

1. Mechanical factors, e.g. slip and shear, in bulk coatings, and temperature effects, e.g. ductile-brittle-transformation-temperatures, and temperature cycle have to be noted. A Pt sandwich layer, for instance, is applied on a Ni-base alloy prior to coating stabilised ZrO_2 to operate above the DBTT of the composite.
2. Duplex coatings such as Cr-Al, Cr-Ti-Si, Cr-Al-Si are best given by applying the first single coat or alloy coat followed by

the top coat, e.g. siliconizing after Cr-Al, Cr-Ti or, Cr before Al.

3. Interlayers are mandatory where undesirable diffusion between substrate and coating has to be stopped. Interlayers will also compensate for Kirkendall void formation which if allowed to coalesce or concentrate, can lead to major non-bonded areas joints and junctions at the interface. Al is applied as an interlayer to a Ti-SiC composite where the Ti substrate can form brittle silicides during service. (Rao & Houska 1983).

Solid state bonding of Al_2O_3 to austenitic stainless steel Type 316 has been achieved using a low pressure (3.1 MPa), low temperature (1173-1473K) bonding of 0.5 micron thick Mo on the substrate steel followed by Ti. Ti/Mo/Ti interlayers have also been given (Hatakeyama et al 1986). Electrodeposited Ni forms the bond layer between Cu substrate and Pt (Ott & Raub 1986;1987). Ni-Cr-Al has been applied as the interlayer bond coat for 410 stainless steel prior to LPPS or air spray of 316 stainless steel (Eaton & Novak 1986).

The role of interfaces in sintering is reviewed (Anon.1982). Controlled precipitation of fine monoclinic needles of ZrO_2 in cubic ZrO_2 increase its toughness and adhesion (Kvernes 1983). A low Young's modulus decreases the chance of brittle fracture occurring during deformations. Ceramic coatings, e.g. $ZrO_2 + MgO$, have a lower modulus than sintered ceramic materials. Residual stresses cause coating failure. All melt coating processes result in significant residual stresses. Further work is needed, to investigate effects of residual stresses in spray coatings, to develop shear adhesion tests as coatings are more often used in shear than in tension, and on the effects of surface embrittlement and grit inclusions (Tucker 1981).

4. "Wetting" a powder-loaded vehicle is better achieved and more uniform when it is hydrophobic, when Al powder is mixed with it for steel aluminizing (Sugano et al 1968).

5. Aluminizing of Ni-base alloys is inherently linked with the Ni/Al diffusion phenomenon. A good documentation of the available literature prior to 1976 is given by Fontana and Staehle (1978). The relative advantages and disadvantages of Ni_3Al and NiAl phases must be noted.

6. Aluminizing of Fe-alloys is done in more than one way, viz. pack, CVD, slurry, cladding and hot dipping. When hot dipping or spraying of liquid metal is done, it is absolutely essential that the molten metal should wet the substrate. The presence of oxide layers generally impede adhesion. However Arnold et al (1977) demonstrate that an oxidizing preheater step followed by entry into a reduction furnace before the substrate enters the liquid metal, actually produces excellent adherence. The alloy should have more than the critical content of the alloying element needed to form a stable, external oxide layer. On Fe-alloys the

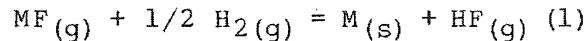
COATINGS: PHYSICAL & MECHANICAL PROPERTIES

oxidizing preheater step induces a predominant iron oxide layer to develop in which the other oxides get dispersed. The reducing section of the process reduces the iron oxide and the surface is readily wetted by the liquid metal.

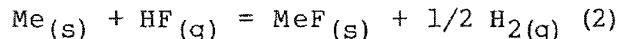
7. Vapour-phase and diffusion type coatings will not adequately coat faying surfaces at a spot-weld or rivetted joint. On such areas a mechanical fastener or closed fusion weld must be used. Fusion welding must be done before the vapour deposition (Gadd et al 1968).

8. CVD coatings exhibit poor adherence when the substrate has been permitted to be attacked by the highly corrosive reactants and/or product gas (Bryant & Meier 1974). For example:

Coating reaction



Metallic substrate reaction



If the free energy of reaction for (2) is less, i.e. more positive than that for (1), then substrate attack can be avoided. Substrates such as Mo-, W-, Ni-, and Ti with a high negative free energy for the fluoride reaction are likely to show poor deposit bonding in chloride-, fluoride-, carbonyl- and carbide-forming media. Factors which affect bonding and adherence in CVD processes are:

- (i) Free Energy of reaction,
- (ii) Reduced activity conditions whence the substrate undergoes alloying reactions,
- (iii) Unfavourable specimen geometry,
- (iv) Reaction in gas phase rather than on the substrate surface which results in a flaky deposit,
- (v) Formation of brittle intermetallics between substrate and coating,
- (vi) Substrate contamination prior to deposition, e.g. by the formation of a thin oxide film, and,
- (vii) Hydriding (or any other precipitate-forming reaction) of the substrate. Generation of hydrogen at the substrate interface is particularly detrimental, particularly in the case of metals which readily dissolve hydrogen. Dissolved atomic hydrogen tends to coalesce to molecular hydrogen and induce stresses resulting in cracking and disbonding due to embrittlement (Bryant & Meier 1974).

Bond coats used to key ceramic coatings show difference in adhesion according to whether the ceramic has been deposited by PVD or CVD (EB-PVD bond coats are usually 50 to 120 microns thick, with surface finish 0.2 to 1 micron). The initial ZrO₂ layer deposited on the alumina of the bond coat is dense and columnar and must be kept below about 2 microns thick to prevent stresses due to thermal expansion mismatch. The outer yttria-stabilized

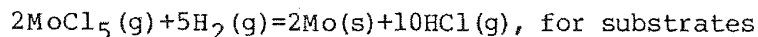
zirconia layer must have lower density for strain tolerance. Mechanical bonding between the ceramic top coat and the metal bond coat in a TBC is an accepted idea. These are experimental conclusions, but the area requires further investigation to clarify diverse bonding behaviour and quantify control parameters.

7.7.2. BOND STRENGTH

Tensile tests for assessing adhesion provide no fundamental data on bonding mechanism, but fracture mechanics methods with a controlled crack path do provide such data (Berndt & McPherson 1980; Ellsner & Pabst 1975; Pabst & Ellsner 1980; Becher & Newell 1977; Becher & Murday 1977; Bascom & Bitner 1977). The cohesive fracture toughness of plasma coatings is much less than that of the same bulk material, due to the lamellar structure. Bond coat interlayers succeed because their metallic lamellae allow plastic deformation; failure near a ceramic/metal interface occurs by brittle fracture between ceramic lamellae or between ceramic lamellae and substrate (Berndt & McPherson 1980).

Adhesion test methods are reviewed in Chapter 9 and reliable data may be generated (Stanton 1973; Bardal et al 1973). Modelling to quantify diffusion bonding of metals has been carried out (Guo & Ridley 1987). Three sub-processes of bonding are proposed: volume and interfacial diffusion coupled with creep, rigid collapse and surface diffusion. An alternative geometry is assumed for the shape of interfacial cavities. Effects of grain size and ratio of phases have also been considered. The time to achieve sound bonding has been predicted to find good agreement with data obtained on a Cu/Ti-6Al-4V experimental system.

Free energy data can sometimes predict adherence of CVD coatings, e.g. CVD reactions such as



with $\Delta G_{\text{f}}^{\circ}$ of the substrate's chloride $< \Delta G_{\text{f}}^{\circ}$ for HCl (both per g atom Cl), non-adherence is expected. This occurs in many systems (Bryant & Meier 1974) but the effect of alloying and gas pressures on activities for the ΔG° calculation must be allowed for. Other factors must also be considered: specimen geometry, thermal expansion coefficient mismatch, surface contamination, and whether solid solutions form (allowing interdiffusion and hence good adherence).

Ion plated coatings have excellent adhesion, even if no alloying or diffusion is possible. Failure often occurs in the metal, not the interface. Bend, tensile, shear and scratch tests gave no failures, in contrast to vacuum deposited coatings. Adhesion is often due to interdiffusion, but ion plating energy (about 100 eV) is only enough to implant to a few atom diameters. Other mechanisms include atom mixing of sputtered substrate with

COATINGS: PHYSICAL & MECHANICAL PROPERTIES

depositing atoms and recoil implantation and ion-aided or radiation aided diffusion. It thus appears that diffusion of only a few atom diameters will give good adhesion. The mechanism is not clear but the adhesion is certainly due to the high energy of deposition (Teer 1983).

Ion bombardment during coating, e.g. sputtering, strongly affects adhesion, perhaps by increasing nucleation site density and so reducing voids (see fig.3-27, Chap.3) (Thornton 1981).

Most plasma coatings have bond strengths below 70 to 84 MPa, but most D-gun coatings and a few plasma coatings have strengths that exceed it. The mechanism of bonding of plasma deposited coatings in many respects is still in dispute (Tucker 1981,1974; Matting & Steffens 1963; Van Vlack 1964). Mechanical interlocking has been considered the most important mechanism by most investigators. It has been shown that bond strength increases with increasing surface roughness in both shear and tensile tests, although it may diminish again above 0.6 to 0.8 microns, rms (Grisaffe 1965; Marchandise 1965). Few published reports have taken into account the detrimental effects of surface embrittlement, peak blunting and grit inclusions when excessive grit blasting is used (Levinstein et al 1961; Leeds 1966).

Plasma sprayed coatings are formed by the impact (100 - 400m/s), deformation and solidification (in microseconds), of liquid droplets, forming overlapping lamellae. Adhesion of plasma sprayed ceramics to metals is poor but is improved by a sprayed bond coat interlayer, e.g. Mo or Ni-Al. The high bond strength between interlayer and steel is easily explained as due to the Ni-Al exothermic reaction and formation of an interdiffusion zone between coating and substrate, but the reasons why ceramic coats adhere so well to the bond coat interlayer needs an explanation (Berndt & McPherson 1980; Ingham & Shepard 1965).

Plasma coating adhesion is thickness dependent, due to internal stresses accumulating with increasing thickness until they exceed the bond strength. Internal stresses in fine powder sprayed coatings rise much faster than for coarse powders. For hard-facings, coarse powder coatings are limited to about 500 microns thick and fine to about 250 microns. This limitation is overcome by using sandwich coatings, e.g. Ni-Al or Mo with the hard coat on top, or by electroplating Ni up to 1mm thick and spraying on top of it; Cr plate is not used as the plasma flame cracks it and because its high hardness prevents surface preparation and leads to poor adhesion. Sandwich coatings perform well under thermal cycling (Malik 1973).

Most of the factors that affect the bond strength of plasma deposited coatings also apply to D-gun coatings. Because of the unusually high velocity of the particles, they are actually driven into the surface of most metallic substrates. Some D-gun coatings are so well bonded that a crack starting in the coating may propagate into the substrate on cyclic stressing. Some

COATINGS: PHYSICAL & MECHANICAL PROPERTIES

substrates require no grit blasting to achieve adequate bonding, since the coating process itself roughens the interface. This embedding/roughening process creates atomically clean interfaces between the coating and substrate over most of the coating area which facilitates chemical bonding and can be likened to the explosive bonding of sheets of metal. This undoubtedly plays a large role in forming the unusually high bond strengths of D-gun coatings. In some cases holding the substrate at constant temperature, e.g. 300°C during D-gun spraying can give improved adherence where a large thermal mismatch is present.

Heat treatment during coating may cause diffusion and improve adhesion by keying on the coating and by causing a gradual transition from substrate to coating. This may not apply to PVD and some CVD processes. Failure may occur within the coating (cohesive failure) or close to the substrate interface (adhesive failure). The adhesion of a coating is controlled by the deformation mechanism of the coating particles during fracture. Metal coating particles deform extensively and much energy is needed for crack growth and so coating adhesion, as measured by fracture toughness, is high compared with ceramic coatings which show brittle fracture.

Plasma sprayed 'self-sealing' composite coatings of a brazing material (Cu-Ni etc), as well as Cr and ZrO₂ are described; bend testing showed no cracks or coating detachment. Strength values are higher than for other types of powder plasma sprayed coatings and further research is needed on such self-sealing types of coatings (Perugini 1973). Arc-sprayed Ti, Nb, Zr and Mo coatings have very high adhesion (>8 kgf/mm²) if produced in pure Ar, attributed to diffusion at the interface. For Ti on a structural steel the diffusion zone width was 20 microns, but insufficient time and temperature prevent the usual form of diffusion. Prior grit blasting gives a high defect concentration which may explain the anomalous diffusion. Adhesion and the diffusion zone width depends on the density, heat conductivity and specific heat (Muller 1973; Steffens & Muller 1973).

Adhesion of wire explosion coatings is excellent as in D-gun coatings, e.g. W on Al fails within the Al. W explosion cladding on mild steel caused the steel surface to sink several microns during the process due to deformation or melting which creates a 1 micron thick melted layer. The strong adhesion is shown to be due to the complete welding of both materials at this boundary, but the weld strength is less than that of a conventional weld due to voids etc. Further studies are needed on this problem. Adhesion tables of plasma sprayed coatings on ceramics and glass are available (Suhara et al 1973; Downer & Smyth 1973). W wire explosion sprayed coating on steel has 24 kg/mm² shearing stress of adhesion, which is the same as that of W itself, and the fracture propagates in the W coating. But W on Cu had only 10 kg/mm² (compared with 28 kg/mm² for solid Cu) and the interface fractured. W and Fe form a solid solution but W and Cu do not and the W/Fe interface thus has a 1.5 micron thick intermediate solid

COATINGS: PHYSICAL & MECHANICAL PROPERTIES

solution layer over 70% of its area which confers great strength (Suhara et al 1974). The adhesion of ion plated W and W-Re coatings is described (Schintlmeister et al 1982).

The microstructure of flame sprayed alumina consists of a series of overlapping lamellae produced by the splat cooling of impinging droplets. Porosities <10% can be achieved, with good adhesion (McPherson 1980). Metastable gamma alumina is formed by flame spraying, not the expected stable alpha form. Flame sprayed bond-coat interlayers of NiCrAl alloy are shown to improve the adherence of $\text{SiO}_2\text{-Al}_2\text{O}_3$ coatings on Ni-Cr and Co-Cr alloys (Kliminda et al 1980). Adhesion tests of CoCrAl, CoCrAlY and CoCrAlHf coatings have been reported (Whittle & Boone 1981).

Angular iron grit blasting gives good adhesion of arc and flame sprayed coatings. A surface roughness factor is defined to relate topography to adhesion (Bardal 1973). Some coatings plasma sprayed with transferred arc onto surfaces not grit blasted, show better adhesion than those sprayed without transferred arc. Their adhesion is beyond the testing range of DIN 50 (as available adhesives do not have strengths exceeding 70 N/mm^2). D-gun coatings have stronger adhesion (Tucker 1981).

The adhesion of flame-sprayed Al coatings on mild steel (irregular interface) is very dependent on surface preparation. Grit type and condition are important but variations of blasting speed and nozzle-substrate distance had no effect. With chilled iron angular grit, adhesive failure was at the interface, but with alumina grit it was within the Al coating. Other grit blasting variables are described (Apps 1974). Plasma air sprayed coatings of Ni, Cr, Mo, Ta and W on Al and steel were found to have melted to form intermetallic intermediate layers which improved adhesion (Kitahara & Asui 1974).

Sheets of Nb and Al_2O_3 pressed together above 1200°C , exhibited a bonding fracture resistance increasing linearly with temperature, varying from 0 at 1300°C to $4 \text{ MN/m}^{0.5}$ at 2000°C at a bonding pressure 5 N/mm^2 for 1 hour (Elssner et al 1978). Presence of some C, O and N (with Nb_2N formation) had no effect.

7.8. INTERNAL STRESSES, STRAIN & FATIGUE LIFE

7.8.1. GENERAL:

Internal stress is an important parameter in coating technology since it often relates to the maximum coating thickness which can be deposited without spalling, irrespective of the coating being produced by PVD, CVD or thermal spraying. It is known that even mild grit blasting will cause serious damage on ZrO_2 coatings. Semi-molten debris contracts on freezing and spalls off the coating. Thermal barrier coatings fail due to cracking. The excellent erosion resistant property of Si_3N_4 is profitably made

use of in gas turbine technology (Godfrey 1983). However, more correlative studies are needed to explain how stresses generated and transmitted through coatings of various types and thicknesses may be controlled, and how coating production can form more uniform and stress-compensating structures. During a coating process, the reaction of the powder particles with their local environment in transit, particularly the extent of their oxidation, and, the stresses generated during coating and in the acting environment are very important in determining the properties of the coatings. Residual tensile stresses may be present in a substrate at a $1/6$ stress gradient against a 2.75 gradient in a TBC upon it, with the coating in compression at the interface (Herman & Shankar 1987; Marynowski et al 1965).

7.8.2. FILM THICKNESS EFFECT & ION-IMPACT STRESSES

Internal stresses present in the substrate and coating have to be taken into account in order to work out a predictable model for the behaviour of a coated component. Internal stresses in thin films may be generated during its formation due to the difference in thermal expansion coefficients between the deposit and substrate materials. Atomic interaction, particularly at the nucleation stage at the substrate/film interface is another source, the effect of which attenuates as the film thickens. Another source is from reflected energetic neutral particles such as neutralized argon ions reflected from the target to produce an atomic peening effect on the bombarded film surface (and substrate). If such particles are in high flux then distorted structures, high defect concentrations and abnormal compressive stress levels can be generated. A working mode for magnetron sputtered alumina has been presented (Roth et al 1987).

Ion bombardment during deposition increases stress by displacing atoms from their lowest energy arrangement, especially for refractory materials. Sputter deposition using planar diodes allows contact of the plasma with the coating. Consequent ion bombardment occurs and electron (100 to 1000 eV) bombardment from the cathode heats and cleans the substrate and causes radiation damage and nucleation sites (Thornton 1981). The relatively high pressure in planar diode sputtering units unfortunately slows down the fast sputtered atoms to near thermal equilibrium with the gas by the time they reach the substrate (Westwood 1976). Triode sputterers can cause Ar trapping in coatings. Magnetron sputterers are generally free of bombardment effects (Thornton 1981). Few measurements exist on how hardness, yield strength etc., are affected by ion bombardment of films during deposition.


Evaporated and deposited films have a tensile stress and sputtered films have a compressive stress, often near yield point. But stress deduced from X-ray lattice parameters may be misleading as intergranular forces are excluded (Mattox 1981). Beam deformation measurements are more meaningful. The stress is also partly a

thermal expansion coefficient mismatch and is mainly of this type for low m.p. materials. On reaching room temperature, mounds or depressions are created by compressive or tensile stresses (Thornton 1981). For sputtered films, higher pressure and temperature and additional sputtering from an oblique angle reduce the stress (Mattox 1981). But compressive stress may be beneficial by not allowing cracks to propagate. Thornton (1981) discusses the effects of working gas species and pressure, apparatus geometry and angle of incidence, on coating stress. Low pressure and angle promote smooth surfaces in compression; higher pressure and angles promote rough surfaces in tension. The compression to tension transition temperature increases with atomic mass ratio of coating to working gas. Effects of substrate bias on stress in sputtered coatings have been mentioned in Chapter 3. Residual stress increases linearly with coating thickness (Tucker 1974; Malik 1985). More studies are needed in which microstructure is related to mechanical properties.

7.8.3. STRESS MODELS:

A heat transfer model has been developed for plasma sprayed ZrO_2 and W coatings to predict effects of internal stress levels. Variation in residual stress distribution as a function of deposition rate and coating thickness was applied, but an extension is needed to include second-order factors such as microstructure, porosity and included oxides. A model is also formulated for sputter ion-coated W, where the dominant feature is the deposit microstructure influenced by the substrate bias voltage. Stresses are accommodated elastically at the substrate/deposit interface as the bias voltage increases and as the film thickens plastic flow occurs with increase in grain size (Rickerby et al 1987). Two new approaches are proposed to relate microstructure to surface stress and surface tension for solid vapour interfaces, considering them at thermal equilibrium. A finite crystal model with rigid planes illustrates that a modification of the bulk equation of state in a crystal slab of finite width can lead to such a difference, and a similar difference can be found between stress and potential density in a fluid in a periodic potential (Wolf et al 1985).

Amongst the in-service stress contributing factors, oxide inclusions play a prominent role. Oxidation results in a volume increase resulting in misfit strains which induce large hydrostatic stresses in the elastic medium around it. The effect of such hydrostatic stresses on diffusion kinetics, dislocation, fracture, pit formation, crack formation and propagation and finally coating failure is considered in another model (Louat & Sadananda 1987). Using oxidation and thermal expansion mismatch as parameters in another model based on an elastic environment has shown that ascribing total elasticity to a coating system, especially to TBC may lead to unrealistic values, incompatible to observed data (Chang et al 1987; Miller 1987). The ceramic is far less

elastic than the alloy bond coat which has different elasticity than the substrate. More work is clearly needed in this area. 

7.8.4. STRESS RELIEF MEASURES:

Plaster (1983) has given a detailed account of impact treatment which is often employed for stress relief or compensation. Its permutations giving more than 21000 types of impact treatment, are possible from the following variables: (i) Abrasives (unlimited choice in solids liquids and vapours) (ii) Pressures (iii) Distance (iv) Angle of impact (v) Material quality and size (unlimited). The scope of impact treatment ranges from the destructive to the decorative. It can be used to blast or carve out a surface. It can produce anti-friction surfaces or surfaces of precise roughness, and it can even erase selectively, misprints which occur during bulk-printing operations to facilitate positioned overprinting of corrected matter. Impact generates stress, which can be detrimental to coating or may be turned into an advantage.

The advantages and beneficial effects of controlled shot peening as a pre-treatment to metallurgical coatings are discussed (Eckersley & Kleppe 1987). Shot peening is also known as impact prestressing, precisely because it induces compressive stresses which compensate stresses generated during the coating process or during service of a coated component. The impact of a high speed pellet creates a dimple of diameter 'd' with a 1/10th depression. The substrate surface stretches and the depth of stretching is about 'd'. The unstretched cone then exerts a compressive force in attempting to restore the surface to its previous state. A treated component may have an imparted compressive stress about 60% of its yield strength. It is argued that since most of the catastrophic failures originate from surface tensile stresses or residual stresses, a pre-stressed compressive state should be an effective compensator, and should be present to extend below all discontinuities caused by surface preparation procedures. The choice of shot for peening is directly related to the material to be treated. To generate a high residual compressive stress the material must be 'shot' with a medium as hard as itself. For high strength steel a hard shot is used; for non-ferrous metals glass, ceramic or stainless steel are used; thin sections are peened with light shots. The critical factors are that material distortion or deep damaging are avoided.

The several areas in a coating process where impact prestressing is beneficial are:

(i) Before grit blasting to offset stress risers created by angular grit. Trailing edges of jet engine blades tend to erode-corrode and/or distort if left untreated.

(ii) To offset negative side-effects of electrodeposited coatings

of Cr, Ni etc. Plated Cr and Ni are brittle and hard and are not only susceptible to crack under load but can also reduce the substrate fatigue strength by almost 50%. Flame deposited coatings do not induce residual tensile stresses like plated Cr and Ni but are brittle and easily generate cracks which continue to propagate into the substrate. Impact prestressing of substrate can offset this condition. High speed steels, titanium and aluminium alloys are shot peened.

(iii) Shot peening is done on coatings when they are to be used under stress-generating conditions, e.g. aircraft landing gears, steam turbine blades etc. Plasma sprayed coatings are consolidated by shot peening, as are silver plated ball-bearings.

7.8.5. STRAIN & FATIGUE

Most metallic coatings have strain-to-failure of less than 1%. D-gun coatings have a higher modulus of rupture than comparable plasma coatings. Some coatings, particularly D-gun coatings are so well bonded that a crack generated in the coating may propagate into the substrate under cyclic stress. The magnitude of the residual stress due to rapid cooling is a function of torch (or gun) parameters, deposition rate, the relative torch to substrate surface speed, the thermal properties of both the coating and substrate and the amount of auxiliary cooling used. Coatings are normally under tension as a result of the residual stress, and this stress must be subtracted from the allowable fracture stress calculated from mechanical property tests of free standing specimens.

Strain and fatigue life results are discussed by Nicoll (1983). The effect of coatings on fatigue life varies (Bartocci 1967; Wells & Sullivan 1968). Some results are shown in Table 7:5. Studies show that if the strain-to-failure of a coating is not exceeded, then the coating will not affect the substrate fatigue strength, e.g. the roots of mid-span stiffeners on gas turbine compressor blades must not be coated, due to extreme fatigue sensitivity, and masking is used. Further research is needed to predict the effect of a specific coating on a given substrate (Tucker 1981). The longitudinal residual strain of 0.4 mm partially stabilized ZrO_2 on a 3 mm thick Al-alloy sheet with a 0.1 mm bond coat of Ni18Cr6Al, was markedly affected by the substrate temperature in a diesel engine combustion chamber; the higher the temperature the greater was the residual compressive strain. The temperature gradient across the coating was not significantly affected by surface cooling. The bond coat had no significant effect on the residual stress in the ceramic but it reduced the stress discontinuity at the substrate interface (Hobbs & Reiter 1988).

Grit blasting prior to coating affects fatigue strength. Coating thickness does not usually affect fatigue strength. Stainless

COATINGS: PHYSICAL & MECHANICAL PROPERTIES

TABLE 7:5

STRAIN FATIGUE LIFE		
Substrate	Coating	Effect
1 Fe alloys	Al, CrAl, PtCrAl	Only very high strain fatigue life is reduced in air at 750°C; cycles to failure reduced 50% at 25°C. Falls as coating thickness increases.
2 Ni alloys	AlPt, Al, CrAl, SiAl CrAl/Pt, NiCoCrAlY	Same as uncoated (900°C, 1500 cycles)
3 IN738	as in 2	as in 2
4 IN738LC	as in 1	as in 1
5 IN738LC	LDC2 (PtAl)	Allows double uncoated stress for a given life for precorroded specimens
6 Nb alloy sheet 20 mil thick	V-(80Cr20Ti)-Si	50% reduction at room temp.
7 Nb alloy XB88	(35W35Mo15Ti.15V)Si	Good at 1000°C
8 FX414	Al, CrAl, NiCoCrAlY	
9 ?	Ni20Cr	Better than uncoated at 900°C
10 ?	Ni20Cr10Al2Hf.1C	Slightly worse than uncoated substrate at medium stress but 100 times worse at high stress

steel coatings decrease the fatigue strength of low alloy steels and Al-alloys (Malik 1973). Al on stainless steel increases its hot fatigue strength (Drewett 1969); a sprayed Al coat reduces its creep resistance while a hot dipped coat increases it.

Both plasma and D-gun coatings consist of many layers of thin lenticular particles but the latter have a higher density and modulus of rupture. The cooling rate may vary significantly with the substrate material and thickness of the coating. As a result of rapid cooling, some coatings have been found to have no crystallographic structure when examined by X-ray or neutron diffraction. Others may have a thin amorphous layer next to the substrate followed by crystalline layers. Many coatings form columnar grains within the splat in one or two layers perpendicular to the surface substrate. High local residual stresses due to the rapid quenching can occur and also non-equilibrium phases may

be present. Both types of coatings have a strain-to-failure $<1\%$. Non-metallic coatings are worse, e.g. a Cr_2O_3 coating on a hydraulic Al cylinder cracked due to the cylinder expanding under pressure. A substrate must be able to support a coating without yielding beyond the coating's strain-to-failure, e.g. a D-gun WC-Co coating gave ten times longer life to steel mill acid line roller guides, but spalling occasionally occurred due to the substrate yielding under impact from steel sheets. The problem was solved by raising the substrate hardness to 55R_C (Tucker 1981).

CVD SiO_2 films are in compressive stress at 1000°C , decreasing with temperature. Silicon oxynitride films from 600 to 8000 A.U. thick are in tensile stress, independent of film thickness and deposition rate (Gaird & Hearn 1978), but parabolic with the nitrogen content. NiCrAlY+Pt coated superalloys are reported to have longer rupture lives and lower creep rates than the substrate material viz. $\text{Ni}_{20}\text{Nb}_6\text{Cr}_{2.5}\text{Al}$ (Strangman et al 1977). Nitrogen embrittlement occurs in hot gas atmospheres, of Al and Al-Cr coatings on nickel superalloys (Schmitt-Thomas et al 1981). Cracking occurs at the interface.

Hydrogen embrittlement of electroplated Ni and Co cermet coatings containing carbides of W, Ti or Cr, was measured by bending a specimen around a fulcrum at a controlled rate. The angle at which it breaks is compared with that for known specimens. Heat treatment at 200°C (3hr) or 300°C (1hr) gave full restoration of the fracture angle. Fatigue strength reduction at 1 million cycles is typically 60% for Cr electroplated steel and is only about 35% for $\text{Co}+\text{Cr}_3\text{C}_2$ cermet electroplate. The stress behaviour of W and W-Re ion plated coatings is described (Schintlmeister 1982). Internal stresses can be measured by a spiral contraction meter (Fry & Morris 1959). A value of 117 MN/m^2 tensile was found for optimum plating conditions which is better than for pure Ni electroplate and shows the stress reduction due to included particles (Kedward et al 1976). More work is needed on ways to stop crack propagation, e.g. by incorporating suitable spherical particles which will arrest cracks which reach them.

Stress levels induced by various surface hardening processes are shown in Fig.7-5. Bars A-G which includes CVD and conventional hardening treatments register lower stress levels than plasma nitriding and vacuum carburizing processes.

7.9. STRENGTH

Strength of hybrid type coated materials present a complex situation at high temperature. Ceramics are of particular interest in this context. They are notch sensitive and have poor impact resistance, have low fracture toughness, but are very resistant to high temperature erosion and corrosion. Duplex ceramic materials are a developing technology and much of their high temperature data as applied to coatings are obscure.

Surface Hardening Process Effects

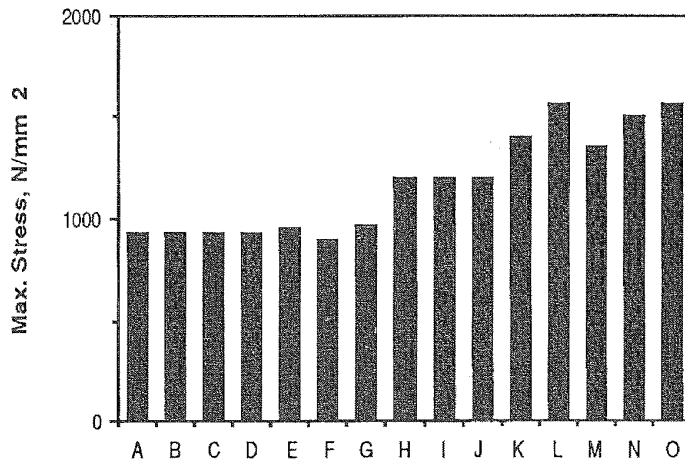


Fig.7-5

Legend	Substrate steel	Surface Hardening
A	Cr-Mo, 722-M24}	VC Layer, TD process
B	H13 }	
C	M2 }	
D	As in A }	Hardened & Tempered
E	As in B }	
F	As in C }	
G	M2	CVD
H	As in A }	Gas or salt-nitrided
I	As in B }	
J	As in C }	
K	As in A }	Plasma nitrided
L	As in B }	
M	As in C }	
N	As in B }	Vacuum-Carburisation
O	As in C }	

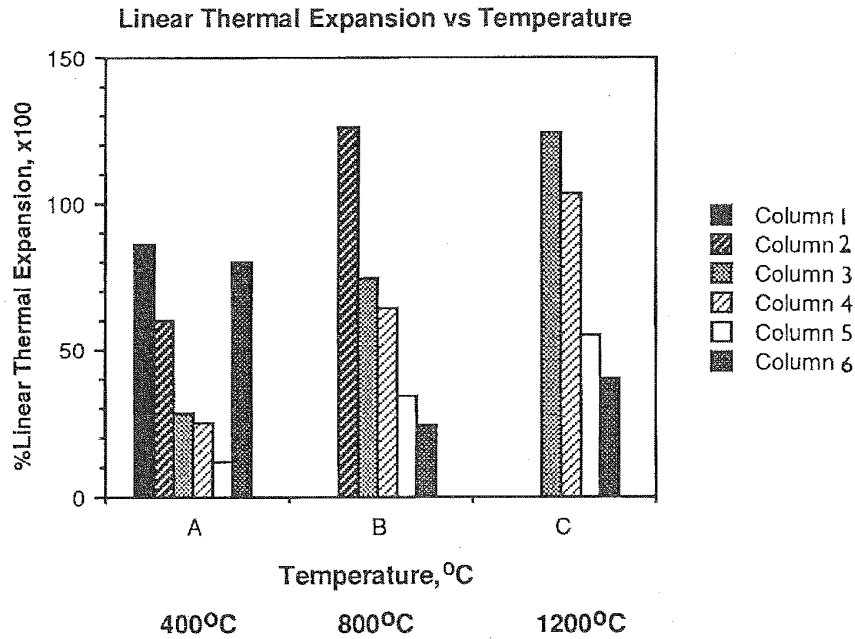


Fig.7-6: Thermal Expansion Characteristics of Al-Alloys, Superalloys & Ceramics

Column	Material	Column	Material
1	Al-Alloys	4	Al ₂ O ₃
2	Superalloys	5	SiC
3	Stabilized ZrO ₂	6	Si ₃ N ₄

Fig.7-6 to 7-8 compare ceramics, superalloys and carbon-carbon composites. (Richerson 1982; Buckley 1988; Hancock 1987). In general, strength at high temperatures can drop to almost half that at ambient conditions. Oxide ceramics, e.g. ZrO₂, HfO₂, Y₂O₃ and ThO₂ are protective carbon-carbon composite at >2000°C but are not strong, while the stronger SiC, Si₃N₄, and HfB₂ can be used around 1800°C, the latter with SiC for short times (Strife & Sheehan 1988). Table 7:6 indicates the effect of aluminide and silicide coatings on substrate strength.

Tensile and creep rupture testing data is relevant in the 0.1 to 1% extension range. Problems of extension measurement are overcome using television systems. PVD Cr by electron beam evaporation was used to produce 1 mm thick Cr films. A submicron columnar grain structure was produced over a wide range of deposition parameters. Brittle intergranular fractures occurred in tests at 25°C to 1000°C, related to intergranular defects reflected in density measurements and linearly dependent on the dissolved oxygen concentration (Anon.1983). Sputtered metal films show a sharp intrinsic stress reversal at low gas pressures, useful for diagnosis of coating quality (Hoffman 1982). Young's modulus

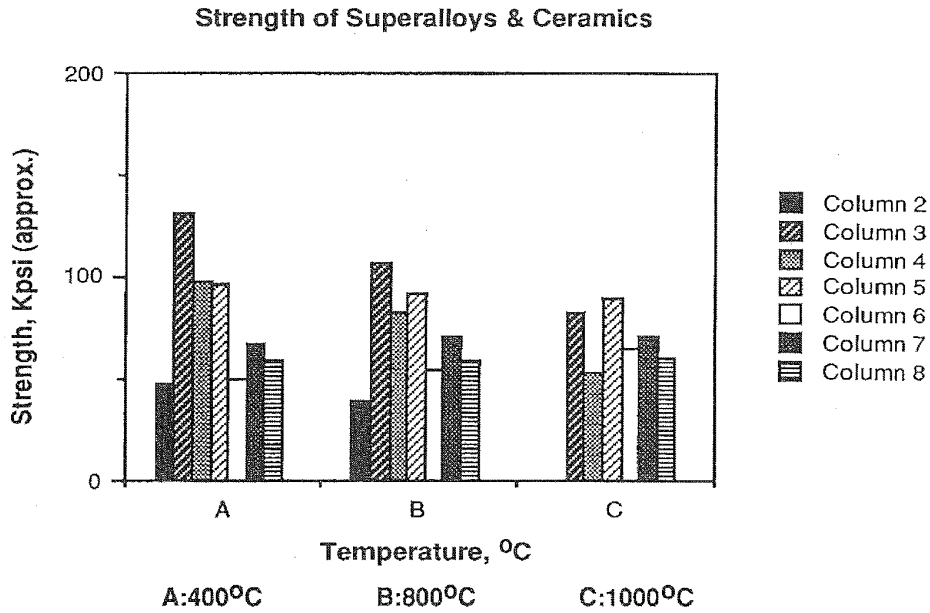


Fig.7-7: Comparison of Superalloy Strength with Ceramics

Column	Material	Column	Material
2	Cast X-40	5	Hot Pressed Si_3N_4
3	Cast IN 100	6	Reaction Bonded Si_3N_4
4	IN 713LC	7	Sintered SiC
		8	Reaction Sintered SiC

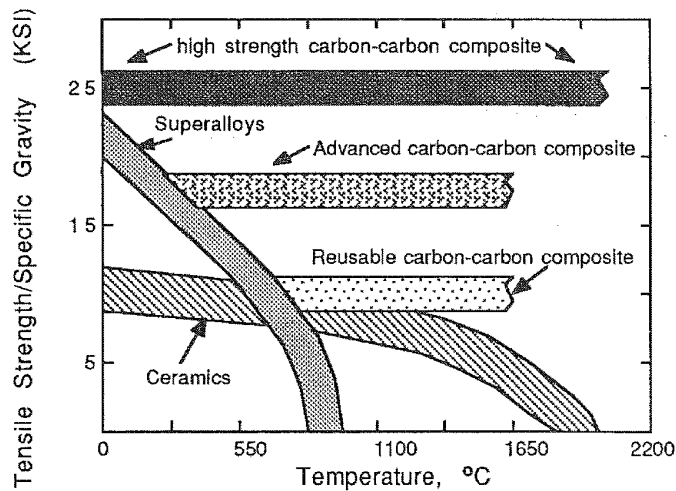


Fig.7-8: Comparative Data (approx.) on High Temperature Strength of Superalloys, Ceramics & Composites

(Buckley 1988)

COATINGS: PHYSICAL & MECHANICAL PROPERTIES

measurements carried out on TiN, TiC, ZrN and HfN by plasma reactive sputtering on type 316 stainless steel substrates showed that porosity lowered the values; TiN was the best with 640 GPa and HfN the lowest at 380 GPa (Torok et al 1987).

TABLE 7:6
EFFECT OF COATINGS ON TENSILE STRENGTH

Substrate	Coating	Effect
Steel	Al	slight decrease
Hastelloy-X	TiSi (CVD)	slight decrease (100-1000°C)
FX414	Al, CrAl NiCoCrAlY	no effect
IN738	Al, CrAl, SiAl	no effect
IN738	CrAl/Pt NiCoCrAlY	no effect
IN738LC	Al, CrAl, SiAl PtCrAl, NiCoCrAlY	slight decrease (20-900°C)
NiNbCrAl (directional solidification)	NiCrAlY/Pt top	increase
Nb alloys	CrTiSi	good to 1200°C
Nb alloys	Ti & TiV	decrease
Nb alloys	Nb15Ti10Ta10W2Hf3Al	decrease
Nb alloys	Nb5W30Hf5Ti3Re	decrease
Nb alloy sheet 20 mm thick	V-(80Cr20Ti)-Si	decreased 25 % at 25 & 1200°C
Tal0W	Sn23Al5Mo	no effect 5 hr at 1440°C

Coatings do not necessarily impair the substrate strength; CVD Ti-Si coatings on Hastelloy X and various coatings on IN738LC belong to this group. But if the cooling in the coating process is too slow the impact strength is reduced, e.g. by allowing carbide precipitation at grain boundaries (Nicol 1983). The strength of FSX414 (Co alloy) up to 1000°C is hardly affected by pack Al, CrAl, and SiAl coatings, but coated IN738LC (Ni alloy) was weaker at 700°C (Strang 1979). Creep rupture and high strain fatigue properties of these superalloys were hardly changed by

COATINGS: PHYSICAL & MECHANICAL PROPERTIES

coating. Metallography showed little interaction between coatings and FSX414 cobalt superalloy, but a needle precipitate (probably sigma phase) extended below the coating into the IN738LC substrate (except for NiCoCrAlY coatings).

CVD W from a WF_6+H_2 reaction mixture has higher yield strength if deposited at $500^\circ C$ (83 MPa) than at $700^\circ C$ (62 MPa), due to a finer grain structure. Further refinement of grain structure and higher strength is obtained by co-deposition of a material which causes re-nucleation, e.g. Re (Blocher 1974; Shim & Byrne 1972; Holman & Huegel 1967). The most effective grain refinement is caused by brushing the surface with a W brush during deposition (Holman & Huegel 1967, 1974; Huegel & Holman 1971), which creates defects by local cold working and momentarily obliterates the gaseous boundary layer through which the reactants must diffuse (thus increasing the local supersaturation. Both effects aid re-nucleation. Similar grain refining occurs during CVD in a fluidized bed of W seed particles; these grow spherically (Blocher 1974) but hot isostatic pressing and rolling gives fine grained sheet (Oxley et al 1965a). Hence a Ta corrosion resistant coating thickness can be reduced by a factor of ten (Oxley et al 1965b).

Fluoride and chloride produced CVD W had equal tensile strengths at $1540^\circ C$ and $1700^\circ C$. Below this, chloride CVD W had lower yield strength but higher ultimate strength. The grain size of fluoride CVD W hardly changed during 5000 hours at $1700^\circ C$, but chloride CVD W showed poor grain growth resistance and an accompanying high DBTT (Bryant 1974). CVD pyrolytic graphite has a $25^\circ C$ flexural strength of 145 MPa which rises to 159 MPa for finer grained material (Blocher 1974).

Rupture strength reduction, e.g. in strong Ni-base alloys, is due to incompatibility between coating heat treatment and those needed to develop optimum mechanical properties in the metal. The coating heat treatment must be adjusted or post-coating heat treatments must be done. Of course, coatings can increase rupture life in corrosive conditions by preventing the reduction of substrate cross section which would occur with no coating.

Strang, Lang and Pichoir (1982) give a general review of alumina coatings degradation effects on substrate creep and strength properties, ductility and fatigue. Coatings of $NiSi_2$, $CrSi_2$ and $NiCrSi$ on Fe, IN100, IN738, Nim90 and IN601, show inward Si diffusion and interlayer reaction and causing strength loss. Specimens with Al in the interlayer had 50% strength loss while those with Cr had 10%. Heat treatment is beneficial (Fitzer et al 1979).

Fine grained fibrous Ni electroplate deposited at the high rate of 30 microns/minute with fast solution flow, using $150 A/dm^2$, had a very high tensile strength of $130 kg/mm^2$ (190 kpsi) (Safranek & Layer 1973). Fine grained electrodeposited Al is 2.4 times stronger than the annealed, rolled metal. Strong electroplated Cr is 6.7 times stronger than the annealed metallurgical

counterpart (Safranek 1974). Strong Co electroplate is 4.7 times stronger than annealed wrought Co. This is due to fine grain sizes. Recrystallisation on heating reduces tensile strength to the normal values. Burnishing (rubbing during electrodeposition) improves mechanical properties (Stoltz et al 1974). The strength of electrodeposited Al and the effect of annealing has been studied (Addison et al 1972). Heat treatment caused severe embrittlement and porosity development due to gas evolution. H embrittlement and fatigue are discussed by Kedward and Wright (1978) for chromium carbide/Co cermet electrodeposits. A reduction in fatigue properties of fatigue sensitive substrates is usual when electroplated. Tensile stress also exists in platings, e.g. Fe, Ni, Co and their binary and ternary alloys.

ZrO₂ coatings on steel substrates have been tested for strength and fracture toughness using four-point bending and double cantilever beam techniques respectively. Strength values of 14.6 - 53 MPa and modulus 20 - 47 kPa were obtained for 0.375 cm thick ZrO₂-20%Y₂O₃ coatings on steel. Predicted values based on a model developed taking into account powder particle heating and its acceleration, as well as substrate residual stress and thermal shock agreed to within 72-88% of the measured data (Eaton & Novak 1986). ZrO₂ with 6 and 20 wt.% Y₂O₃ or 10 and 15 wt.% CeO₂ showed a greater toughness to cohesive fracture than adhesive fracture. For ZrO₂-CeO₂, the tetragonal structures coatings were tougher than fully stabilized coatings; for 10wt.% CeO₂ addition toughness varied from monoclinic > transformable tetragonal > non-transformable tetragonal; for 15 wt.% CeO₂ both tetragonal types > monoclinic > cubic; for 6 wt.% Y₂O₃ non-transformable tetragonal >> cubic > monoclinic; the highest strength level was registered for the 20 wt.% yttria ceramic (Heintze & McPherson 1988).

7.10. DUCTILITY, CREEP

The Ductile Brittle Transition Temperature (DBTT) is the lowest temperature at which a ductile 90° bend can be formed on a specified radius. If the as-coated alloy has 90° bend ductility at room temperature, bend tests done after oxidation exposure will quickly reveal ductility loss due to interdiffusion, entry of atmosphere contaminants and other effects not readily detected by visual inspection. Specifications for such bend tests are available (Natl.Acad.Sci. 1970) and are widely accepted. It is suggested that pile-up and work hardening theories include the inner grain structure in cases where alloys are hardened by a second phase. The grain boundary properties and structure are influenced by impurities or particle inclusions. Ultra-fine grain inclusions are found to provide ductility to high strength materials if surface preparation eliminates micro-cracks. In steady state creep calculations of complex alloys, introducing grain size influence (Hall-Petch stress) as one of the internal stress parameters provides rationalization in relating optimal grain

COATINGS: PHYSICAL & MECHANICAL PROPERTIES

size to maximising creep resistance. Controlling the grain boundary structure and grain size can lower crack growth rates, their initiation and propagation (Lasalmonie & Strudel 1986).

Sputtered coatings deposited at low substrate temperatures have many structural defects, while those deposited at high temperatures approach bulk properties. Simple metals with structures at the zone 1/zone 2 border (Fig.7-2; p.301) have high strength and hardness but little ductility. Dense zone 1 coatings have similar hardness but little lateral strength (Thornton 1981). In zones 2 and 3 the grain sizes increase with T/T_m and the strength and hardness fall towards bulk annealed values and ductility rises. In contrast ceramics deposited at low T/T_m have low hardness but approach bulk values at high T/T_m . Alloys have smaller grains and better phase dispersion than conventionally produced alloys (Westwood 1984), perhaps giving better corrosion resistance.

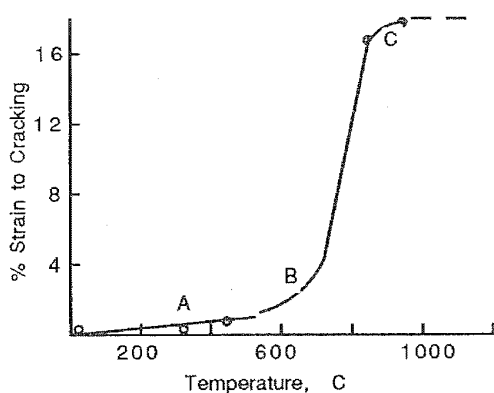
Electron-beam-evaporated Ni films vacuum deposited at < 0.3 times the melting point has uniform columnar half micron grains and is free of defects. It has the same hardness and yield strength as conventional Ni sheet and better creep ductility. Films condensed at 0-35 times the melting point had larger 2 to 3 micron grains. Hardness and yield strength were slightly lower but creep properties were erratic due to abnormal grain growth. Codeposition of alumina with Ni gave an equiaxed homogenous film with 0.3 micron grains, fully dense. Strengthening effects were observed with good hardness and hot creep resistance (Jacobson 1981). Alumina was on grain boundaries below 0.4 vol.%. Ni+ZrO₂ films were also studied.

Hardness, strength, ductility, creep and thermal conductivity can be controlled by microlaminar layers formed by alternate condensation from electron beam heated evaporation sources, e.g. Fe/Cu, Cr/Cu and Cu/Ni coatings from 0.1 to 300 microns. But Ni/Cu microlaminates are structurally unstable due to interdiffusion, forming a homogeneous solid solution. Microlaminates containing Cr can have twice the hardness and strength of pure Cr and also high ductility (pure Cr has no ductility). Superplasticity occurs for Fe/Cu microlaminates of 0.5 microns thickness, due to formation of islands of Fe in a Cu matrix. The steady state creep in Fe/Cu decreases sharply when the layer thickness equals the grain size (30 microns). Thermal conductivity is much reduced (below that of either component) for microlaminate layers, (see section on hardness) and these give possible thermal barrier coatings which have ductility, unlike ceramics (Movchan & Bunshah 1982).

Coatings can vary from brittle (MCrAlY, Al>12%) to relatively ductile (MCrAlY, Al<8%) and exhibit a range of DBTT. Reducing the Al and Cr contents reduces the hot corrosion resistance while increasing the ductility, and a compromise can be reached with overlay coatings (Nicoll 1983). Brittle coatings withstand cyclic engine conditions if the lower temperature is above the DBTT of the coating. The low-Al beta-NiAl phase can accommodate about 1%

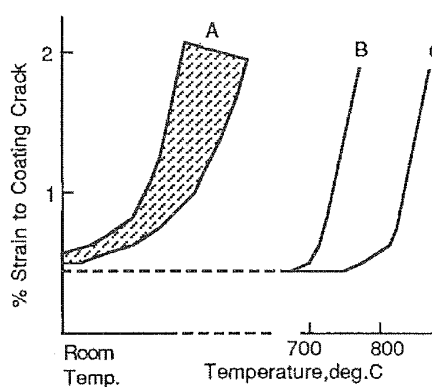
COATINGS: PHYSICAL & MECHANICAL PROPERTIES

tensile strain at 650°C with deviation from ductility occurring at 540°C; for high-Al beta-NiAl, the DBTT is about 815°C. The DBTT of MCrAlY overlays however, is from 350°C to 500°C and so these coatings can withstand a wider range of cyclic temperatures (Wing & McGill 1981). The 'strain to fracture' test gives the ductile-to-brittle transition temperature (DBTT) by observing the coated surface by telescope during a hot tensile test and measuring the strain at which the coating spalls or cracks. Plotting these values against temperature gives the DBTT; Fig.7-9 shows data on CVD SiB₂ coated on superalloy IN 738LC and Fig.7-10 compares the DBTT of overlay coatings and diffusion aluminide coatings. Some superalloy creep and fatigue test results are reviewed by Nicoll (1983).



A: Elastic substrate, Coating delaminates;
 B: Substrate begins to become plastic;
 C: Substrate failure, Coating stays plastic

Fig.7-9: SiB₂ Deposited by CVD on IN 738LC Superalloy Effect of Temperature on Strain to cracking



A: Ductile Overlay; B,C: Aluminide
 B-Low Al, Diffusion Coating
 C-High Al, As Coated

Fig.7-10: Trend in DBTT of Ductile Overlay & Aluminide Coatings

A low DBTT is desirable (see Table 7:7). Adding Ti to an Si coating on IN738 increases the DBTT from between 450- 700°C to 850-1000°C. For Si-base coatings on IN-738LC, Nimonic 105 and IN-939, the DBTT rises with strain rate and with grain size. Presence of small particles lowers the DBTT. N embrittles Cr, H embrittles steels and Cu, and O embrittles Cu and W. It is desirable to reduce brittleness inducers such as Si and Al (Nicoll et al 1979). Decreasing the coating thickness can lower the DBTT. Cr has a DBTT just above room temperature, but N contamination unfortunately increases this to over 600°C. Coatings offer protection from this effect. Noble metal coatings have very low N solubility. Aluminides containing Fe and Ti and silicide coatings have also been evaluated (Natl.Acad.Sci.1970). Pt aluminides are less ductile than MCrAlY overlays and further development is

COATINGS: PHYSICAL & MECHANICAL PROPERTIES

needed to improve this aspect (Wing & McGill 1981). The resistance to embrittlement during air oxidation of Cr-base alloys can be measured by the DBTT. Plasma sprayed Cr+10vol.% yttria was an effective coating. Other coatings studied were Li-doped yttria-stabilized chromia (Clark 1971).

Sol-gel ceria and CVD ceria and silica coatings on 20Cr25Ni-Nb stainless steel were oxidised with a load of half that calculated to rupture after 10000 hours at 825°C, in CO₂. The creep rate of the CVD silica coated steel was lowest and of sol-gel ceria was highest. This was consistent with theories of the oxidation-induced creep of the stainless steel; the ceria stopped oxide exfoliation and as the oxide is in compression it aided creep of the coated steel. Uncoated steel exfoliates its oxide, reducing its creep. CVD silica coated steel suffered almost no oxidation and hence had good creep properties (Bennett 1983).

Microhardness measurements show that arc-sprayed Ti coatings become hard and inductile if reactive gases are not excluded. But absence of oxygen forms droplets which do not easily wet the substrate, as oxygen (liquid oxide) reduces surface tension. So controlled amounts of O₂ are added. A thick-walled Cu tube arc spray coated with Nb can be reduced by drawing by about 20% without any coating damage or loss (Muller 1973). The high cooling rate of arc-sprayed Ti gives some metastable beta Ti in stable alpha Ti. Nitrogen causes a decrease in beta Ti, an increase in internal stress, solution expansion of the mixed crystal, a hardness increase and ductility and adhesion decrease (Steffens & Muller 1974). Spraying in pure Ar is essential. The ductility of D-gun and plasma coatings is limited. Even metallic coatings show a strain-to-fracture of <1% (Tucker 1974).

Structure and property relationships for electrodeposited coatings are discussed by Safranek (1974) and others (Sadak & Sauter 1974; Chen et al 1974; Stoltz et al 1974). As with sputtered coatings, fine grained coatings have much better strength etc., than columnar structures (which can be avoided by correct plating conditions). Proprietary brighteners give a banded or lamellar coating, also promoted by periodic current reversal. Cracking of highly stressed deposits often show a banded structure (Safranek 1974).

The effect of coatings on creep rate is shown in Table 7:8.

COATINGS: PHYSICAL & MECHANICAL PROPERTIES

TABLE 7:7

DUCTILE-BRITTLE TRANSITION TEMPERATURE

Substrate	Coating	Effect
Ni alloys	NiAl, AlCr/Ta	DBTT is 700°C for low Al and 800°C for high Al
Cr5W.1Y	NiCr	Ln & Y reduce DBTT.
Cr5W.1Y	NiCrW	N increases it
Cr5W.1Y	Pt, Pd, Al	N increases DBTT
Cr5W.1Y	Cr ₅ Al ₈ (FeCr) _x Al _y	increases from 250° to 420°C
Cr5W.1Y	NiCr, NiCrW Ni ₃₀ Cr, Ni ₃₀ Cr ₂₀ W	After 100 hr at 1150°C the DBTT was 540°C.
	same + 4 Al same + barrier layers of: W, W1%ThO ₂ , W25Re, & W	After 1260°C it was 870°C
IN 738LC	Si base coatings	25 to 1000°C Increases with strain rate Increases with grain size Decreases if small particles are present
IN 738	Si	DBTT is 500°C
IN 738	NiCrAlY/ZrO ₂	DBTT is 700°C for NiCrAlY, no DBTT for ZrO ₂
Nim 105	Si base coatings	25 to 1000°C Increases with strain rate Increases with grain size Decreases if small particles are present
Nim 105	Si	DBTT is 400°C
Superalloy	Co15Cr10AlY	DBTT is 250°C
Superalloy	Co22Cr12AlY	DBTT is 750°C

=====
Note: A low DBTT is desirable, to prevent coating cracking on passing through this temperature.

The NiAl phase is brittle at 25°C, and like all b.c.c. structures it has a brittle-ductile transition at around 720°C (or more, depending on Al content - NiAl has a wide stoichiometry range). Gas turbine temperatures are above this, but transients can cause cracking. More ductile coatings are needed. High Al "NiAl" coats are fine grained, precipitation strengthened and more resistant to thermal fatigue. After some use, outward diffusion of Ni leads to a pure NiAl phase with a weak columnar structure. Re prevents the ductile-brittle transition.

Table 7:8

EFFECT OF COATINGS ON CREEP RATE

Substrate	Coating	Effect
1a steel	CeO ₂ (sol gel)	Reduces creep
1b steel	SiO ₂ (CVD)	Increases creep
1c steel	hot dip Al	Reduces creep
1d steel	sprayed Al	Increases creep
2 Ni superalloy	AlPt	Pack aluminising heating irreversibly increases creep
3 IN738LC	Al, CrAl, SiAl PtCrAl, NiCoCrAlY	No change at 750° & 850°C
4 FSX414	as in 3	as in 3
5a Nb alloys	Nb15Ti10Ta10W2Hf3Al	Reduces creep
5b Nb alloys	Nb5W30Hf5Ti3Re	Reduces Creep
5c Nb alloys	CrTiSi	Good at 1200°C

=====
Note: The effect of coatings on creep rate is generally small. The creep rate in SO₂ and in melts is decreased by a coating.
 =====

7.11. HARDNESS vs WEAR & EROSION RESISTANCE

7.11.1. BASIC ASPECTS

Hard materials may be categorized broadly into three classes based on the types of chemical bonding prevalent, viz. metallic, covalent and ionic. Transition metal borides, carbides and nitrides, e.g. TiC, VC, WC, TiB₂, TiN, are predominantly metallic in character; borides, carbides and nitrides of Al, Si and B are covalent; oxides of Al, Be, Ti and Zr are ionic. At a glance, all are in a broad group as ceramics, but a simple bonding model does not define these materials, nor is there a sharp division. The transition metal ceramics - borides, carbides and nitrides, considered to be some of the hardest and most chemically inert materials known, are ascribed with a complex bonding structure combining covalent, metallic and ionic bonding (Sundgren et al 1986b). All the compounds are distinctive with high hardness and high melting points, but they differ in other physical properties. The linear thermal expansion coefficient decreases in general from ionic to metallic to covalent hard materials. The first have the lowest modulus of elasticity. Tables 7:9 and 7:10 give a general trend in properties as applied to coated materials (Holleck 1986).

COATINGS: PHYSICAL & MECHANICAL PROPERTIES

TABLE 7:9

TREND IN PHYSICO-CHEMICAL & PHYSICO-MECHANICAL PROPERTIES OF HARD COATING MATERIALS

Decreasing Tendency in Property	Trend in Chemical Bonding
Melting Point	Metallic -> Covalent -> Ionic
Stability	Ionic -> Metallic -> Covalent
Thermal Expansion Coeff.	Ionic -> Metallic -> Covalent
Hardness	Covalent -> Metallic -> Ionic
Brittleness (Toughness)	Ionic -> Covalent -> Metallic
Interaction tendency Adherence to Metallic Substrates	Metallic -> Covalent -> Ionic
Multi-Layer Compatibility	Metallic -> Ionic -> Covalent

TABLE 7:10

TREND IN PHYSICO-CHEMICAL & PHYSICO-MECHANICAL PROPERTIES OF BORIDES, CARBIDES & NITRIDES

Decreasing Tendency in property	Trend in the Ceramics
Melting Point	Carbides -> Borides -> Nitrides
Stability	Nitrides -> Carbides -> Borides
Thermal Expansion Coeff.	Nitrides -> Carbides -> Borides
Hardness	Borides -> Carbides -> Nitrides
Brittleness (Toughness)	Nitrides -> Carbides -> Borides
Interaction Tendency Adherence to Metallic Substrates	Borides -> Carbides -> Nitrides
	Borides -> Carbides -> Nitrides

Factors which fix coated material properties are three-fold:

- (i) Fabrication parameters - temperature of the substrate and the process, reactant-product interaction, and stresses created by thermal, ionic, particle and process impacts;
- (ii) The Constitution of - the Substrate, Coating and the Substrate/Coating system,
- (iii) Microstructure - grain size, grain orientation, grain boundaries; density (porosity)

COATINGS: PHYSICAL & MECHANICAL PROPERTIES

Optimization of the properties of hard materials must then examine the fundamental relationships in the context of the high temperature regimes which are encountered in practice, on the following basis:

1. Bonding characteristics of the specific materials
2. Stoichiometry
3. Phase relationships and transformations
4. Anisotropy
5. Specific properties of miscibility - solid solution or inter-metallics formation etc., within the coating candidate hard materials as well as the substrate.

Further criteria of hard material selection then depends on the interaction of its surface as a hard coating with the environment and the workpiece (if it is a tool finish), its own hardness, fatigue strength, fracture toughness and ability to accommodate stress, its adherence and interaction, if any, with the substrate and thermal expansion mismatch. Problems arise because good adherence at the substrate/layer interface cannot rule out surface interactions, and high hardness varies inversely with high toughness. Necessity for increasing hardness and strength means acceptance of decreasing toughness and adherence (Holleck 1986).

Tribological coatings have excited considerable interest in nuclear and other energy areas apart from the traditional machine tool industry because of their relative inertness to chemical reactions, lower thermal conductivity, resistance to erosion and ability to accommodate friction. The resistance they provide in nuclear applications to static adhesion, galling in vacuum environment, wear (wear scars can induce stresses), friction in the absence of conventional lubricants, static adhesion (of metallic surfaces in static contact) and chemical resistance has been reviewed (Lewis 1987). The general conclusion for hard coatings is that metallic hard materials appear to be very suitable and versatile except for their chemical response to environment, ionic hard materials are particularly suitable as surface finishes because of their high stability and low interaction tendency, but to get the best out of the coating/substrate system with an optimum wear resistance, only multiphase and multilayer coatings may be envisaged (Gurland 1988; Quinto 1988; Grunling et al 1987; Lewis 1987; Holleck 1986; Hillery 1986; Sundgren et al 1986; Sundgren & Hentzell 1986). Data processing for wear optimization has been enabled for more than 30 coating and surface treatment processes (Syan et al 1987; Kramer & Judd 1985).

7.11.2. HARDNESS & WEAR

Hardness of a material provides a measure of its ability to resist plastic deformation, and fracture toughness is a measure of its resistance to crack propagation and fracture. Coatings for tool materials have to be dominantly hard in order to function as

COATINGS: PHYSICAL & MECHANICAL PROPERTIES

a tool without suffering undue deformation, but they also have to be sufficiently tough to withstand bending loads imposed by cutting forces, and to sustain shocks generated by interrupted cuts at high speeds and feed rates. With a compromise between hardness and fracture strength achieved, the service life is decided by the progressive wear and erosion. Hard coatings for other high temperature applications have to normalize their hardness and toughness with respect to the thickness required and the response of their thermal characteristics to environment and load.

The several forms of wear are (Gurland 1988; Hillery 1986; Child 1983):

(i) Adhesive wear (galling, scuffing, seizing) - which occurs particularly severely between mutually soluble pairs while in sliding contact, and often occurs in inert environments where even thin oxide films are absent to separate sliding components; and this could lead to micro-welding. As such welded areas formed at asperities (high points) shear and get plucked out during repeated sliding from the weaker (softer) surface, severely roughened surfaces result.

(ii) Abrasive wear which results from circular or linear sliding motions, normally with an acting load, of hard particles, cutting, impacting or ploughing into surfaces which are less hard;

(iii) Fretting wear characterized by low-amplitude loads and/or motion causing localized pitting (erosion); wear due to subsurface fatigue cracks is called delamination wear (Child 1983).

(iv) Corrosive wear which occurs as products from corrosion contribute to chemical and mechanical interaction to any of the three types given above, and,

(v) Diffusional wear which develops at high temperatures by selective constituent diffusion resulting in weakening areas and crater formation.

When the coating thickness is small compared with that of the substrate, its deformation will first follow that of the base material. At high temperatures interdiffusion, ageing and cyclic parameters and other factors interfere. Creep deformation is determined by the load and it is a volume effect, and fatigue causes locally concentrated damage (Grunling et al 1987). Under mild abrasive wear thin coatings fail due to localized detachment at the grooved intersections caused by the abrasive particles, and thicker coatings support contact stresses elastically and degrade by microchipping or a polishing mechanism. Severe abrasive wear causes thick coating failure by cohesive fracture. Under erosion conditions thick coatings survive angular particle impact for longer times while thin coatings perform well under blunt erodents. Internal stresses induce thin coat spalling when eroded or scratched (Rickerby & Burnett 1987).

COATINGS: PHYSICAL & MECHANICAL PROPERTIES

Hardness is a good first approximation for adhesive and abrasive wear, for materials of the same type, but not for wrought materials (Tucker 1981). Earlier results of wear tests have been reviewed (Tucker 1974). Gregory (1980) reviews the wear resistance of materials and the improvement in wear resistance produced by surface welding. Hardness is related to wear resistance if comparable microstructures are considered. High wear resistance is not necessarily associated with low friction; soft materials may be good lubricants but do not wear well. A very hard smooth surface with small inclusions of a soft metal or a lamellar solid, e.g. MoS_2) is recommended, obtainable by ion implantation (Dearnaley 1973). Optimum coating thicknesses for best wear resistance are very thin, e.g. 2 microns for MoS_2 , due to the need to conduct heat away, which is difficult for MoS_2 in a resin binder coating. Areas of wear are usually limited and ion implantation can be applied to small regions of a bearing or shaft (without dimension change) to keep costs down. Ba ion-implanted into Ti-1Al-4V gives oxidation and fretting fatigue resistance; 40% Ba was still present after 10 million fretting cycles (Mattox 1981). When the matrix of a hardfacing alloy is Fe, Ni, or Co, the alloy will typically contain C, Cr, W and Mo. Higher amounts of these increase carbide formation and wear resistance. Good wear resistance is obtained from plasma sprayed alumina or chromia + silica.

Laboratory experiments have shown that implantation of a wide range of materials with gaseous ions, especially nitrogen, can cause a reduction in mild abrasive wear by factors typically 2-10, provided operating temperatures remain below 400°C . Work at A.E.R.E. Harwell, has focussed on analysing the mechanism of improved wear resistance as well as the production of prototype implantation equipment.

The latest development at Harwell (Gardner 1987) is the large "Blue Tank" ion implantation machine, currently the biggest in the world. This can treat workpieces up to 2 metres maximum dimension and 1016 kg weight using a bucket-type ion source capable of generating 35mA of nitrogen beam current over an 800mm diameter treatment area. This machine enables increased flexibility and reduced unit treatment costs for nitrogen ion implantation and an accessory monitors the nitrogen dose to an accuracy of around 20%. Examples of large items treated in the "Blue Tank" include racing car crankshafts, printing cylinders, crushing rollers, confectionery processing rollers and large plastic processing moulds.

A series of papers from Harwell deal with the various aspects of ion implantation and its role in improving adhesive and abrasive wear, resistance. Dearnaley (1985b) discusses the various categories of wear and shows that because wear rates under abrasive condition are very sensitive to the ratio of the hardness of the surface to that of the abrasive particles, large increases in working life are attainable as a result of ion implantation. Under adhesive wear conditions, the wear rate appears to fall

COATINGS: PHYSICAL & MECHANICAL PROPERTIES

inversely as the hardness increases and, it is advantageous to implant species which will create and retain a hard surface oxide or other continuous film in order to reduce metal-metal contact. In a review report from Harwell UK, Goode (1985) compares various surface treatments for metallurgical applications including modified ion implantation techniques. The possible mechanisms by which ion implantation can be used to improve wear and to strengthen metals and other materials have also been reviewed (Dearnaley 1986; 1987). These include,

(i) The pinning of dislocations by the segregation of interstitial species such as N, C or B for instance in steel (Dearnaley et al 1976),

(ii) The introduction of obstacles to dislocation movement consisting of fine dispersion of hard second phase precipitates, e.g. nitrides (Hutchings 1985),

(iii) Reduction in the coefficient of friction as a means of lessening subsurface stresses during sliding (Hubler et al 1985),

(iv) Modification of the work-hardening mechanism that takes place during wear so as to render the material more self-protective (Dearnaley et al 1985),

(v) Implantation of one or more species such that the surface is rendered amorphous, and so generally possesses a low coefficient of friction which may be combined with the presence of a high content of strongly-bound constituents (eg. TiC) (Follstaedt et al 1983), and,

(vi) Ion bombardment in the presence of sufficient oxygen to cause its take-up, eg as an oxy-nitride in reactive metals, such surfaces having improved lubricity and freedom from galling (Oliver et al 1984).

The effect of temperature reached during nitrogen ion implantation of tungsten carbide and steel has been studied (Dearnaley et al 1985b). Implantation below 200°C softens tungsten carbide, but at higher implantation temperatures significant hardening can be achieved.

Thermochemical and surface heat treatments are also used to combat wear, e.g. carburizing, nitriding, nitrocarburizing, boronizing, chromizing, CVD and PVD (thermochemical) and induction, laser and electron beam hardening (surface heat treatments). A hard 'case' of 5 to 10 microns is enough except for heavy loading (gears, bearings) if the core material is soft. Surface treatments or coatings allow the advantages of a composite: cheap but tough core and a hard surface (Child 1983). Earlier reviews on wear resistance are: (Lang 1983; Hurricks 1972; Donovan & Sanders 1972; Gerdeman & Hecht 1972). Wear resistance test methods are reviewed in Chapter 9.

Sections 7.11.3 to 7.11.8 consider hard materials studied and developed variously in the context of wear and erosion applications and production routes. TiN dominates to a large extent; again, a representative picture may be had, and it is out of scope here to cover the entire literature output.

7.11.3. HARDNESS vs APPLICATION

Before deciding which coating to apply for wear resistance it is important to assess the reasons for the wear. Wear may involve mechanical separation of small particles, corrosion, thermal shock or mechanical stress. If due to the scouring action of hard particles, a hardfacing alloy may be suitable. If due to oxidation, Co-C-Fe alloys etc., may be suitable; Co-base alloys are known for their low temperature and high temperature (1000°C) wear resistance (Coutsouradis et al 1987). An intentional oxide dispersion deposited under conditions that do not significantly oxidize the metal matrix is far superior to a coating heavily oxidized during deposition, both in wear resistance and mechanical properties.

Smoothest coatings do not always give the lowest friction, e.g. a nodular brush finish gives lowest friction in liquid Na (Tucker 1981). Self-welding of mostly static components can be prevented by coating, e.g. load pads on fuel ducts of a Na-cooled nuclear reactor - stainless steel, stripped of its oxide by the liquid Na, is self-welding but this is prevented by a D-gun chromium carbide-nichrome coating.

7.11.4. HIGH TEMPERATURE HARDNESS & HARDFACING

Requirements for hot wear resistance are (Child 1983):

- high hot hardness (resistance to thermal softening),
- structural stability (temper resistance),
- retention of adherent oxide films to act as lubricants,
- high thermal fatigue resistance, and,
- corrosion resistance.

The improved wear resistance of hard carbide layers is not at the expense of lower fatigue strength. For best fatigue properties, plasma nitriding or vacuum carburizing is needed. Oxide and fluoride films reduce high temperature friction, oxide films having temperature independent friction coefficients (Child 1983; Bhushan 1980).

Comprehensive reviews on tool wear are listed: Gurland 1988; Quinto 1988; Wolfe et al 1986; Sundgren & Hentzell 1986; Knotek et al 1986; Dearnaley & Trent 1982. Properties of types of hard-surfacing alloys are shown in Fig.6-19 (p.275). Hardness achieved by various processes is compared in Fig.7-11. Fig.7-12 shows the life increase of pins for Al die casting, due to Nb coating.

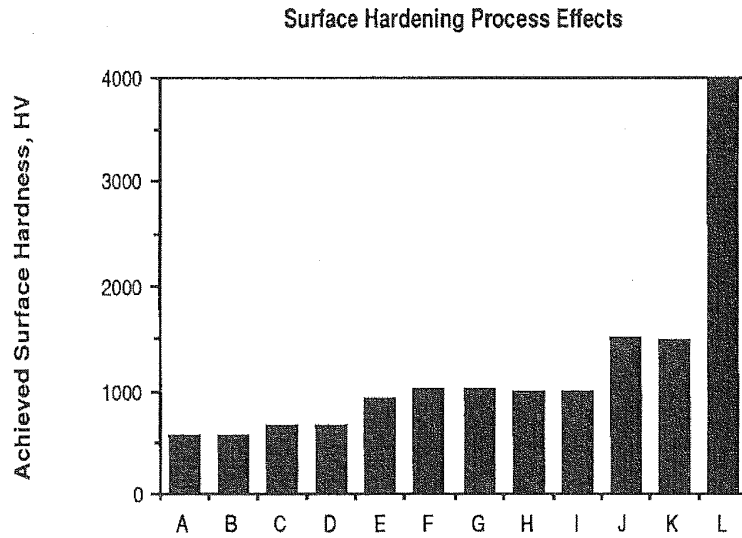
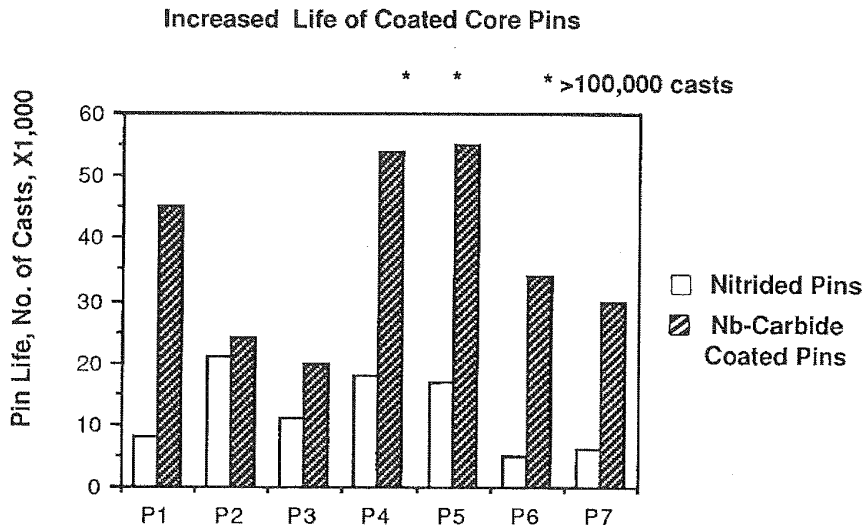


Fig.7-11

Legend	Type of Steel	Surface hardening
A	Mild steel	Ferritic nitro carburising
B	0.4%C steel	Induction & flame hardening
C	0.5%C steel	As in B
D	Cr-Mo-steel	} Nitriding
E	Cr-Mo-V-steel	
F	Cr-Mo-Al-steel	
G	High alloy tool steel	
H	Most steels	Carburising
I	Carbon steel	Carbo-nitriding
J	Mild & Tool steels	Boronising
K	Carbon & Tool steels	Chromising
L	Tool Steel	Toyota Diffusion Process



Life increase of core pins for aluminium die-casting,
due to niobium carbide coating.

Fig.7-12

Friction and wear of alumina coatings with various pins is discussed in pin-on-disc wear tests (Kohno & Kuwahara 1982).

7.11.4.1. Hardened Surfaces:

Chromised carbon steel is hard and brittle with good wear and abrasion resistance and low friction coefficient. Chromised low carbon steel is ductile (Drewett 1969). The main problem of boriding steel by diffusion saturation is the brittle surface layer produced and the method is little used. Combined diffusion coatings based on B, Si, Al etc., with multiple saturation give a high hardness, wear resistance, bonding and corrosion resistance (Samsonov 1973). Addition of Ta and Nb increases the m.p. of an Al coating which reduces interdiffusion and hot erosion. A nitrogen plasma of 10000°C for a few minutes surface hardens steel by nitrogen and 10 microns below the surface the hardness was 5 times more than the untreated steel. Ti and Ta can be similarly hardened (Lee & Ariyasu 1979). TiN is about 5 times harder than hardened steel and has low friction against steel. X-ray diffraction and electron microscopy were used to investigate the hardening behaviour of ion-nitrided SUS304 austenitic stainless steel as opposed to the usual ferritic nitriding steels (Urao et al 1982). Hardsurfacing but non-uniform wear was registered for high dose ion implantation of carbon or boron on Ti-6Al-V alloys (Bolster et al 1987).

COATINGS: PHYSICAL & MECHANICAL PROPERTIES

Ni-Cr-B-Si hardfacing alloys are used for wear resistant coatings, e.g. in producing glass bottles (Knotek & Lugscheider 1974). They can be applied as a self-fluxing powder by welding or by fusing in a furnace (slightly oxidising, or vacuum). Volume diffusion of the B into the steel occurs, giving increased hardness as for boronized steel. The growth mechanism of Fe_2B , FeB , and FeB_{1+x} by powder boride reaction with Fe indicated that reactions proceeded mainly at discrete points of low boron activity with an inward diffusion controlled process resulting in continuous layer growth. The outer layers are thus structurally disordered and mechanically weak (Palombarini & Carbucicchio 1987). Plasma spraying can also be used for boriding; the consequent phase transformations are discussed (Pilous 1981). Laser assisted boronizing of austenitic steel surfaces gives a higher compaction of CVD coats and improved bonding (Steffens 1983). At least 15 microns of $\text{FeB} + \text{FeB}_2$ surface layers on steel gives wear resistance (Child 1983). For thicker layers (to reduce erosion), monophase FeB_2 should be used, to avoid cracking. Boronized surfaces wear 100 times less than untreated steel. Amorphous borides $\text{Ni}_{20-21}\text{M}_{2-3}\text{B}_6$ where M is Ti, V, Nb or Ta have shown good wear and corrosion resistance. They were plasma sprayed atomized powders (Lugscheider et al 1987). Low wear and friction resistant properties of ion beam deposited tribological BN (Miyoshi et al 1985) and CVD composites of TiC-TiB_2 (Hollech et al 1985) are worth noting. Moulds and dies given CVD boriding (Ni-B) have hardness of $\text{HV}850 \text{ kg/mm}^2$ and wear better (Mullendore & Pope 1987).

Cemented carbide inserts, both coated and uncoated with TiC, TiN or alumina, were used to cut EN8 and EN24 steels. Rake-face TiC coatings wore by atomic diffusion and plastic deformation while TiN coatings and uncoated WC-Co wore by atomic diffusion. Alumina rake coatings wore by plastic deformation. Flank wear of coated and uncoated tools was by atomic diffusion. Alumina and TiN coatings resisted groove formation better than TiC. Grooves formed by oxidation and by fatigue cracking, both of which were prevented by cutting in jets of Ar or N_2 . Cutting temperatures attained by the tool edge are about 1125°C , for EN8 steel cut at 183 m/minute. Turbine components, e.g. the midspan shroud of the blade is carbide coated. Fan and compressor blade dovetails and disc slots are also carbide coated for fretting wear (Hillery 1986). Erosion-corrosion resistant coatings of TiN and Ti_5Si_3 or TiAl_3 on Ti owe their hardness to the nitride, and their oxidation resistance to the silicide or aluminide. Fe-Cr-C hardfacing alloys for high temperature use have been produced by a manual metal arc welding technique. The hardface alloy consisted of large primary M_7C_3 carbides in a eutectic mixture of austenite and more M_7C_3 . Hardfacing alloys usually depend upon 3 layers to avoid dilution of the top layer by the base material, but thick deposits lead to weld cracking. Diffusion barrier layers are warranted for this purpose (Svensson et al 1986).

A baseline coating composition of a nickel alloy bonded Cr_3C_2 formulated with Ag, BaF_2 and CaF_2 was designed for wear resis-

tance at 900°C for aerospace and advanced heat engine applications (Sliney 1986). Very hard WC coatings with interlayers of Ti, Ta, W, Mo and Si between WC and stainless steel have been evaluated (Srivastava et al 1986).

Nitrides, particularly TiN and its combinations are one of the most widely investigated materials groups, both as applied and surface transformed coatings (Dearnaley 1987). Ion nitrided Fe-Ti alloys (1.07, 2.08, 2.58 wt.% Ti) increased in hardness with increase in Ti. Gamma Fe₄N was the surface layer with TiN as small dispersed precipitates (Takada et al 1986). Plasma nitrided Type 316 stainless steel also show Fe-rich surface layer with sub-surface Cr-rich nitrides. Peak hardness occurred at a 10 micron depth as ageing at 700°C increased the solubility of Fe₄N (Sundaraman et al 1987). Ion plated 3 micron TiN on cemented carbide showed tempering effects inducing lattice contraction (Perry et al 1988). A new material - Tribocor 532N is formed by surface nitriding a Nb-30Ti-20W wt.% alloy produced by conventional melting methods. TiN forms preferentially, but as the Ti level decreases Nb enters the reaction resulting in a fine structure of complex nitrides in a Nb-W-rich matrix. Nitriding at 1350-1900°C is parabolic with Ti showing the greatest mobility and affinity to nitrogen. Tribocor is developed for high temperature wear and corrosion resistance with greater hardness than WC-4.5%Co (Ziegler & Rausch 1986).

Frictional force and thermal shock caused the H 13 steel tool failure of ion-plated nitrides (Wiiala et al 1987). Ion beam deposited BN on non-metallic substrates for wear resistance showed good affinity to SiO₂ but not to GaAs or InP (Miyoshi et al 1987). ZrN deposited by cathodic arc plasma process outperforms TiN by a factor of two in cutting Ti-alloys and is marginally superior on other conventional steel substrates (Johnson & Randhwa 1987). The same ranking has been shown with (Ti,Al)N as an intermediate for ion plated Zr-, Ti-, Ti-Al- and Ti-Al-V-nitrides, with an interesting feature of substrate polishing prior to coating yielding equivalent wear resistance to doubling deposit thickness from 3-5 microns (Molarius et al 1987). High rate reactive sputtered nitride (and carbide) deposits have shown diverse ranking in wear resistance to the two above and also on different substrate steels. On 4340 steel the ranking order was TiN, TiC, ZrC, HfC, ZrN and HfN, and on 1045 steel it was TiN, HfC, ZrN, HfN, TiC and ZrC (Sproul 1987). A comparison of the overall defect levels of nitrides produced by all these methods could elucidate the reasons for divergence of wear results.

7.11.5. RUBBING SEALS

Compressor rub coatings, labyrinth seals and turbine gas path seals are yet to be developed to long-term acceptance and service levels. The incursion of a vane or blade tip into the seal can result in wear of either or both the components. The blade/shroud

clearance problems have been addressed by the application of abrasive tips to the blades. 'Borazon', a cubic boron nitride has been useful but it has poor thermal stability and does not last long. MCrAlY alloys, which have been successful as overlay coatings have also served well as gas path seals. TBC such as ZrO_2 and its variations have been tested for ceramic gas path seals, and in diesel engines (Hillery 1986; Levy & Macadam 1987; Keribar & Morel 1987). Above $250^\circ C$ or in vacuum, fluid lubricants are unsuitable. Solid lubricants are used, usually as thin coatings containing a binder, but adherence is often poor and failure occurs by peeling or by accumulation of soft wear debris. Ion implantation has resolved this problem to some extent by providing surface additives without the form of a coating which could peel off, and with no change in dimensions nor any surface roughening (for coating keying) required. Mo and S implantation gave a considerable decrease in friction. Pb, and Ag are good such lubricants in vacuum, but not in air due to oxidation (Dearnaley et al 1973).

Rubbing seals for ceramic gas turbine engine regenerators must provide a low leak seal between exhaust and inlet air while continuously rubbing the abrasive regenerator, in a high temperature corrosive atmosphere subject to repeated thermal shock. Low friction is needed to minimise rotation energy losses. Requirements are <25 microns per 100 hours for both matrix and coating and a friction coefficient of <0.35 . Conventional solid lubricants (graphite, MoS_2) oxidise below $500^\circ C$. Plasma sprayed NiO- CaF_2 on Inconel 601 were studied at $760^\circ C$ (Moore & Ritter 1974). Ideally, this type of composite coating with a hard (NiO) matrix containing a small amount of soft (CaF_2) material, will have friction no higher than that of the soft material and wear no higher than the hard material.

Rubbing surfaces for liquid Na cooled nuclear reactors must resist liquid metal corrosion and irradiation. Chromium carbide in a 15 vol.% nichrome binder and Tribaloy 700 gave good results when applied as a D-gun coating, the only disadvantage being that it requires a line of sight with impact angles $>45^\circ$ (Lewis 1987; Johnson et al 1974). A composite powder of Ni5Cr3Al coating on bentonite core at a coating to core ratio 4:1 has been applied by thermal spray for high temperature abradable seals (Clegg & Mehta 1988).

Boron nitride deposited on 440-C bearing steel substrates by ion-beam extraction of borazine plasma was friction tested against various transition metals, viz. Ti, Zr, V, Fe, Ni, Pd, Re and Rh. The 2 micron thick BN included some oxide and carbide picked up during the tests, and oxygen adsorption was mainly responsible for increasing friction. The higher the affinity to oxygen the higher the friction (Miyoshi et al 1985). Oxides have been found effective in reducing sliding wear, but neither friction nor wear is eliminated completely (Glascott et al 1985). TiN sputter deposited and ion plated on bearing steels provided improved resistance to rolling fatigue for steels but gave varied perfor-

mance on softer copper-alloy substrates (Hochman et al 1985). Ion nitrided steel surfaces register lower coefficients of friction but are columnar in structure (Spalvins 1985).

7.11.6. HARDNESS & EROSION RESISTANCE

Erosion may be considered as deformation wear of brittle materials and cutting wear of ductile materials. The maximum erosion wear of brittle coatings occurs at perpendicular impact angles and of ductile coatings it is maximised at oblique angles of 15-30° (Raask 1988; Hillery 1986). Large particle ingestion, typically at 90° affects the leading edge of a turbine airfoil. Further downstream in the compressor, particles tend to be smaller and are centrifuged towards the rotor periphery. Here the erosion affects the airfoil above midchord as well as the trailing edge at low impact angles. Erosion resistant coatings are important for gas path seals and for nuclear reactor applications (Hillery 1986; Nicoll 1983; Schwarz 1980). Erosion is combatted by hard coatings and its effect varies with particle size, velocity and angle of incidence, the last factor being the most crucial. It is thus obvious that no single coating can resist both low and high angle erosion impacts. Chromium carbide- and tungsten carbide-based coatings are being used in power recovery turbines and gas turbine compressor sections. A high temperature erosion testing apparatus built for their evaluation is described by Sue & Tucker (1987).

Erosion and corrosion occur together in coal gasifiers (Wright 1987; Meadowcroft 1987) and have been studied at 870°C with alumina and magnesia particles at 180 m/s in a burner rig (Barkalow & Petit 1979). Alumina-forming alloys resist erosion oxidation and hot corrosion better than chromia-formers. Hot corrosion-erosion is much worse. A comparison of the wear and erosion resistance of coatings is given in Figs.7-13a,b and 7-14a,b,c. Erosion-oxidation and erosion-hot-corrosion histograms are given for comparison in Chapter 8. Table 7:11 (Yee 1978) details the wear resistance of coatings.

T A B L E 7 : 11

ABRASIVE WEAR RESULTS OF SOME COATED AND UNCOATED MATERIALS*

Test material	Treatment or coating**	Thickness (μm)	Hardness (HV)	Relative Volumetric Wear
<u>Steel</u>				
Ck15N	Annealed normally		180	165
100Cr6H	Hardened, tempered at 150°C		840	72
100Cr6V3	Hardened, tempered at 500°C		300	111
X5CrNi189	Annealed		275	124
34CrNiMo6	Quenched and tempered		330	108
X220CrMoV12H	Hardened, tempered at 150°C		810	48
<u>Electroplating</u>				
Ck15EH	Hard chromium	50	1050	23
CuZn40	Bright nickel	50	580	97
Ck15G	Dull nickel	50	560	106
<u>Anodizing</u>				
AlMgSi	'Ematel'	20	450	63
<u>Bath Nitriding</u>				
Ck15	'Tenifer'	8-10	640	73
<u>Spray Coating</u>				
NiCrBSi	Plasma, remelted		700-800	33
Mo	Flame sprayed		800	79
Cr ₂ O ₃	Plasma		700-900	159
Al ₂ O ₃	Plasma		850-950	127
WC-Co	Plasma		800-1000	106
Cr ₃ C ₂ -NiCr	Plasma		500	50
<u>Chemical Vapour Deposition</u>				
105WCr6	TiC(1050°C)	12	3200	3.5
C100	W ₂ C(550°C)	30	1900	4.8
100Cr6	Vanadized	30	2400	7.5
C100	Vanadized	30	2400	9
C100	Borided	100	1600	12
100Cr6	Borided	100	1600	14
Ck15	Borided	100	1600	30

* From ref.159 of Hara et al (1978).

** Vanadizing by pack cementation at 1100°C, 4 h; boriding by pack cementation at 900°C, 3 h.

Wear resistance & Hardness vs Coating Method/Material

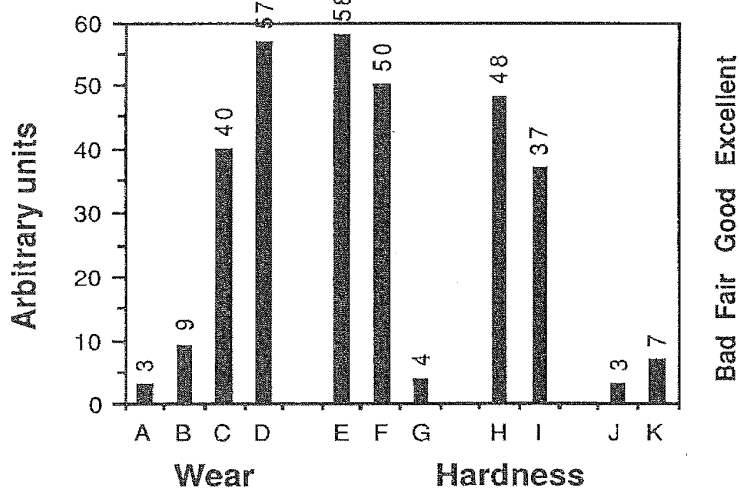


Fig. 7-13a

Legend	Coating Method	Material Or Coating
A	---	Hard Chrome
B	---	Wrought Steel
C	Plasma	WC-Co
D	Detonation Gun	WC-Co
E	----- " -----	91WC-9Co
F	----- " -----	85WC-15Co
G	Plasma	88WC-12Co
H	Detonation Gun	Al ₂ O ₃
I	Plasma	Al ₂ O ₃
J	Plasma	Ni
K	Plasma	58Co25Cr10Ni7W

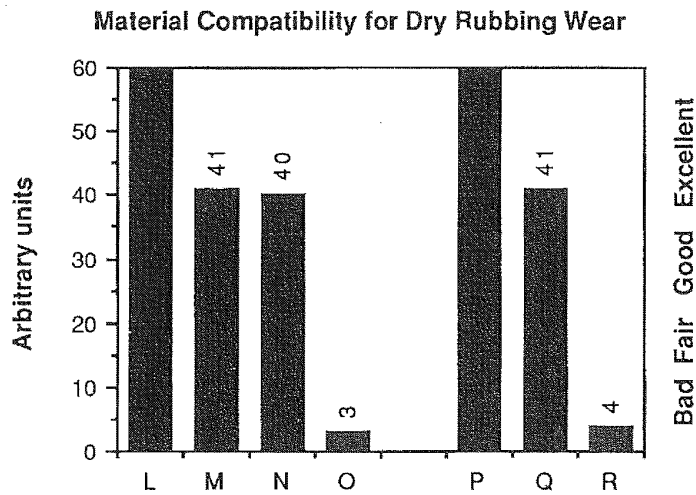


Fig. 7-13b

Legend	Coating Method/Material	vs	Coating Method/Material
L	Detonation Gun/WC-Co		GA Mechanite
M	-----"-----/WC-Co		440C Stainless Steel
N	-----"-----/WC-Co		Detonation Gun/WC-Co
O	-----"-----/WC-Co		Inconel-X
P	-----"-----/Al ₂ O ₃		Haynes-25
Q	-----"-----/Al ₂ O ₃		Hastelloy-C
R	-----"-----/Al ₂ O ₃		Detonation Gun/Al ₂ O ₃

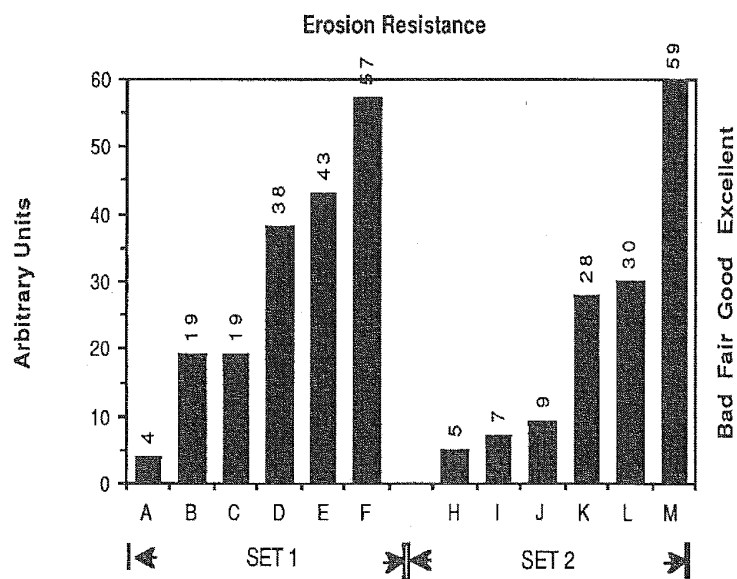


Fig.7-14a

Legend	Coating	Legend	Coating
A	CoCrAlZr	H	IN738 } Chromia-
B	CoCrAlTi	I	X-40 } formers
C	CoCrAlSi	J	MA754 }
D	CoCrAlHf	K	IN738 } Alumina-
E	CoCrAlY	L	(Al Coating) } formers
F	CoCrAl	M	Si ₃ N ₄

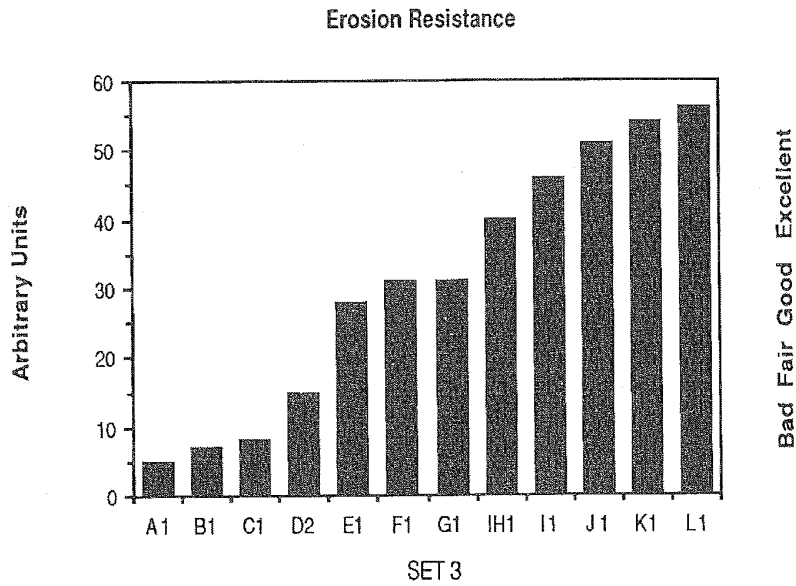


Fig.7-14b

Legend	Substrate	Coating
A1	TRW1900	--
B1	SM200	--
C1	SM211	--
D1	IN100	--
E1	IN717	--
F1	IN713LC	--
G1	PDRL162	--
H1	B1900	--
I1	PDRL162	Al
J1	IN100	Al
K1	B1900	Al
L1	IN713LC	Al

Erosion Resistance

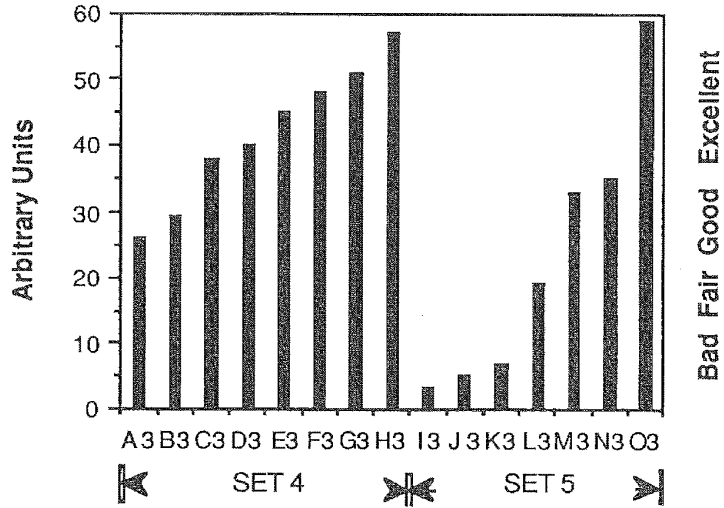


Fig.7-14c

Legend	Substrate	Coating
A3	Haynes C9	none
B3	Hastelloy X	none
C3	Hastelloy X	Al
D3	Hastelloy X	Haynes C3
E3	Hastelloy X	CrAl
F3	Hastelloy X	Al-Cr-Si
G3	Hastelloy X	Al-rich Al-Fe
H3	Hastelloy X	Al
I3	HA 188	none
J3	IN738	none
K3	X 40	none
L3	MA 754	none
M3	IN 738	NiAl
N3	IN 738	CoCrAlY
O3	Si ₃ N ₄	none

7.11.7. HARD COATINGS - ROUTE RECORD

7.11.7.1. PVD Coatings:

The microhardness and tensile properties of Ni, Ti and W vapour condensed coatings were studied by Movchan and Demchischin and Bunshah. Zone 1 structures show high hardness, decreasing rapidly to zone 3 which has the hardness of the annealed metal. Increasing deposition temperature (on going from zone 1 to zone 3) gives larger grain size, low strength, higher ductility and lower hardness. Both hardness and yield strength varied as the inverse square root of the grain diameter (Hall-Petch relationship) (Bunshah 1974). Variation of microhardness with temperature for Al_2O_3 , ZrO_2 and TiC , is quite different from metals. It falls from zone 1 to zone 2 but rises in zone 3. The high zone 3 hardness of TiC ranks it second to diamond (Raghuram & Bunshah 1972).

PVD wear resistant TiC , TiN and Ti(C,N) coatings onto low temperature substrates usually gives poor adherence and film morphology. A low N_2 pressure improves adherence, as does a thin Ti film (Pepper 1978; Brainard & Wheeler 1979; Matthews & Teer 1980), and vaporization in $\text{C}_2\text{H}_2 + \text{N}_2$ (Enomoto et al 1982). The hardness of BP coatings on Mo has been measured (Morojima et al 1979) and decreased as the B:P ratio increased from 1 to 1.5. Very hard, wear resistant ceramic coatings are obtainable by activated reactive evaporation (ARE), reactive sputtering and ion plating. TiN coatings by reactive ion plating are used on twist drills, cutting tools, dies and moulds (Teer 1983). ZrN is used on cutting tools (Kirner 1973). Low temperature, $<400^\circ\text{C}$, deposition of tribological 20% yttria-zirconia, TiB_2 and B-18 wt.%Si produced on steel, Cu- and Al-alloys showed good wear resistance. Excellent thermal and wear resistance were shown by zirconia coatings on copper and Al-alloys (Prater 1986). Cathodic magnetron sputtering of Mo alloyed with carbon or nitrogen, on 304L steel were found superior to hard chrome in corrosive, cyclically stressed and abrasive wear conditions (Danroc et al 1987).

Modified arc evaporated (Union Carbide) TiN coatings were found more erosion resistant than those produced by other PVD and CVD methods. A wide range of hardness values has been reported for TiN from 340-3000 HV which is felt to be primarily due to the crystallographic orientation and presence of a second phase such as Ti_2N (Sue & Troue 1987). Magnetron sputtered Cr-C and Cr-N coatings show much greater wear resistance than Cr (Gillet et al 1983). Solid solution hardening of $(\text{Hf,Ti})\text{N}$ was found when deposited by a high rate reactive sputtering process using a dual-cathode configuration (Fenske et al 1987). Amorphous alumina coatings on grey cast iron produced by rf magnetron sputtering have measured 300HV0.05 hardness and a tensile strength of 300 N/m^2 (Roth et al 1987).

Ion implantation of interstitial species like N and C has major effects on surface-related mechanical properties (Herman 1982;

COATINGS: PHYSICAL & MECHANICAL PROPERTIES

Hale et al 1982; Zhong-yin et al 1982; Delves 1982; Roberts & Page 1982). The lattice distortion is analogous to the effect of shot blasting the surface and increases hardness. The relation between wear and oxidation in ion-implanted metals has been discussed in detail (Dearnaley 1982); ion implanted species on oxide grain boundaries or dislocations block fast diffusion paths. Ion implantation has succeeded where oxidation and stresses coexist. Ion implantation by inert gases acting on a sputtered TiB_2 film on stainless steel improves the erosion resistance to He^+ and D^+ , which is of importance to the first wall of fusion reactors (Padmanabhan & Sorensen 1982).

Several workers report that PVD coatings give superior performance to their CVD counterparts. Claims such as this have to be treated with caution since a number of process and coating/substrate aspects have to be taken into account: Magnetron sputtering vs CVD - Konig (1987); Steered Arc Evaporation vs CVD - Boelens & Veltrop (1987); Plasma assisted activated reactive evaporation vs CVD - Bunshah & Deshpandey (1986). A state of art report of all CVD and PVD is made by Sundgren & Hentzell (1986). The implication of PVD via different deposition processes on tool wear models has been discussed (Kramer & Judd 1985; Kramer 1986). Results reported by Quinto et al (1987) would be of interest in this context. At room temperature, PVD microhardness values were significantly higher than the CVD products, but both registered the same values at $1000^\circ C$. TiN by PVD, IP, MS and AES; TiAlN, HfN and ZrN by PVD and MS and all by CVD were studied. TEM studies confirmed that the high residual compression growth stresses of all PVD coatings were associated with lattice distortion and fine grain size. Thermal expansion mismatch between coating and substrate was responsible to the low residual stresses in high temperature CVD coatings. Thin coatings, about 5 microns thick have also been examined (Quinto 1988). Bulk material structure and property relationships can be extrapolated to some extent for both PVD and CVD coatings, but substrate/deposit features will be unique to coatings only.

7.11.7.2. CVD Coatings:

CVD Ti, Cr and Al carbides and TiN coatings are used to increase wear resistance in many machining operations. TiC, VC, NbC and Cr_7C_3 are used on tools, valves, in die casting, metal cutters and in magnox reactors to reduce sliding drag (Child 1983). CVD carbides produce a continuous chip when cutting steel tools and segmented chips when cutting pearlitic cast iron. Tools coated with TiN- Al_2O_3 -TiC stay 200 degrees (C) cooler (Dearnaley et al 1986). CVD TiC on ball bearings shows very good wear resistance and has high hardness up to $35000 N/mm^2$ (Boving & Hintermann 1987).

Codeposition of SiC with CVD pyrolytic C gives increased wear resistance, applicable to rocket nozzles (Blocher 1974). Hot hardness of $2150 kg/mm^2$ has been measured for CVD SiC on graphite

COATINGS: PHYSICAL & MECHANICAL PROPERTIES

(Morojima et al 1986). Siliciding of grey cast iron by CVD (H_2+SiCl_4) at 960° to $990^\circ C$ produced an adherent and wear resistant coating (Samsonov 1973). Below 960° the adherence was poor and above $980^\circ C$ the coating was thin on parts distant from the gas entry. A 30 micron CVD film of Ta is used on subterrene graphite heat receptors to resist hot rock temperatures of 1700 to 2000K (Stark et al 1974). Very high (10 to 20 GN/m²) hardness at $1500^\circ C$ is reported for CVD Si_3N_4 (Niihara & Hirai 1982).

7.11.7.3. Electrochemical & Chemical Coatings:

Cr plating is the most extensive electrodeposited coating for wear resistance, usually 20 to 500 microns thick. The effect of changing the deposition conditions and heat treatment for 1 h at 400, 600 and $800^\circ C$ of the conventional deposit on abrasive wear has been assessed. Conventional deposits produced at $55^\circ C$, 4000 A/m² had hardness of HV 9.0 GN/m², and had a surface crack network. Crack-free deposits produced at $72^\circ C$, 1600 A/m² showed a hardness of 5.5 GN/m². The conventional deposit in the as-plated condition was a factor of several superior to those heat treated or crack-free (Gawne & Despres 1985).

Failure of a wear resistant WC-9%Co binder coating may be caused by surface fatigue causing spalling. This is prevented by a more impact resistant WC-15%Co coating, which is used on gas turbine engine compressor blades (Tucker 1981). 30% chromium carbide powder electrolytically codeposited in a Co matrix has excellent wear resistance (Kedward & Wright 1978). These coatings have been successful for gas turbine aircraft engine parts, at 15 to 125 microns. Worn Al alloy pistons can be salvaged by such 250 micron coatings (Kedward & Wright 1978). Wear resistance up to $700^\circ C$ is given by a Co + Cr_3C_2 cermet coating which provides a hard glaze of Co_3O_4 debris retained by Cr_3C_2 (Cameron et al 1979); wear resistance is also partly due to an hcp lattice. Tensile stress in AlN coatings is due mainly to differential thermal expansion on cooling but the net stress is compressive (Zirinsky & Irene 1978) and increases with deposition temperature. Adding Si_3N_4 sharply reduces the net stress into the tensile region.

Electroless Ni-P deposits are used as wear resistant coatings. The unlubricated wear characteristics have been examined (Ma & Gawne 1985). A standard rubbing test of like-on-like shows electroplated Ni+WC cermet coatings to be better than other Ni cermets but all the Ni based coatings had unacceptably high wear rates. Co+ Cr_3C_2 was more wear resistant than Ni or Cr based cermets. Co forms oxides with lower friction than oxides of Ni, Cr or Fe. Moderate wear occurs at $200^\circ C$ and very low wear at $300^\circ C$ to $700^\circ C$. A hammer wear test is more arduous and assesses the coating cohesion and adhesion also. Co+ Cr_3C_2 shows good wear properties, nearly matching plasma and flame sprayed Co+WC deposits and equalling plasma sprayed Co alloy X-40 (Kedward et al 1976). Excellent high temperature wear resistance (unlubricated friction wear tests) of Waspaloy has been reported with Co+ Cr_2O_3

electrodeposited cermets at 300-700°C, the resistance attributed to a Co_3O_4 glaze layer (Thoma 1986).

7.11.7.4. Sprayed Coatings:

D-gun and plasma coatings are mainly used for wear resistance (adhesive and abrasive) (Tucker 1974). Considerations for wear resistant coating selection have been given (Tucker 1981). The effect of powder feed composition and size, in plasma spraying of wear resistant carbides, and results of friction tests are discussed. The use of $\text{NiO} + \text{CaF}_2$ (plasma sprayed from powders) for coating truck turbine engine heat exchanger seals is described (Clegg et al 1973).

The mechanical properties of plasma and D-gun coatings are anisotropic because of their splat structure and directional solidification. Plasma sprayed ZrN on steel in argon atmosphere was hard (945-1045 VHN) but showed poor oxidation resistance and a sharp thermal expansion coefficient (Derradji et al 1986). The hardness of a detonation gun coating is generally higher than that of a plasma coating of the same composition. Hardness is usually reduced for a given material if the coating is applied in an inert atmosphere as compared to spraying in air. A typical wear test machine has rollers touching at different speeds, the roll diameter and weight loss being measured. This is used to select candidate materials for diesel engine testing. Plasma sprayed alloy coatings containing 20 to 30% free graphite gave promising results (Solomir 1973).

D-gun coatings are often much harder than plasma coatings of similar composition due to their higher density and cohesion. The high bond and cohesive strength of D-gun coatings allow their survival to impact, temperature and fretting (Barnhart 1968). Hardness varies with cooling rate if relative differences occur in various phases which form (Tucker 1974). Erosion (Sue & Tucker 1987) and fretting (Lindgren & Johnson 1987) wear tests have been reported on D-Gun coatings of Cr_3C_2 -NiCr(A) and Cr_{23}C_6 -NiCr(B) on steels and superalloys. The coatings were distinctly superior with bond strength greater than $6.9 \times 10^4 \text{ kN/m}^2$ to those produced by plasma spray which showed 30% lower hardness due to porosity. The D-gun coatings had an apparent metallographic porosity of 1%. The two chromium carbides were similar in fretting wear but coating B was more resistant to spalling and did not affect the substrate creep-rupture properties. Coating A underwent structural changes to Cr_7C_3 .

The microhardness of arc sprayed Ti Nb and Mo is low (ductile coating) if gas/metal reactions are avoided (Steffens & Muller 1974). Wear mechanisms of thermally sprayed hard facings such as Ni_3B and carbides are discussed (De-jie et al 1982). Flame sprayed 13% Cr steel coatings are used for wear resistance (Gagnet 1969). NiAl powder or Ni-graphite (75%-25%) are flame sprayed to give abradable seals (Messbacher 1975). The lower

density (than plasma spraying) gives better coatings for this purpose. Grey cast iron has long been used for diesel piston rings as its graphitic structure prevents seizing (Solomir 1973). But at high power the wear becomes unacceptable and so hard Cr coatings are applied. But this needs good lubrication. Flame sprayed Mo (successful in petrol engines) corrodes.

Arc sprayed mixed metal coatings and pseudo-alloys (e.g. Cu + stainless steel) are wear, erosion and abrasion resistant and can be deposited at high rates to give thick coats on large components with bond strengths around 30 N/mm². Plasma sprayed Mo/Mo₂C coatings resist wear, Mo being the ductile matrix. An inert atmosphere is necessary to stop oxidation of the Mo₂C and loss of Mo ductility. Mo/Mo₂C composite coatings have low friction (Steffens 1983). Although plasma-deposited materials are softer than the wrought materials, they are much more wear resistant. Wrought alloys develop piles of debris but no debris occurs with plasma-deposited alloys as their structure limits the sizes of adhered wear particles. Addition of a small amount of alumina to aluminium bronze results in almost the same wear resistance as pure alumina, without increase in hardness (Tucker 1974).

7.11.8. WEAR vs MULTI-COMPONENT & MULTI-LAYERED COATINGS

It is evident from the discussion and information given in the preceding sections of this chapter that a considerable improvement in wear resistance can only be met by product optimization on a multiple-component, multiple-phase, multiple-layer concept. Ternary nitrides have been investigated and other systems and process methods may be expected to follow.

An increase of 200% of tool life has been achieved by diffusion boriding tool steel with Co-W-B followed by CVD TiC-TiCN or TiC-Al₂O₃ (Zachariev & Zlateva 1987). TiC-Al₂O₃ composite and TiC/Al₂O₃ layer deposited on stainless steel by direct electron beam evaporation showed greater abrasive and adhesive wear loss when compared with TiC by the ARE process (Memarian et al 1985). Steered arc evaporated TiN (6-7 microns thick) showed 42% lower flank and crater wear than TiN by random arc evaporation and 10 micron deposits by CVD. Steered arc evaporated TiHfN (2.5 microns thick) and TiNbN (4.9 microns thick) were both superior to the TiN (Boelens & Veltrop 1987). Magnetron sputtered TiHfN, TiZrN and TiVN also show a similar improvement in wear characteristics (Konig 1987). A two-fold increase in high temperature drill cutting both in terms of wear and oxidation is reported for TiAlN against TiN. Oxidation resistance extended from 550° for TiN to 800°C for TiAlN. The coatings were sputter ion plated (Munz 1986; Jehn et al 1987).

Innovations in multi-phase, multi-layer and multi-component wear resistant-deposits require reliable data on phase relationships of the metals and ceramics involved. Detailed discussions are

COATINGS: PHYSICAL & MECHANICAL PROPERTIES

presented by Holleck (1986), Sundgren & Hentzell (1986) and Konig (1987). Nitrides of similar lattice parameters and structures can be co-deposited more effectively and to give better resistance. Thus TiN can be combined with CrN, NbN, HfN, VN and ZrN but not with MoN, TaN or WN (stoichiometry not shown) (Konig 1987). Combinations of B₄C with LaB₆, TiB₂, ZrB₂, SiC and Al₂O₃ in binary and some ternary combinations have all resulted in 30-60% improvement in wear (Holleck 1986). Carbo-nitrides and oxy-carbonitrides of Ti and many other metallic and ceramic systems are listed (Sundgren & Hentzell 1986). A graded layer ceramic seal system developed from plasma spray has been a candidate aerospace coating. Inconel 713 substrate is given a NiCrAl bond coat followed by four layers of ZrO₂, viz. with 60% CoCrAlY and 15% CoCrAlY as the first and second layers on top, followed by 100% ZrO₂ and a porous zirconia as the topmost layer (Hillery 1986). Many more such sealing, thermal barrier, wear- and erosion-corrosion resistant coating composites are expected to be common in future high temperature coatings.

CHAPTER 8

Chemical properties of coatings

8.1. INTRODUCTION

The output of literature on alloy degradation is varied and voluminous, and it is difficult to do justice to all of this here; a reasonable cross-section is given in this chapter which reviews in brief, the influence of chemical factors on the durability and performance of coatings used for high temperature systems. It is difficult to determine any single package in explaining degradation, categorized by specific environment, mechanism or types of coating. The same coating can be applied by various processes, and each process is inherent with its own advantages and incorporated defects which can initiate coating failure later in service life. The chapter may be viewed in four main areas, divided into a number of sections for clarification. Coating/substrate/environment aspects in general are given at the outset, followed by the prevailing conditions for degradation of coatings in gas turbines - marine, power- and aero-engines, and in coal conversion systems, nuclear technology and tribology. The fundamental aspects of chemical reactions and examples in all aspects of chemical degradation, viz. general oxidation, hot corrosion, sulphidation, carburization, and erosion-corrosion form the third area. The fourth area examines the degradation of specific coating systems. References quoted in all sectors have been selected on a representative basis and should provide useful sources for further information.

The references listed below will be particularly useful in determining the direction and emphasis on aspects which need to be considered for high temperature investigations:

COATINGS: CHEMICAL PROPERTIES

Conclusions published in the 1986 symposium on high temperature corrosion (Lacombe 1987); Workshop questionnaire and summary on high temperature corrosion (Rahmel et al 1985); Reviews on:-

- coatings in energy-producing systems (Stringer 1987; Fairbanks & Hecht 1987; Hancock 1987; Peichl & Johner 1986),
- the role of oxide scale point defects (Gesmundo 1987),
- electrochemistry of hot corrosion (Rapp 1987; Rahmel 1987),
- erosion (Wright 1987) and corrosion (Meadowcroft 1987) in coal combustion and conversion processes,
- oxide/metal interface and adherence - compositional fluctuations (Newcomb & Stobbs 1988), fracture mechanics (Hancock & Nicholls 1988), stresses and cohesion (Schutze 1988), improvement on adhesion (Stott 1988), protective oxides on gas turbine components (Rhys-Jones 1988).

8.2. COATING/SUBSTRATE/ENVIRONMENT vs DEGRADATION

8.2.1. GENERAL:

The deterioration of a coating and its eventual failure is primarily linked to:

- (i) The process by which it is applied,
- (ii) Its metallurgical compatibility with the substrate, and
- (iii) The joint response of coating plus substrate to the operating environment.

Coating failure associated with the coating process can arise in four ways:-

Coating composition, nucleation and build-up,
Coating thickness and uniformity,
Coating/substrate bonding - adhesion,
Coating defects, e.g. pores, cracks, disbonding and microstructure formed in as-processed condition and/or heat treated condition.

Chapters 3-7 review the process and physical aspects of high temperature coatings which control the above aspects. In brief, the coating composition is decided on the basis of the operating environment and the substrate on which it is applied. Deposition processes which are line-of-sight have to align substrate/target geometry to achieve uniform 'cover'. All processes resort to mechanical and electrical devices in moving the substrate and/or target to achieve uniformity in deposition, and not rely entirely on ionic, particle and physical mobility. Appropriate surface preparation and temperature control have to be exercised for ensuring sound adhesion, while controlled substrate exposure w.r.t. its geometry enables achievement of desired thickness, coherence and uniformity of the coated product. Ion bombardment or implantation for creating compressive stresses, or, negative

bias to substrate to be sputtered are also used as a substrate pretreatment apart from chemical cleaning with a view to improving adhesion. Shot peening or grit blasting of the substrate or an interlayer of oxide ensures good coating nucleation and adhesion. Heat treatment as a post-coating step is often necessary to improve substrate-coating bonding.

Coating processes incorporate physical defects such as pores, voids and microcracks via nucleation, dislocations and crystal growth during the build-up of the deposit on the substrate; they can also cause interlayer structural changes, or substrate-coating interactions and interdiffusion leading to compositional and microstructural changes. The porosity in plasma and D-gun coatings is partially interconnected and so may have a strong influence on the corrosion rates of the coatings. Some D-gun coatings have sufficiently small pores to be unimportant in oxidation (Wolfla & Tucker 1978) but may not be ignored in hot corrosion where molten media are involved, and the porosity of plasma coatings have to have a post-treatment sealing of the top layer to render them acceptable. Heat treatment is not essential but may have to be considered. Columnar morphology is particularly unwelcome in hot corrosion environments regardless of how chemically resistant the coating may be. The evolution of barrier and multiple sealant layers compensate this physical inadequacy of an otherwise satisfactory coating.

The porosity of flame sprayed ceramic coatings can be greatly reduced by chromate impregnation, making these useable in hot corrosion conditions. Porous coats achieved by plasma spraying can be of advantage, as are microcracked and segmented ceramic coats like ZrO_2 (+ MgO , Y_2O_3 etc), for accommodating thermal shocks. However, microcracks can expose thermal barrier coats to selective leaching, e.g. of Y_2O_3 by molten salts (Pettit & Goward 1982). NiCrAlY (bond layer)/Cr intermediate coat/ ZrO_2 - Y_2O_3 (thermal barrier) exposed to Na_2SO_4 + vanadates caused total ceramic spallation in 100- 200 hrs with selective attack on Y_2O_3 while Cr was unaffected (Kvernes 1983). Thermal-mechanical (freezing) effects of condensed salts which penetrated porous coatings and disruptive chemical reactions between environment and coatings can both cause coating failure (Lau & Bratton 1983).

In the low temperature range, sealants can be applied for use up to $150^\circ C$ (Tucker 1983). A new high temperature adhesive, LARCl-13 can provide high strength bonds up to 300° and can be used up to $600^\circ C$ for short periods (St.Clair & Progat 1985). Its use as a pore filler appears promising. Bronze shaft sleeves handling saturated brine in a chlorine processing plant provided good service at $175^\circ C$ when it was applied with an epoxy-sealed machinable metallic plasma undercoat and plasma deposited chromium oxide sealed with epoxy (Tucker 1983). Aluminium-bronze coatings on aluminum alloy substrates of aircraft landing gear bearings are corroded when the hydraulic fluid gets contaminated with salt water in marine conditions. A plasma coating virtually identical to the substrate and its subsequent sealing solved the corrosion

COATINGS: CHEMICAL PROPERTIES

problem.

At high temperatures however, plasma coatings have to be sealed by sintering and sometimes given supportive mechanical treatments (Tucker 1983). Laser sealing plasma coats of MCrAlY (M=Fe, Ni or Co) reduced the porosity to about 4 vol.% for dense coatings and about 10% for more porous coatings (Bhat et al 1983). The as-plasma-sprayed coatings revealed Al and Y segregated as thin splats. The Al_2O_3 developed on oxidation was discontinuous. The porosity caused premature degradation by internal sulphidation and reduced mechanical strength while the chemical inhomogeneity would also contribute to the former. Plasma spraying with 5 wt % Al yielded only 1% Al in solution with Ni, while Al and Y segregated to thin splats. Laser treatment resulted in a four-fold increase of Al content in the top layer, while Y segregated to the coating/laser treated zone interface. Laser treatment also consolidated the outer 20-25 micron layer which provided a coherent continuous 5 micron layer of Al_2O_3 even during thermal cycling at 1100°C. However, laser treatment produced an outermost layer of slag which recorded a weight loss during thermal cycling. Slag formation can be prevented by laser surface modification in inert atmosphere or vacuum and by post-peening.

Laser fusion, laser irradiation or merely LST as it is termed, has been applied to aluminided and chromided superalloys and electrodeposited Cr (Galerie et al 1987), to PAVD SiO_2 coatings (Ansari et al 1987). Ni-10Cr and Ni-20Cr develop the protective Cr_2O_3 layer on identical mechanism; the oxide nucleates at the alloy grain boundaries which provide rapid diffusion paths for Cr and preferential oxide nucleation sites for internal oxide precipitates, and the healing layer is established initially at their intersection with the surface; stepwise extension into the grains promotes lateral growth, and thereof the cover of the healing layer. Ni-10Cr, at 1025°C, was found to be slower in developing the self-healing cover due to surface insufficiency of Cr. LST resulted in a change in surface microstructure, and provided rapid diffusion paths via retained alloy grain boundaries and twins which resulted in the 10Cr alloy evening up with the 20Cr alloy in self-healing (Stott et al 1987).

Burman and Ericsson (1983) have achieved plasma coating consolidation by HIP and EB. EB remelting prevented big oxide inclusions while allowing fast diffusion of Ni^{++} , and a 6% strain resistance prior to cracking. Although HIP treatment allowed only 3% strain release; it prevented Ni^{++} diffusion and retained oxide inclusions which could act as diffusion barriers. Both EB and HIP post-treatments of FeCrAlY plasma coats on Alloy 800 (Fe-base) and IN 738 improved oxidation by a factor of 10, the HIP treated surface developing a smooth oxide scale and the EB treatment yielding a nodular scale. Laser melting using a gas flow shield results in a high cooling rate to cause microcracks while EB is done in vacuum and can implement controlled cooling. The former has to be monitored to minimise slag forming. LSA and LSM have been improved with many modifications rendering them more versatile (Powell &

Steen 1981; Gnanamuthu 1979; Draper 1981, 1987; Bass 1981; Burley 1982).

Bond strength is very sensitive to variations of the plasma spraying process and to microstructural alterations during service life. A controlled precipitation of fine monoclinic ZrO_2 toughens up a cubic ZrO_2 at thicknesses greater than 0.5 mm (Kvernes 1983). The first order rule-of-thumb for thermal fatigue is that coatings have 1-2% ductility at the temperature of occurrence of maximum strain and should possess enhanced thermal fatigue resistance compared to elastically brittle coatings. Ceramic coats, especially, spall due to transient thermal stresses with failure occurring within the ceramic, near to but not along the ceramic/metal interface (Pettit & Goward 1982). A metal felt in between the metal substrate and the ceramic coat can help to accommodate shear stresses resulting from thermal expansion mismatch (Kvernes 1983).

Sol-gel-applied CeO_2 and SiO_2 coatings on preoxidized steel exhibit a low corrosion rate in CO_2 at 825° , the oxidation of steel itself having been reduced by a factor of 3 to 4. The improvement is thought to be due to reduction in spalling during thermal cycling as an alpha quartz layer formed during the sol-gel process was incorporated in the growing oxide scale (Bennett 1983). Abrading the alloy coated surface prior to oxidation delays spalling (Hutchings et al 1981). ODS alloys in this respect are superior to ordinary superalloys (Lowell et al 1982), their lower thermal expansion causing reduction in spalling of the oxide layer. One method of combating corrosion fatigue and pitting of low pressure turbine blading (AISI alloys 403 and 630) and other surfaces washed by steam condensate is by coatings. The Southern California Edison Company have tested a number of nickel-gold electroplates (Kramer et al 1982). Coating selection for future prototype blade applications was based on a composite ranking of both laboratory and field specimen performance. The results indicated that fused powder Teflon, a nickel-cadmium diffused electroplate and ion vapor deposited aluminium all have significant benefits worth further investigation in field exposures.

8.2.2. EFFECT OF ION IMPLANTATION ON DEGRADATION

A drastic reduction in degradation of steels by oxidation drew attention to ion implantation as a surface modification method. The effect of ion implantation on high temperature oxidation has been extensively reviewed (Bennett & Tuson 1988; Bennett 1981). The surveys cover the oxidation behaviour of implants like Y and Ce in metals such as Ti, Zr, Cr, Fe, Ni and Cu as well as a range of stainless steels to Fe-Ni-Cr-Al alloys. Aluminized coatings are also discussed. In all cases beneficial effects could be obtained by selecting the right dopant as well as the optimum dosage. Several elements, metals and non-metals were ion implanted and some resulted in an increase in corrosion rate.

COATINGS: CHEMICAL PROPERTIES

Radiation damage and effect of dosages of ion implantation were considered responsible for the onset of failure of the modified surface. Other workers also affirm that radiation damage and implant atomic radius are important parameters, along with solubility, compound and ternary oxide formation (Pons et al 1982).

Subsequent investigations indicate that any radiation damage to the lattice due to ion bombardment during implantation is annealed out at or below the oxidation temperature used. Ion bombardment also causes sputtering which has complex effects on oxidation. The physical effects of ion implantation can be best established by examining the effect of self ion implantation. For this purpose, variation of ion dose, dose rate, bombardment temperature and annealing temperature prior to oxidation, are particularly informative. Only when the role of radiation damage, sputtering etc., has been ascertained can the more complicated chemical influence of impurity atoms be distinguished.

Although the shallowness to which ions are implanted was predicted as a weakness in the technique, this has turned out to be its unique strength. Because the implanted element is confined initially to a near surface layer its subsequent redistribution has provided detailed and unique information about atomic migration mechanisms during oxidation. Also, the technique has provided further insight that could not have been obtained by any other procedure, that many elements, e.g. Y and rare earths on the oxidation of austenitic and ferritic stainless steels, acted through strategic location within the oxide film. Ion implantation also has the advantage of independence upon mutual solubilities which can provide mechanistic understanding of the role of specific elements in the thermal oxidation behaviour of metals and alloys. The implantation of Y in Ni-Cr alloys does not lead to grain structure change and this is an advantage for comparing the beneficial percentage with an alloy where change in grain structure occurs. Y implantation has been found to reduce oxidation and spalling of oxide in the stainless steel used for cladding nuclear fuel reactors (Bennett et al 1986). Doses as low as 2×10^{16} Y⁺ ions/cm² have been shown to have a strong and long-lasting effect at temperatures up to 950°C. In contrast, most implanted impurities in Si were found to increase oxidation rate (Holland et al 1988).

The review by Bennett and Tuson (1988/89), addresses the improved oxidation characteristics of Cr₂O₃ and Al₂O₃ forming alloys in detail and reviews recent oxidation studies on ion implanted alloys particularly over the last five years. These cover studies in O₂ and CO₂, of Fe, Ni and Co base alloys implanted with Y, La, Ce etc.. The review gives a critical discussion of the possible mechanisms.

Ion implantation has established that the dramatic influence of many elements is derived from their incorporation into the oxide during the early stages of oxidation (Bennett et al 1976; Bennett 1983) and that a dispersion of reactive oxides is more effective

than the corresponding metal (Hou & Stringer 1988). Another positive effect observed in 20Cr-25Ni-Nb stabilised stainless steel was that implantation of Y and Ce extended the scale growth induced by the low temperature oxidation process to higher temperatures, up to 1000°C (Bennett et al 1987).

In all scales, the reactive element was located in a continuous band, probably acting as markers for the original metal surface. In some cases Y_2O_3 segregated at grain boundaries provided the source of Y in the band. Parallel observations confirmed that segregation of reactive elements also occurred for alloy additions. The most probable mechanism (Stringer et al 1972) is that the dispersed reactive element oxide particles on an alloy surface act as heterogeneous nucleation sites for the first formed oxides, thereby reducing internuclei spacings and hence the time for subsequent lateral growth. A discussion of the role of segregates in blocking diffusion along grain boundaries indicates that the most probable mechanism could be due to complex defect formation, by vacancy-rare earth association, increasing the activation energy for diffusion along segregated short-circuit paths (Nagai & Okabayashi 1981; Duffy & Tasker 1986).

Numerous models have been proposed to account for the enhanced adhesion of ion implanted materials. These have been reviewed in detail recently (Moon 1988). In any system one or more can apply and no fixed rule exists. The beneficial effect of implanted materials could be due to reduction in stress, oxide keying or pegging, chemical bonding of the scale-substrate interface, vacancy sink provision or impurity gettering. All these possibilities have been discussed in the review by Bennett and Tuson (1988/89).

Several of the mechanisms identified by numerous experiments in reducing corrosion rate are summarised below (Dearnaley 1987):

1. The production of a coherent film of material that resists diffusion of anions and cations, e.g. Al_2O_3 following high dose implantation of Al^+ (Bernabai et al 1980).
2. The blocking of short-circuit diffusion paths through the scale, e.g. at grain boundaries (Bennett et al 1985).
3. Modification of oxide plasticity, e.g. to allow the relief of growth stresses without cracking (Bentini et al 1980).
4. Modification of electronic conductivity and hence the defect population (the classic Wagner-Hauffe mechanism).
5. Electro-catalytic processes may occur which can influence reactions, e.g. in moist atmospheres, involving ingress of hydrogen or OH.

Oxidation of binary Ni-33 and 20Cr, IN 939, Rene N4, FeCrNiNb, and FeCrAl alloys with implanted Y, Ce, Ar, Pt, Zr, Al, Ca and Si have been scrutinised. The implanted dose, the test duration and the alloy condition, e.g. pre-oxidised, etc., are factors which influence the oxidation rate, and often without any

COATINGS: CHEMICAL PROPERTIES

improvement or, when it does retard, it does so for a limited duration. The protection is not comparable to that obtained by the element incorporation as an alloy constituent in the coating or the substrate (Srinivasan 1987). The effects of Al and B implantation on Fe-oxidation were studied (Brown et al 1985; Galerie et al 1982). Fe and Cr ion implantation into Fe had detrimental effects on its oxidation rate at 400°C at 0.1 torr. Self-implantation caused increased oxidation due to more diffusion paths in the oxide and the benefit of Cr lasted only until the 200 nm thick implanted layer was oxidised (Howe et al 1982).

La implantation to a dose of 10^{17} ion/cm² on 20Cr/25Ni/Nb-stabilized stainless steel (also containing 0.9%Mn and 0.6%Si) was oxidized in CO₂ at 825°C up to 9735 h. The beneficial effect was evident in scale adherence during thermal cycling. Microstructural changes were manifested in finer Cr₂O₃ grains and an intermediate region of La-rich spinel between the outer Mn(Fe,Cr)₂O₄ spinel and inner Cr₂O₃+spinel, beneath which was a continuous band of Cr₂O₃ and internal SiO₂. The implanted La while oxidizing also acted as a marker due to its low diffusivity. A major consequence of the improved adherence was that the steel was prevented from pitting attack (Yang et al 1987).

The effect of Ni, Ar, C, Cr and Li ion implantation into Ni was studied for oxidation resistance at 1100°C in O₂. NiCr₂O₄, LiO₂, etc., impeded scaling and later dissolved in the scale, doping the NiO. A long term effect occurred in all cases, the oxidation rate eventually becoming higher than that for pure Ni (Stott et al 1982a). Unimplanted Ni-20%Cr and Cr-implanted surfaces gave spalling scale on cooling, but Y and Ce implanted surfaces resisted spalling (Stott et al 1982b). Similar effects of Y and Ce on steel are reported (Bennett et al 1982). Cr and Ni-implanted Ni developed a NiO scale more faceted, more mismatched and generally smaller with more extensive stress during growth. The initial slower rate gave way to much higher rates at longer times. A doping effect on a semi-conductor NiO is ascribed as the cause (Stott et al 1982c; Peide et al 1981).

Two ternary oxides were detected on Al-implanted Fe at 727°C after 100-120 h. FeAl₂O₄ was ascribed to cause a blocking effect (Pons et al 1982). But Fe-15Cr-4Al alloy implanted with Al in a 25 micron thick surface layer showed no significant influence on its oxidation behaviour in air at 1100°C (Smith et al 1987). An Al implant dose $<1 \times 10^{17}$ ions/cm² had no effect on the oxidation rate of Fe-6 at.% Al alloy at 900°C. Ion mixing of Al and Al₂O₃ on SiO₂ improved adhesion, increasing with the ion dose, with the best adhesion enhancement obtained by implants which produced glassy phases with Si-O-Al bonding (Galuska et al 1988). Comparison of oxidation rates of ion implantation treatment and LST of boron-alloyed iron showed that LST reduced the rate better. The scale morphology seemed to be responsible with the implant oxidized sample showing FeB₂O₄ as top scale followed by FeO, Fe₃O₄ and Fe₂O₃ sequentially beneath. The LST sample scale analysed to a top layer of Fe₃BO₅, Fe₃O₄+Fe₂O₃, FeBO₃ and B₂O₃ at the metal-

/scale interface (Pons et al 1986).

When 0.86% Y was alloyed with this FeCrAl, oxide spallation was reduced for at least 3271 h while Y with Al registered an improved behaviour for a limited duration (784 h). The beneficial effect of Y is inferred to be within the oxide film rather than the subscale (Bennett et al 1980). Y implantation was carried out on FeCrAl alloy with and without Y (0.19 wt.%) and Y added as a sulphide. Oxidation in air at 1050°C showed that the rates of FeCrAl with and without yttrium sulphide were the same. FeCrAlY registered improved adhesion with convoluted scale formation. Pegged alumina scales on FeCrAl were cracked and non-adherent; the scale was adherent in the implanted alloy but with no change in the convoluted morphology. Y added to FeCrAl as an alloy normally forms flat scales but Y implantation at fluences of 10^{15} and 10^{17} ions/cm² did not achieve this. Helium bombardment on scales formed on implanted alloys exhibited local blistering (Smeggil & Shuskus 1986).

Fig.8-1a shows the parabolic oxidation rate constant of Al-implanted FeCrAlY was less by a factor of 140 in tests at 1100°C (Bernabai et al 1980; Bennett 1981). Annealing Y-bearing Fe-Cr-steels is good and is thought to be due to either a lowering of the diffusivity of spinel-forming elements, or a degree of pre-oxidation of Y in the annealing pO₂. A similar mechanism is envisaged for the influence of Y implantation on Ni-Cr, Fe-Ni-Cr and Fe-Ni-Cr-Al alloys but does not appear to be well supported. Yttrium dissolution in the oxide layer changes the growth rate and composition and gives then an improved adherence. But the oxidation rate of the Fe-Ni-Cr-Al alloy is hardly affected; see Fig. 8-1b, 8-1c and 8-1d (Pivin et al 1980). A beneficial effect has also been reported for 20/25/Nb steel by Ce and Y in CO₂ at 825° and seemed to have originated during the early stages of subscale development, negating any initial detrimental influence caused by radiation during implantation. CeO₂ and Y₂O₃ grains modified the mechanism of growth of FeCr(MnNi) spinel with a thinner Cr₂O₃ underlayer. Outward cation grain boundary diffusion was arrested by the ingrained CeO₂ and Y₂O₃. The change caused in the microstructure resulted in increased adhesion. The formation of a continuous, weak, fracture-prone layer of SiO₂ was inhibited as scale modification occurred (Bennett 1984).

The effects of ion-implantation on Cr₂O₃-forming alloys appears to be variable, but often beneficial in air or oxygen environment. The same cannot be said for Al₂O₃-forming alloys. Most of the studies reported are on Fe-base alloys in air or O₂ atmospheres only.

Implantation of Y and Ce improves oxidation resistance of chromia former alloys but that of Al or noble gas results in little or no beneficial effect (Bennett et al 1980; Antill et al 1976). Pre-oxidation followed by yttrium implant in IN 800H has been shown to be beneficial (Kort et al 1986). The oxidation rate at 1020°C was reduced by 45% for this alloy when Y-implanted. However, when

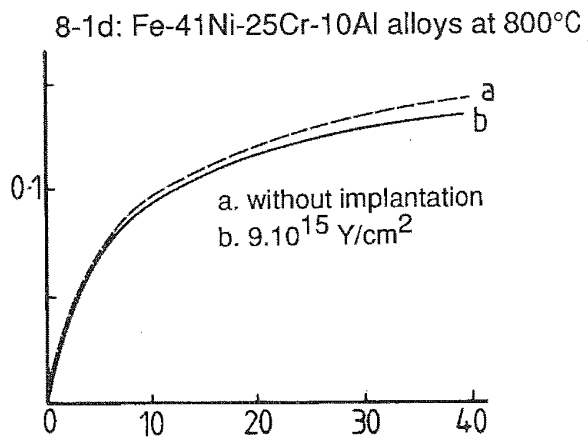
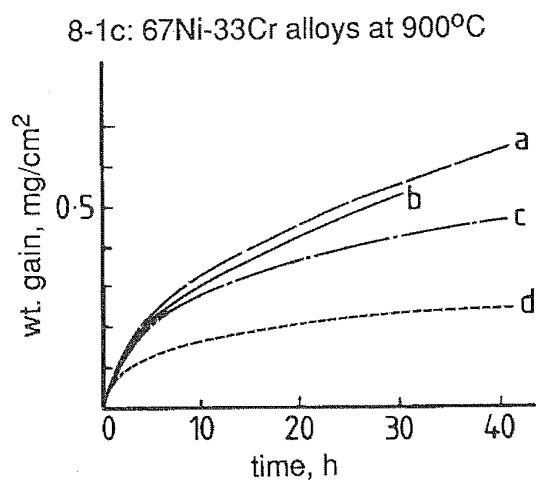
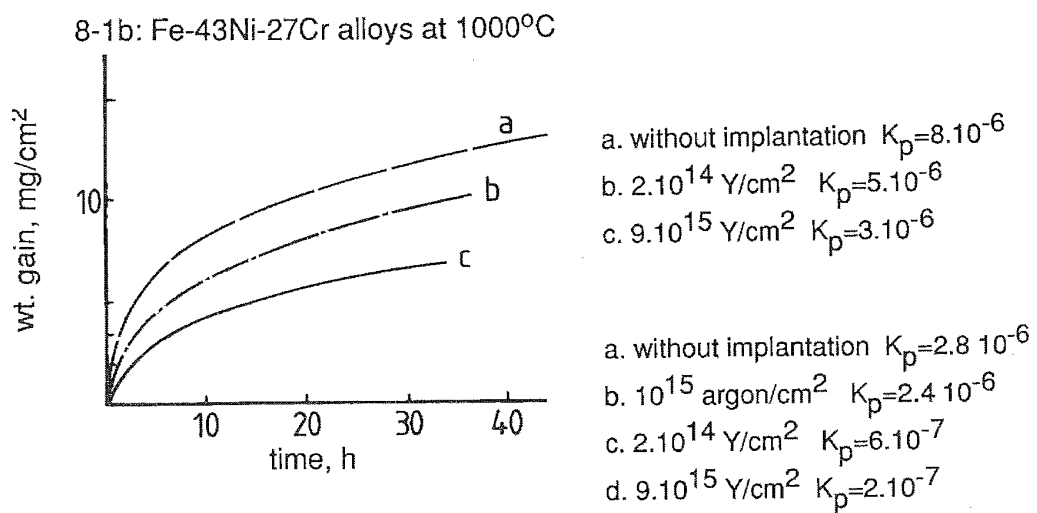
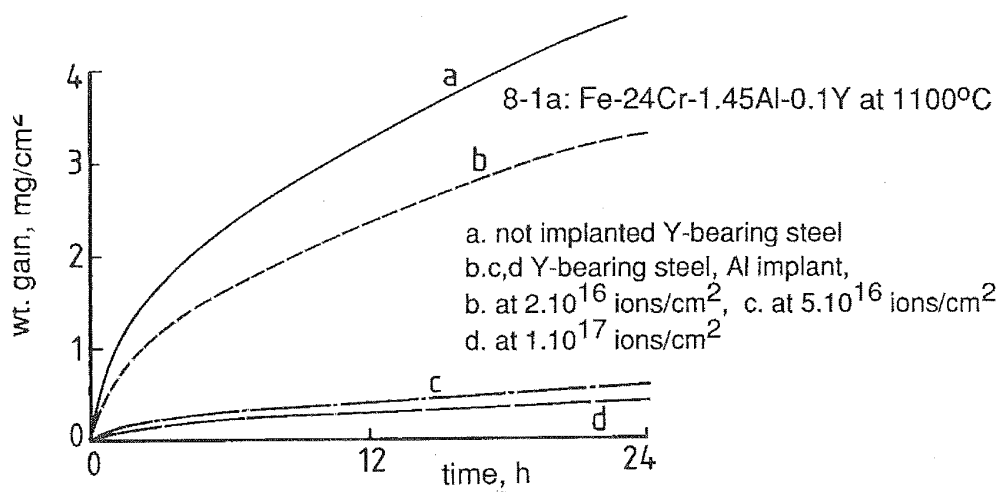


Fig.8-1 (a-d): Effects of Ion Implantation on the Oxidation of Fe- & Ni-base Alloys.

exposed to H_2-H_2S at $560^\circ C$, Y-implantation has no effect on the alloy sulphidation rate without pre-oxidation. A 70% decrease occurs for the pre-oxidized, implanted alloy in the first 50 hours but the mass gain rate accelerates to twice the non-implanted alloy in 150 hours. Implantation of Kr shows a similar initially slow but accelerating later effect, but over much shorter durations and Al implantation has no beneficial or detrimental effect. A similar pattern of an initial decrease in rate (95%) and later acceleration (x3) in 200 hours is observed in $H_2-H_2S-O_2$ at $640^\circ C$ (Polman et al 1987).

CoCrAlY overlay coating implanted with yttrium and oxidised in air at $700-1000^\circ C$ developed voids which occurred in the initial stage of oxidation and was found to be dependent on the distribution of Y on the alloy surface. Implanted Y reduced the extent of interfacial void growth and increased the oxide film thickness. Implanted cobalt had no effect (Sprague et al 1983). Si and Y implants in CoCrAl and CoCrAlY alloys conferred resistance to exfoliation during thermal cycling (Smeggil et al 1984a, 1984b). Al implantation in NiCrAl and NiCrAlY alloys did not affect the alumina-forming characteristics or pattern. The oxide scale exfoliation of alumina formers did not seem to be automatically associated with any microstructural damage/changes brought about at the implantation stage. Implantation of $^{32}S^+$, however clearly resulted in cracked scale growth and exfoliation at $1050^\circ C$, 24 h in air. In the sulphur implanted NiCrAlY large (>1 micron) dark precipitates, of Y_2S_3 devoid of Ni, Cr and Al, were found 10 microns below the scale metal interface, while the actual implantation could not have been more than a few thousand angstroms deep (Smeggil et al 1985). This movement of sulphur inwards and Y segregation from Ni, Cr and Al can be explained in conjunction with the non-adherence of the alumina-former alloy, on the basis of the fact that yttrium which is normally available for oxide adherence is now not available at adequate levels at the metal/scale interface as sulphur getters the subsurface Y. It could be inferred that at low sulphur potentials Y_2S_3 would form preferentially even before Cr; the implanted sulphur appears to force reaction with yttrium, preventing its outward diffusion when it reaches the required activity through internal diffusion. A similar argument has been put forward earlier (Abderrazik et al 1984).

From the above discussion it may be inferred that most of the degradation studies are in oxygen or air. Very few studies are available on hot corrosion (Bhat et al 1983). Ion implantation has been used to successfully reduce the corrosion/erosion type wear of burner orifices used in oil-fired power generating plants and thereby, increase their in-service life (Bennett 1981). The process has beneficial features recognized in nuclear technology, tribology and to a good extent in most carburization/oxidation environments but has yet to be explored for adapting to more aggressive environments.

COATINGS: CHEMICAL PROPERTIES

Particular experimental areas requiring more comprehensive cover are :

Comparison of the scale (at a point in time where thickness is the same in both cases) of implanted and unimplanted substrates to shed more light on the mechanism of scale adhesion.

The variation with scale thickness of the temperature drop required to cause spalling from the implanted substrate.

Mechanistic studies in sulphidising environments as well as mixed environments.

Although ion implantation has become an accepted technique in corrosion research, it has yet to be used practically for corrosion protection. The present scale up of implantation equipment would make this economically viable. The crucial factor however, in determining the practical applicability is the demonstrated persistence of the beneficial influence of implantation on degradation.

8.2.3. DEGRADATION AFFECTED BY PROBLEM AREAS IN SUBSTRATE/COATING COMPATIBILITY

Several problems occur at the process stage which affect the coherence of the resultant substrate-coating complex. Intermetallic compound formation, diffusion, interdiffusion, effect on ductile brittle transformation temperature are the main influencing factors, which could create gradient-type changes in substrate and coating compositions in regions near the interface, create stresses, undesirable phases and precipitates, all of which could adversely influence the protective capacity of the coating. Other effects are vaporization, selective attack, mechanical strain and creep effects, effects on microstructure and phase formation, and thermal shock and fatigue.

These are discussed below with a few examples:

Intermetallic Compound Formation:- Ir coatings on Nb, Mo and W form intermetallics which reduce the original coating thickness.

Diffusion:- In Ti and TiV foils on Nb alloys, interstitial compounds (which strengthen the substrate) diffuse to an external sink (such as a coating containing Group IV elements).

In MoSi₂ coatings on Nb alloys, Ta10W, Mo alloys and W, oxygen diffuses in and embrittles Nb and Ta alloys. Mo and W form volatile oxides. The composition and coherence of the coatings are affected. MoSi₂ and NbSi₂ coatings on Nb show that Si diffusion occurs from an outer silica layer through an (Mo+Nb)₅Si₃ interlayer and depletes the coating of Si. In NiSi₂, CrSi₂ and NiCrSi coatings on Fe, IN738, IN100, Nim90 and IN601, inward diffusion

of Si reacts with an interlayer and decreases strength.

In coatings of Al, CrAl, MCrAlY etc., on IN100, nitrogen penetration forms carbonitride and stresses cause cracks. AlPt coatings on superalloys form an undesirable sigma phase due to inward diffusion.

Interdiffusion:- Coatings designed for hot corrosion resistance usually contain higher Cr and Al than the substrate component alloys. High temperature exposure over long periods increases the levels of both elements in the interdiffusion zone, which will lower the Cr and Al at the scale/environment interface and thus the renewal capacity, while also causing embrittlement at the interdiffusion zone. In 200 h at 1000°C the following surface compositional changes (at.%) at the near surface region occur as 200 micron thick oxide scale forms on a NiCrAlYSi alloy (Grunling et al 1987):

0.4Si alloy:- Al 17 to 8.5; Cr 25 to 30; Ni 43 to 55;
4Si alloy :- Al no change: Cr 23 to 29.5; Ni 48 to 31;
changes in 2%Si and 4.6% si alloy were not as significant.

At intermediate temperatures the sigma phase formation is possible. Al appears to be considerably affected by temperature gradients with a 1% drop across 10, 2.8, 2 and 1.4 mm at temperature gradients of 0, 100, 200 and 300°C/mm respectively. Increasing gradients and exposure time cause steeper profiles; grain boundary diffusion of coating elements could get enhanced which results in greater penetration depths. Decrease in low cycle fatigue limits with corrosion and interdiffusivity for LDC 2 coated IN 738 is illustrated (Grunling et al 1987).

Sputtered TiC applied as a diffusion barrier between Al and CoSi₂ breaks down at 500°C to form Co₂Al₉ and Ti₇Al₅Si₁₂ at 550°C (Applebaum & Murarka 1986). In Ni₃₀Cr, and Ni₃₀Cr₂₀W with and without 3Al, or Mo barrier layer, or W-1%ThO₂ barrier layer, or W₂₅Re barrier layer, embrittlement occurs at 1150°C due to interdiffusion and at 1250°C due to nitrogen. In Al coatings on Ta and Ta₁₀W, interdiffusion forms Ta-Al phases at 1150°C. NiAl coatings on Ni alloys degrade due to interdiffusion. Reactive diffusion occurring when exposed to high temperature over a period (termed as the soaking time) were found to induce a continuous change in the local compositions of both the coating and substrate, which in turn changed the growth of precipitates and surface oxidation. PVD-NiCoCrAlY on Udimet 520 developed the detrimental sigma-phase in this manner which affected both the microstructural stability as well as oxidation resistance. Tested on soaking up times over 500-2000 h, the system showed a sharp change between 1000 and 1500 h (Zambon & Ramous 1987).

It is proposed that three stages of interdiffusion be recognized during the degradation of a substrate/coating system. The stages can be tagged by measuring the solute loss from the coating and the variation of the surface concentration with time taking note

COATINGS: CHEMICAL PROPERTIES

of the coating thickness. In isomorphous systems with constant diffusivity, stages 1 and 3 are closely related to the coefficients of the square root diffusivity matrix [r] - an asymptotic approach to the final coating composition, and in binary and ternary systems any improvement in interdiffusion in stage 1 will be reflected likewise in stage 3. But higher order systems, including ternary show kinetic behaviour dependence clearly on the coating composition. Taking a Ni-Cr-Al system it has been demonstrated that decreasing %Cr decreases the Al-diffusion rate from the coating to the substrate. Changing %Cr in the range of 10 at.% results in a x10 reduction of the time taken to lose 50% Al from the coating (Thompson & Morral 1987).

Internal Oxidation:- In Hf20Ta coating on Ta and IrHfTa on W, oxidation occurs via coating defects at 1800°C. CrTiSi coating on Nb also undergoes similar degradation by oxidation in air via coating defects. In TaAl₃-Al coating on Ta, internal oxidation occurs in air at 1600°C.

Ductile Brittle Transition Temperature (DBTT):- Applying Cr₅Al₈ and (Fe-Cr)_xAl_y coatings on Cr5W.1Y by the pack cementation coating process causes recrystallization of the substrate due to thermal effects and increases the DBTT from 250 to 420°C. Table 8:1 lists the DBTT of typical diffusion and overlay coatings determined at a 1% fracture strain (Nicholls & Hancock 1987):

TABLE 8:1

DUCTILE-BRITTLE TRANSITION TEMPERATURE OF DIFFUSION & OVERLAY COATINGS

Coating	DBTT, °C; Range
Co-35%Al	970
Ni-35%Al	740
Ni ₂ Al ₃	570- 710
Ni ₃ Al	730 - 900
NiAl	868 - 1060
Siliconized:-	
Nimonic 105	350
IN 738LC	560
IN 939	510
Co15Cr10AlY	250
Co18Cr9AlY	235
Co23Cr12AlY	740
Co27Cr12AlY	910
Ni38Cr11AlY	430
=====	

Miscellaneous Substrate/coating Effects:-

Chromalloy W-3 and PFR-30 on Nb alloys: Coatings vaporize; poor adherence, cracking, non-uniformities, occurring in air at 1420°C.

SiO₂ and CeO₂ on steels: Iron oxides destroy coating.

ZrO₂ (MgO or Y₂O₃ stabilised): Vanadates (from diesel fuel combustion) attack the MgO or Y₂O₃.

SiO₂ on 9Cr-steel: Cracks due to mechanical strain allows oxidation in CO₂.

Al on Fe alloy: Phase transformation occurs and Al-deficient FeAl phase starts to degrade in air at 750°C.

NiCrAlY/Pt coating: Coating thermal process affects substrate microstructure and creep strength.

ZrO₂-12%Y₂O₃/Ni16Cr6Al.6Y duplex coating on superalloys: Salt melts absorbed by coat porosity and then thermal shock failure follows; acid fluxing hot corrosion mechanism also occurs. The problems however, are not universal but dependent on the service arena.

8.3. ENVIRONMENTAL CONDITIONS FOR COATING DEGRADATION

Table 8:2 surveys the many types of coatings and process routes used in high temperature environments. Table 8:3 surveys the substrate/coating/environment interaction situation and effects. Chapter 1 has introduced the problems encountered in high temperature systems. Microstructure (Buhler & Hougardy 1980) and diffusion profile studies have provided the means for selection of coating component elements (Fitzer & Maurer 1979).

8.3.1. FLUIDIZED BED COMBUSTORS - COAL GASIFIERS

Fe-Cr-based alloys are the predominant structural materials and are also coating candidate materials. Ni and Co, in large proportions are detrimental to the coating or alloy service life and are not cost-effective for the industry, being more expensive than iron to produce and fabricate. The problem areas are summarised in Table 8:4 and Fig.8-2.

High temperatures and pressures prevail in the processing components for coal preparation and feeding systems, and the effluent streams vary from slag and liquid slurries to gas entrained with fly ash. Erosion-corrosion including wear is a problem of equal or greater magnitude than hot corrosion itself, in coal combustion and fluidized-bed systems (Raask 1988; Wright 1987).

TABLE 8:2

TEMPERATURE & ENVIRONMENT INTERACTION - THE RESPONSE OF THE ALLOY EXPOSED TO HOT CORROSION, EROSION & WEAR

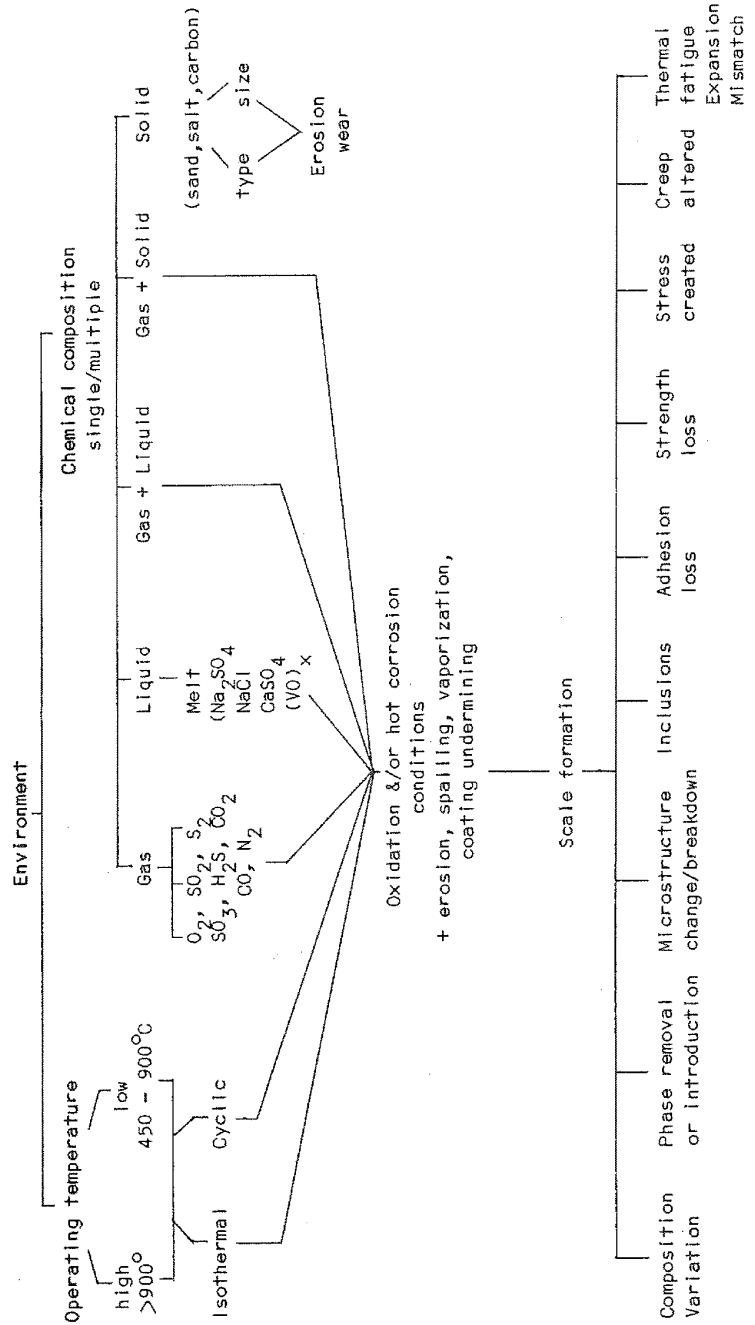


TABLE 8:3

CHARACTERISTICS OF COATINGS OBTAINED BY DIFFUSION PROCESSES(A) & BY OVERLAY(B)
 (A Survey of interest to service in high temperature and hot corrosion environments)

Coating Process	Type	Average Coating Thickness, μm	Advantages (coded)	Coating Material
PVD - sputtering, evaporation, ion-implantaion, ion-plating.	B	75-100 (can vary)	(b),d	Ce, CoCrAlY, FeCrAlY NiCrAlY, NiCoCrAlY, ZrO ₂ (Y ₂ O ₃)
CVD -inert/vacuum media	A,B	Variable	b	Al, Ni-Cr, Si, SiB, TiSi SiO ₂
CVD - pack cementation	A	100	b	Al, AlPt, Cr, CoNiCrAlY, Si, SiAl
Spray - vacuum and air plasma, d-gun, flame, slurry laser spray, plasma sintering.	A,B	150-400; can be varied	a,(b),c,d	Al-Si, CoCrAlY, FeCrAlY, NiCrAlY, NiCoCrAlY, Ni-Cr-Si
Cladding, Surfacing	B	Can vary	a	NiCrSi
Sol-gel	B	1	(c)	Ceria, SiO ₂
Galvanic	A	100 can vary	(c)	Ce, Cr, CrFe

Code: a - suitable for repair work; b - good adhesion; c - suitable for thermal barriers; d - Composition can be easily varied. Brackets indicate average performance.

=====

COATINGS: CHEMICAL PROPERTIES

Conventional combustion systems (steam boilers), atmospheric and pressurized pressure fluidized-bed combustors (AFBC,PFBC), and some gasification systems use pulverized and sized coal. Coal-oil mixtures, coal-water mixtures are used which reduce emissions of oxides of nitrogen. Coal washing is done in some cases, to reduce sulphur emissions. Gasification reactor systems have compromised in efficiency to circumvent materials design problems required by the advanced systems proposed in the 1970s. The cool water integrated gasification unit is one such operational plant. Erosion-corrosion is a severe problem in coal liquefaction systems, and rapid corrosion of equipment in the distillation stage was found to be due to the concentration of amine hydrochloride fractions with a boiling point of 240^o-280^oC (Keiser et al 1981). WC-Co coatings have retarded the erosion problem but are expensive to renew very frequently. Borides, carbides and nitrides have also been tested for erosion control with Si₃N₄ giving the best erosion-hot-corrosion resistance (Wright 1987). Cladding and LPPS coatings are generally used.

Boiler Tube Failures & The Problem Spectrum

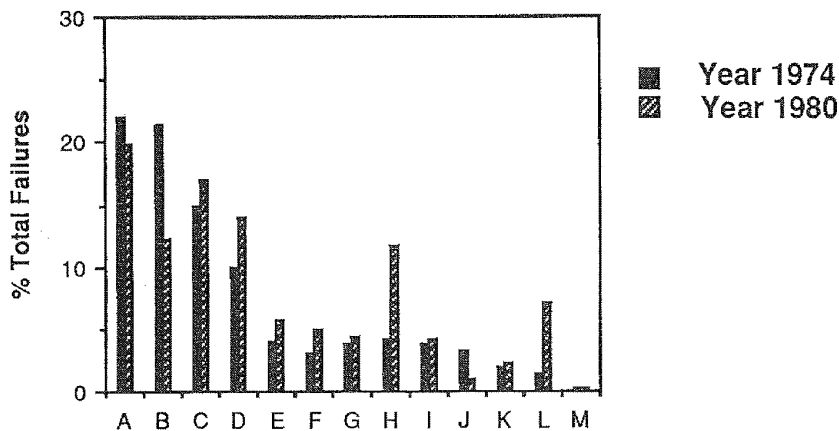


Fig.8-2

Column	Cause of Failure	Column	Cause of Failure
A	Mechanical Design	B	Weld Defects
C	Excessive Heating	D	Erosion of Sootblower
E	Corrosion due to water & Steam	F	Blocking Effects
G	Mixed Causes	H	Erosion due to Dust
I	Defects in Tubes	J	Wrong Materials
K	Mechanical Damage	L	Fireside corrosion
M	Other Operational Factors		

TABLE 8:4

CORROSION ASPECTS WHICH HAVE CAUSED NEAR-TOTAL SHUT-DOWN OF PULVERISED COAL-FIRED PLANTS

Corrosion Areas	Status
Dew-point Corrosion: Air heaters, ducting and stack locations	Alternative material for mild steel not yet in full operation; mechanism of attack reasonably clear; replacement economics under review.
Exfoliation: Oxide scales on ferritic & austenitic re-heaters and s/h steels; shut down caused via tube blocking and turbine erosion.	Spalling in austenitic steels predictable and under control; Ferritic spalling predictable but less clear for compensation.
Furnace using coals high in sulphide/chloride - damage of furnace wall tube.	Existence diagrams of the oxide-sulphide-chloride regimes vs temperature on many resistant alloys and mild steels are available. The mechanism of chloride effect and influence of carbon and sulphides are reported.
Heat flux effects	Corrosion rates predictable theoretically; plant data available; controlled investigations not widely reported.
Integrated action of stress-strain-oxidation at stress points/transition joints on gas and and steam sides.	Maximum threshold of effects predicted theoretically. Some pilot investigations available in published literature.
Multi-lamination and oxide-thickening of Superheaters and re-heaters on the steam-side. Superheater tube the coal used. corrosion.	Predictability reported; laboratory simulation not known to be reported. Damage caused by high sulphide/chloride coals documented. Corrosion mechanism yet to be clearly explained vis-a-vis the coal used.

=====

The environment in coal gasification is predominantly reducing unlike in a gas turbine with oxygen potential varying over a large range of 10^{-1} - 10^{-14} in a cyclic pattern. The temperatures are not very high but in the region of 650- 900°C. Because steam and limestone are used, the environment has H_2/H_2O , $CaO/CaSO_4$ reactions as well as those of C/CO , CO_2 , S_2 and some chloride.

COATINGS: CHEMICAL PROPERTIES

Thus the reaction environment consists of S_2 , SO_2 , CO , CO_2 , H_2S , H_2O , HCl , with carbon and unreacted fuel particles, with CaO and $CaSO_4$ creating erosion conditions (Meadowcroft & Manning 1982). In the U.K. furnaces operate around 160 bar at $350^\circ C$, and the heat exchanger units run at a metal surface temperature of $450^\circ C$ in the evaporator tubes and $650^\circ C$ in the superheater tubes. Co-extruded tubes are feasible if fabrication of the 50Ni-50Cr clad can be overcome, so that the niobium-stabilized Type 310 steel component can be replaced with another class of steel as the inner tube (Meadowcroft 1987).

3.3.2. THE GAS TURBINE ENVIRONMENT

The environment presented during the operations of a gas turbine is complex and variable but mainly oxygen-rich with sulphur and chloride as chemical contaminants and erodents such as salt particles and pyrolytic carbon. An appraisal of surface-oriented problems for gas turbine applications appears to be as shown in Table 8:5 (Pettit & Goward 1983).

TABLE 8:5

<u>Problems</u>	<u>Aircraft</u>	<u>Marine</u>	<u>Utility</u>
Oxidation	Small	Medium	Medium
Hot Corrosion	Medium	Large	Small
Interdiffusion	Medium	Large	Medium
Thermal Fatigue	Small	Medium	Large

Table 8:6 indicates the factors leading to degradation and the environmental conditions which are conducive to create them. Table 8:7 summarises the industrial turbine environment.

Gas turbines are run on a wide range of fuels from natural gas and high sulphur diesel to the highly refined aviation fuels. The ambient atmosphere is generally highly oxidizing with a high air to fuel ratio. The flame temperature reaches $2000^\circ C$. The full potential of the hot gases from the combustor confronts the blade section, with the thermal energy from combustion transformed to mechanical energy. The role of protective coatings is to maintain the integrity of the blades and guide vanes over extended periods. Cooling passages in the blades keep their temperature down. The first stage nozzle guide vane with a low design stress is the hottest at $900-1150^\circ C$ and is subjected to severe thermal stresses and hot corrosion. The turbine rotor blade suffers a high creep stress because of the centrifugal force; it also undergoes thermal cycling and mechanical fatigue at $800-1050^\circ C$, the second stage vanes and blades operate about 100 degrees below that of the first stage.

TABLE 8:6
LEVELS OF LOADING EXPECTED IN GAS TURBINES FOR AIRCRAFT APPLICATIONS

Type	Type of Loading	Effective Limits of Parameter	Detrimental effect
Mechanical	Centrifugal stress	170 N/mm ²	Cyclic strain in all temperature ranges
	Stress gradients:		Formation of cracks in the coating
	i. local	e.g. + 30 N/mm ²	
	ii. time-dependant (temperature & gas pressure variations)		
	Gas velocity	up to 600 m/s	Stripping of the coating erosion, mechanical removal
	Impact by external media		Spalling of the coating
[T, σ : lifetimes from 1000h to 5000 - 10,000h]			
Chemical	Oxygen excess	12% by volume	Oxidation and corrosion depletion across surface or local attack
	Fuel contamination, e.g. sulphur	0.3w/o permissible 0.01w/o usual	Alloy impoverishment
	Air intake contamination, e.g. sea salt, industrial atmosphere	up to ~1 ppm	Roughening of the surface
	Pressure	up to 25 bar	
	Flow rate	up to 600 m/s	
Thermal	Temperature range: in combustion gas	up to 1400°C	Diffusion processes
	in component local	up to 1050°C	Changes in structure
	Temperature gradients influenced by time	up to 200°C/mm up to 100°C/s	Mechanical stresses

COATINGS: CHEMICAL PROPERTIES

TABLE 8:7

SERVICE CONDITIONS IN HEAVY DUTY INDUSTRIAL
GAS TURBINES

Pressure	: p = 10 bar approx.
Max. Gas Velocity	: 300 m/s
Mechanical Stresses	
During Operation	: up to 16Nmm^{-2}
Frequency Range	: 150 - 2000 Hz
Temperature Variations:	200°C/min.
Temperature Gradient	
(normal to surface)	: 200°C/mm
Deposit Constituents	: 1 mg/m^3
	CO, CO ₂ , SO ₂ ,
	SO ₃ , H ₂ O, O ₂ ,
	N ₂ , CaO, MgO,
	K ₂ O, SiO ₂ ,
	Fe ₂ O ₃ , Zn, V,
	SO ₄

Turbines which operate under marine conditions ingest salt from the sea. In general, industrial aero-engines last longer than military craft. The high altitude aero-engines use highly refined fuels and pure air; coatings under these conditions are subjected to high temperature oxidation. Low altitude marine engines use lower quality diesel fuel in salty air under gas + solid conditions, an ideal condition for hot corrosion over a wide temperature range. V/STOL aircraft engines are subject to severe cyclic stresses leading to thermal fatigue. Turbines used in power generation use medium to low quality fuel and face hot corrosion by vanadium and sulphur products and erosion problems. An alumina coating for instance, may go through a damage and repair cycle with adequate reserve of aluminium activity in an oxidation-erosion environment. A hot corrosion environment could flux the Al₂O₃ compelling support by Cr₂O₃ with a duplex, triplex and multicomponent coating. It has been shown that attack from contaminants can be a high probability because both Na and K can build up to high levels of concentration if untreated potable water is used for water injection which later evaporates (Hsu 1987). Erosion and abrasion are caused by sand, salt or carbon particles (EUR 1979).

Na₂SO₄, NaCl, and in some cases, vanadic oxides present the additional threat of molten salt which changes high temperature oxidation into hot corrosion conditions. However catastrophic corrosion can occur if a molten reaction eutectic product can form in purely gaseous conditions (Simons et al 1955; Hocking 1961; Vasu 1965; Alcock & Hocking 1966; Hancock 1968; Viswanathan & Spengler 1970; Vasantasree 1971; Brown et al 1970; Vasantasree & Hocking 1976; Holder et al 1977; Mrowec & Werber 1978; Birks 1970; Wood et al 1978; Strafford 1976). The reactant environment

is composed of O_2 , SO_2 , SO_3 , Na_2SO_4 , $NaCl$ with sand, salt and pyrolytic carbon particles. The superalloys used in gas turbines are mostly Ni-Cr- and Co-Cr base, the Fe-Cr- base alloy series being used mostly under reducing conditions like in coal gasifiers, fluidized-bed combustion and in nuclear technology.

Degradation in gas turbines is predominantly temperature oriented, be it hot corrosion by chemical factors or corrosion induced by physico-mechanical factors, with cyclic conditions aggravating all types of corrosion. The temperature parameter is classified in three main ranges, where the low range is set over $600-750^\circ C$, the intermediate over $800-900^\circ C$ and the high range above $1000^\circ C$. The regions $750^\circ-800^\circ C$, and $900^\circ-1000^\circ C$ are overlap regions and are dependent on the specific alloy and coating system. All other working conditions are complementary. Most of the studies reported are carried out at atmospheric pressure but some high pressure rigs and high pressure laboratory studies have also been carried out (Conde et al 1982; Ma et al 1984; Ma 1983).

Interdiffusion plays an important role; coalescent Kirkendall voids reduce adhesion strength and cause coating failure by substrate parting; creep and thermal fatigue are common modes of turbine degradation. At high temperatures Al in an aluminide or an MCrAlY not only undergoes oxidation but it also diffuses inwards into the base metal (Smialek & Lovell 1974). At $1100^\circ C$, a CoNiCrAlYTa coating put through cyclic oxidation was shown to undergo interdiffusion with Co and Cr diffusing inwards while Ni diffused outwards (Mevrel & Pichoir 1984; Peichl & Johner 1986). In a NiCrAlZr/Ni22Cr system the Al was completely consumed in 15 h at the same temperature (Nesbitt & Heckel 1984). Linear porosities created by Kirkendall voids could reach as high as 70% in 400 h at $1100^\circ C$, and such porosity can lead to separation of coating from substrate even without any external influence (Peichl et al 1985; Gedwill et al 1982). Alloys such as MOO2 which contain W (9.5 wt% in this case) tend to form W-rich plate-like and cubic phases over quite narrow temperature ranges, e.g. found at 1050° but not at $1100^\circ C$ in this case (Peichl & Johner 1986). MCrAlY coatings tend to develop precipitates of needle-like phases, often described as sigma-phases at the substrate/coating interface (Grisaffe 1972; Pichoir & Hauser 1980; Moorhouse & Murray 1979; Lang & Tottle 1981). These acicular precipitates induce embrittlement and introduce intergranular cracks proceeding to transgranular paths in the coating. Plate-like precipitates on aluminided IN100 showed nitrogen in Auger analyses at 95-101 ppm levels in the precipitates, against the 14-20 ppm in the alloy, which was tied up with Ti(C,N) and formed between 800° and $1000^\circ C$ with a maximum at $950^\circ C$ (Meisel et al 1980).

Localized low temperature hot corrosion occurred in CoCrAlY coating on a Stage 1 blade of LM2500 high pressure turbine after 600 h on a North Sea oil platform. Internal oxidation with a corresponding volume increase had generated enough mechanical stress to cause spalling. The influence of a molten salt attack was evident

COATINGS: CHEMICAL PROPERTIES

after 10000h. Spitt defect incorporated during the EBPVD of a CoCrAlY caused lifting and spalling of coating on a similar turbine blade after 21500 h in service at intermediate temperatures. Other defects which can be EBPVD-process generated are leaders and flakes. Alloys with high chromium levels are reasonably resistant to intermediate temperature attack, but not lower chromium alloys which require protective coatings. Additions of Hf, Zr, Pt, Ce and Ta to MCrAlY-type coatings have improved the service-life. Superalloys are normally used in a coated state for high temperature operations because of the danger of losing Cr by formation of its volatile oxide CrO_3 . Single crystal alloys, directionally solidified alloys and mechanically alloyed products have brought in considerable improvement in service life. 1% Hf incorporated as a laser-clad alloy with Ni, Cr and Al in the ratio 10:5:1 was found to improve oxidation resistance at 1050°C of Inconel 718 when clad by underfocus lasing rather than an overfocus deposit. The NiCrAlHf alloy clad was uniform in the second phase with undissolved Hf particles. The reduction in oxidation rate was reasoned to be due to competitive reactions wherein the HfO_2 would act as sinks for excess vacancies, thereby reducing void formation and thus improving adhesion (Singh et al 1987).

Aluminiding with and without Pt, MCrAlY and thermal barrier layered coatings are further advances made in gas turbine alloy coating technology. Degradation in these coatings occurs by preferential loss of one phase, e.g. beta phase reduction in CoNiCrAlY produced by LPPS after 600 h cyclic oxidation at 1050°C in a hot gas stream of 0.3 Mach and cyclic frequency of 1/h; the coating however, was still sound. An uncoated single crystal Ni-base superalloy MOO2 collected sub-surface voids within 400 h under the same conditions. A Pt-modified aluminide coating was observed to have the subsurface voids covering the whole of the gamma-prime depleted zone (Peichl & Johner 1986). Many overlay formulations of cobalt alloy compositions have also been made (Coutsouradis et al 1987).

A qualitative survey of gas turbine alloys hot corrosion resistance is shown in histograms, Fig. 8-3 to 8-7.

Gas Turbine Hot Corrosion Resistance, Isothermal, 700°C

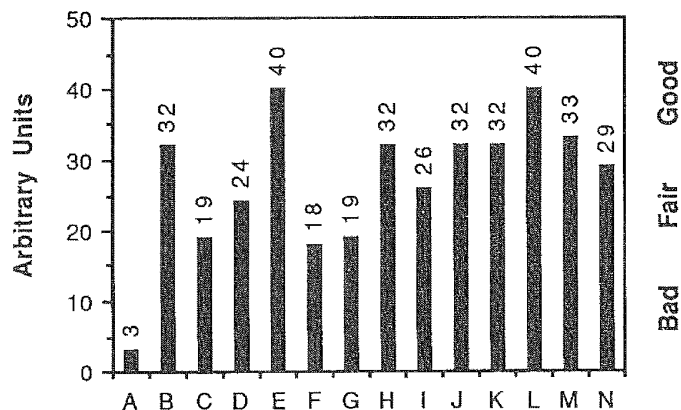


Fig.8-3: Hot Corrosion Resistance of Coated Superalloys

Legend	Substrate	Coating and Conditions
A	Superalloy	ZrO ₂ (pSO ₃ = 10 ⁻²)
B	Superalloy	ZrO ₂ (pSO ₃ = 10 ⁻³ , no salt)
C	*	CoCrAlY
D	Superalloy	CoCrAlY
E	*	Co26Cr11AlY
F	*	CoCrAlY
G	Superalloy	CoCrAlY/Pt
H	Superalloy	Pt/CoCrAlY
I	*	NiCoCrAlYHf
J	*	NiCoCrAlY
K	*	NiCrAlY
L	*	NiCrSi
M	IN738LC	Cr
N	Nim80A	Cr

Note: *indicates that the substrate used was not stated. Pre-annealing, NaCl content of test environment and other conditions cause big variations in hot corrosion rates. For these reasons it is very difficult to produce even semi-quantitative histograms like the ones displayed.

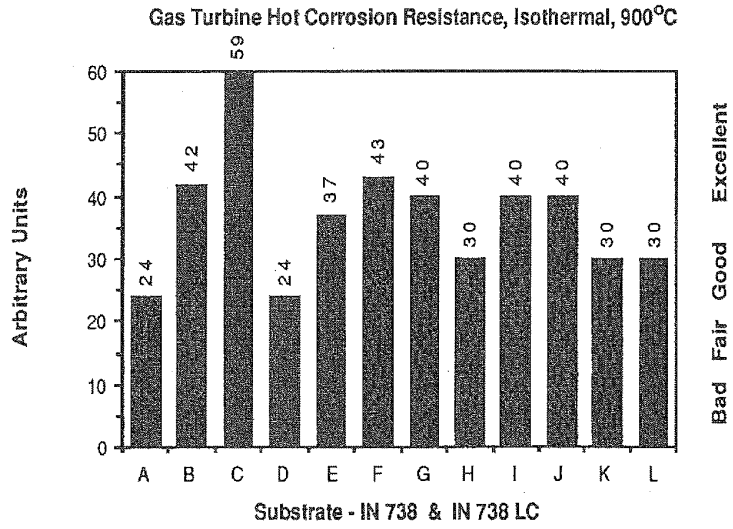


Fig.8-4

Legend	Substrate	Coating & Conditions
A	IN738	none
B	IN738	NiAl
C	IN738	57Co25Cr3Al10Ni5Ta0.2Y
D	IN738LC	none
E	IN738LC	Cr
F	IN738LC	Si
G	IN738LC	Si-Ti
H	IN738LC	CrNiSi
I	IN738LC	CoCrAlY
J	IN738LC	CrAlY
K	IN738LC	CrAlCe
L	IN738LC	PtAl

Gas turbine Hot Corrosion Resistance, Isothermal, 900°C

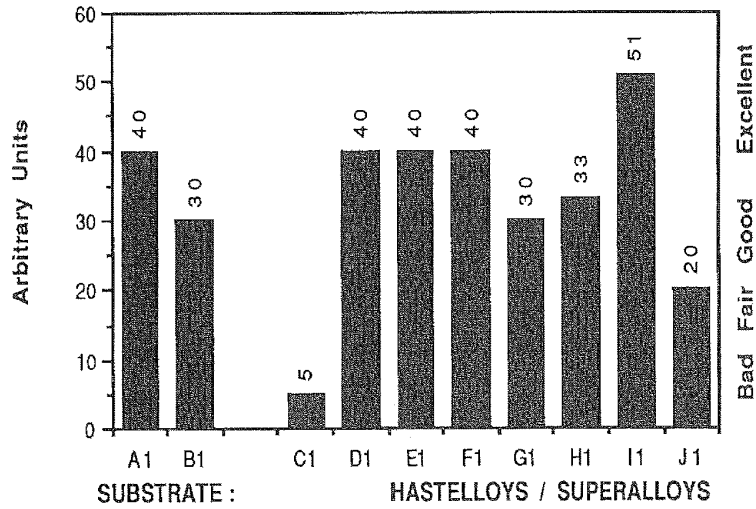


Fig.8-5

Legend	Substrate	Coating & Conditions
A1	Hastelloy-X	CrAlY
B1	Hastelloy-X	CrAlCe
C1	Superalloy	Ni16Cr6Al0.6Y/ZrO ₂ .12Y ₂ O ₃ duplex coat
D1	Superalloy	Ni20Cr11Al0.4Y/ZrO ₂ .8Y ₂ O ₃ duplex coat
E1	Superalloy	2CaO.SiO ₂
F1	Superalloy	MgO-NiCrAlY Cermet
G1	Ni-Superalloy	PtAl
H1	Superalloy	CoCrAlY
I1	Superalloy	ZrO ₂ (pSO ₃ , no salt)
J1	IN700	CrAl

Gas Turbine Hot Corrosion Resistance, Isothermal, 900°C

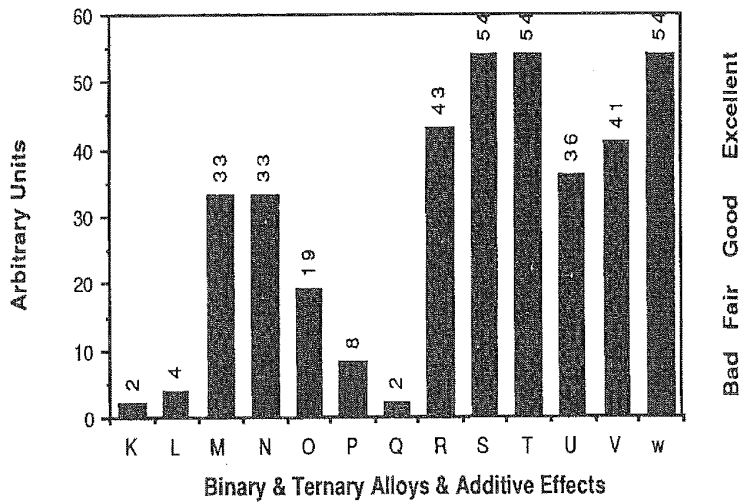


Fig.8-6

Legend	Substrate	Coating / Conditions
K	B1900	none
L	Ni20Cr	none
M	Ni20Cr	Si^
N	Ni30Cr	Ni25Cr12Al1.1Y^
O	Co30Cr	Co22Cr6Al1.1Y^
P	Ni8Cr6Al	none
Q	Ni6Cr6Al16Mo	none
R	Ni15Cr6Al	none
S	Ni16Cr3.4Al	none
T	Ni16Cr3.4Al2Mo2W	none
U	Ni16Cr3.4Al2Mo2.6W	none
V	Ni16Cr3.4Al2Mo2.6W0.1C	none
W	Ni25Cr3.4Al2Mo2.6W0.1C	none

^only cases wherein coatings have been applied; others have been tested as individual candidate coating materials.

Gas Turbine Hot Corrosion Resistance, Isothermal, 900°C

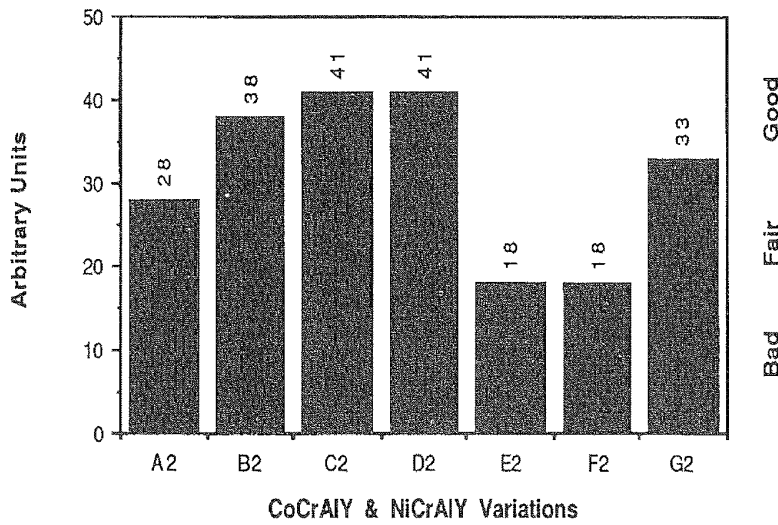


Fig.8-7

Legend Coating /Single Material Tested *

- A2 CoCrAlY*
- B2 CoCrAlY*
- C2 Co26Cr11AlY*
- D2 CoCrAlHfPt*
- E2 NiCrAlY*
- F2 NiCoCrAlY*
- G2 NiCoCrAlYHf*

*Authors do not state the substrate

8.3.3. NUCLEAR TECHNOLOGY AND TRIBOLOGY ENVIRONMENTS

Corrosion problems in reactors are mostly encountered in the coolant and sealing systems. Carburizing and oxidation forms of degradation prevail which result in highly active oxide spallation. Carbon deposition interferes with heat transfer and causes erosion and crevice corrosion problems. The reactant environment is generally composed of $\text{CO}_2 + 2\% \text{CO}$ with 300-350 ppm CH_4 , 200-300 ppm H_2O , 200-300 ppm H_2 . Carbonaceous deposition occurs from the catalysed degradation of a gas phase precursor derived from methane radiolysis, with the Fe and Ni constituents of the catalyst steel (Bennett et al 1984; Bennett 1982). Oxidation can be controlled and is not a serious problem but carburization is. Mechanical wear and abrasion is aggravated at high temperatures. Coatings vary from electroless Ni on steel for protection at 100°C in pressurised water reactors against boric acid, to aluminides and other coatings for much higher temperatures (Gras 1987).

Systems are tested in prototype nuclear processes for assessment. Be on steel, Monel, Mo, Cu and graphite (Dua et al 1985), and TiC on Mo (Fukutomi et al 1985) are used to reduce plasma contamination and power loss in Tokamak nuclear fusion reactors. Helium coolant in high temperature gas-cooled reactors can cause corrosion due to impurity inclusions such as CO, CO_2 , H_2 , CH_4 and H_2O . Incoloy 800, Nimonic 75 and Inconel 617 have been tested. An instability temperature T_i is tagged & found to be alloy dependent, particularly with activity of Cr. CO forms as a reaction product between the surface oxide and the carbon in solution and initiates the damage. T_i was found to be 907°C for IN 800H and 807°C for Nimonic 75. Decarburization occurs in the latter alloy at 850°C . Wet helium was found to suppress this reaction in IN 800H and reduce it in Nimonic 75 (Grimmer et al 1987). This temperature dependence is clarified further into three regions, and for Inconel 617, below a critical temperature of 830°C simultaneous oxidation and carburization occur in the helium coolant. Carburization reoccurs at 930°C with evolution of CO, thus severely limiting the alloy function. Between these two temperatures normal oxidation as in undiluted oxygen-containing gases, occurs (Christ et al 1987). Thermon 4972 is found to be similar to Inconel 617 in mechanical and creep rupture properties but with superior oxidation properties due to the formation of $\text{Mn}_{1.5}\text{Cr}_{1.5}\text{O}_4$, which prevented both further oxidation as well as a carbon transfer process (Huchtemann & Schuler 1987). Enhancement of oxidation by tellurization has also been recorded for an SUS 316 stainless steel fast reactor fuel cladding (Saito et al 1987). Significant reductions in weight gain and oxygen penetration of V-15Cr-5Ti (a blanket alloy for fusion reactor) was found when it was covered by vapour deposited Cr. The environment was He with 100 vppm H_2 impurity at 650°C . Without the protection of Cr, vanadium oxides cause severe degradation above 600°C (Tobin & Busch 1987).

The main concern of all aspects of degradation in nuclear technology is that the industry has to have a very long-term, fool-proof solutions to all its problems in view of the prospective risks involved when failure occurs. Physical degradation, and tribological aspects predominate over chemical degradation; this has been discussed in Chapter 7. The temperature range is wide from 100° to 650°C in which ferritic and austenitic steels as well as low carbon steels are employed. Chemical degradation is viewed in conjunction with the reducing effect of liquid sodium coolant in fast breeder reactors, where Na can reduce the protective oxides on steel by forming sodium chromite. This leads to the exposure of the bare metal to problems such as wear, fretting, static adhesion, galling and friction. 40 micron thick aluminide coatings on IN 718 which are fabricated as slip rings to fit recesses of grid plate holes have been successful. The coated material withstood more than 3000 cycles between 530°-200°C and damage was negligible even up to 627°C. D-gun coatings are under review (Lewis 1987).

8.4. CHEMICAL DEGRADATION MECHANISMS

8.4.1. GENERAL:

The environmental conditions discussed in the previous section show that the chemical factors controlling and influencing degradation are composed of several reactants under cyclic and isothermal conditions and mixed situations such as erosion and stress. The coating which confronts them is often as nearly multicomponent as the substrate itself. The mechanism by which a multicomponent substrate/coating/reactant configuration leads to coating degradation and termination of component service life is, needless to say, complex.

The fundamental thermodynamic and kinetic principles which govern the primary reactions are available in the references listed and are beyond the scope of detailed conventional treatment here. The judgement that has to be exercised in the context of practical systems is in deciding how far results from an equilibrium state or a simple system can be extrapolated. Many reactions occur in a non-equilibrium state, the phase rule could be inapplicable and mass transfer and heat transfer reactions have to make assumptions not always valid. Yet, fundamental studies are vital to an understanding of the problem, especially in understanding diffusion phenomena. This section merely introduces work carried out in the fundamental field with reactions involving only air and oxygen for oxidation, followed by the more complex hot corrosion, sulphidizing, sulphating and carburizing reactions. The influence of NaCl which was recognized at a very early stage of gas turbine research by investigators in the U.K. and in other countries in Europe, is also considered. This chapter also includes a summary of the outcome of a panel meeting for a co-ordinated attempt at

COATINGS: CHEMICAL PROPERTIES

addressing fundamental aspects of high temperature corrosion which warranted further research (Rahmel et al 1985).

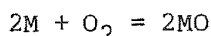
The general flowsheet for surveying the degradation mechanism starts with three main parameter blocks (Table 8:8):

TABLE 8:8

a. The Coating	b. The Environment	c. The Temperature
1. all metallic	1. all gas	1. low isothermal
2. all ceramic	2. gas+solid	2. high isothermal
3. metal & ceramic	3. gas+liquid	3. cyclic with iso-thermal residence periods
	4. gas+liquid+solid	

A few simple cases of chemical reactions with oxygen as the reactant are considered in the following three sections.

8.4.2. CASE 1: Bivalent metal + Oxygen = Metal Oxide



$$\Delta G^{\circ} = RT \ln pO_2; \text{ or, } pO_2 = \exp (\Delta G^{\circ} / RT), \text{ where,}$$

pO_2 is the equilibrium oxygen pressure and ΔG° is the free energy of formation for the reaction as written at T, the temperature in Kelvin. This is the baseline for a typical oxidation reaction. Most metals, precious metals excepted, form stable oxides at prevailing oxygen pressures at almost all temperatures. A few exceptions are elements such as Si, Mo, W and Cr, which can also form volatile oxides under certain operating temperatures and pressures. Fig.8-8,a-c, show the scale growth monitored as mass change viewed w.r.t. time.

(i) If the oxide scale is dense and protective, the scale growth will follow parabolic kinetics (Fig 8-8a) expressed as

$$dw/dt = k_p/w$$

where w is the weight change per unit area (can be expressed also in terms of oxide scale thickness, or thickness of metal lost/reacted or consumed), with time t, over an area A; k_p is the parabolic rate constant. The oxide layer, if coherent and completely covering, becomes a barrier between the coating it covers and the reactant, and with time, the oxidation rate levels off to a low value.

(ii) A non-protective scale will follow linear kinetics as in Fig.8-8b; the coating continues to oxidize until all of it is

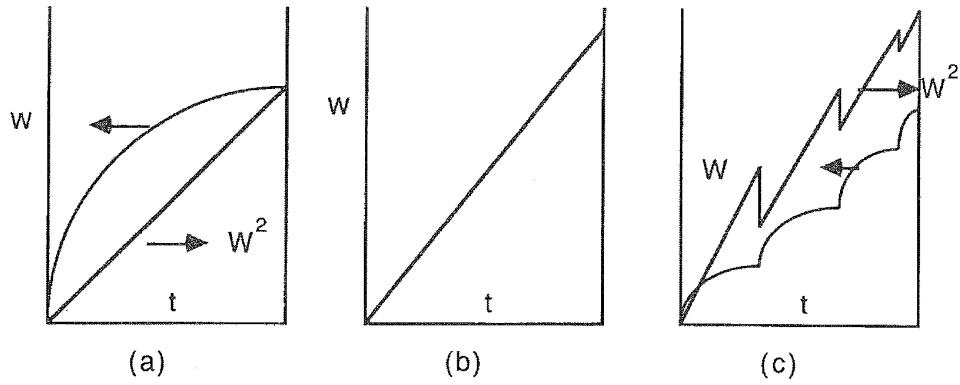


Fig.8-8 (a,b,c): Scale Growth Kinetics

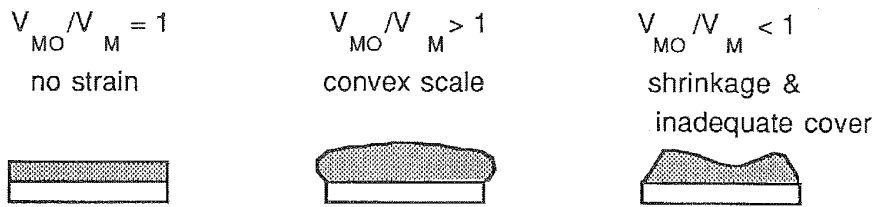


Fig.8-9 (a,b,c): Scale/Substrate relationship

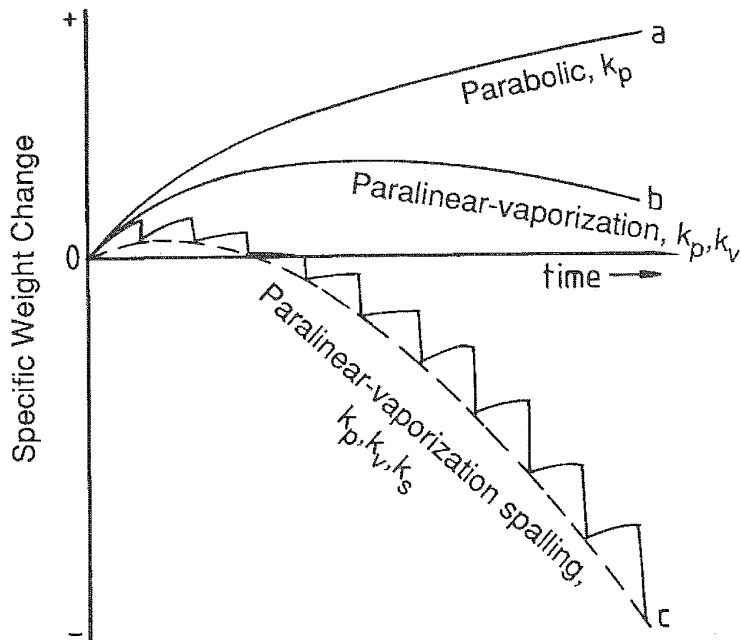


Fig.8-10: Typical Modes of Weight Change with Time for Different Types of Oxidation Behaviour.

COATINGS: CHEMICAL PROPERTIES

consumed.

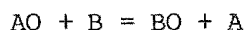
Cases (i) and (ii) in Fig. 8-8 illustrate the simple configuration $a_1 + b_1$ at c_1 or c_2 (using notation given in Table 8:8). When the configuration $a_1 + b_1$ at c_3 prevails, then the physical and mechanical stability of the oxide MO is subjected to the thermal stress-fatigue situation. The oxidation pattern shown in Fig. 8-8c will then occur. The ratio of metal oxide molecular volume: metal atom volume influences the strain under which the metal oxide is stretched (or convoluted) laterally on the metal surface (Fig. 8-9 a,b,c). The stress causes spalling even in isothermal conditions resulting in a make and break pattern. This is aggravated under thermal cycling conditions, c_3 . Configurations, especially a_3 with b_4 and c_3 , present the most aggressive conditions, introducing mechanical and physical factors to interact with chemical reactions, demanding scale adherence, strength, plasticity to accommodate thermal stresses and fatigue. Equations relating temperature and stress to predict the initiation of spallation have been proposed (Evans & Lobb 1984). Vaporization of one or more of the products along with constitutional changes arising from diffusion and phase related problems, when more than one metal is involved, push the substrate/coating endurance to extreme limits. Fig. 8-10 shows the mode of weight change with time when protective oxide, vaporization and spalling occur during oxidation.

8.4.3. CASE 2: Multiple elements + Oxygen = Multiple oxides:

The oxidation of each metal is governed by its activity in the alloy and the free energy of oxide formation; a metal oxide of higher negative free energy (lower equilibrium p_{O_2}) can form at the dissociation pressure of an oxide with a higher p_{O_2} of oxide formation. Scale growth and oxide predominance is temperature dependent and is determined by the relative diffusion rate of the species, with the most stable oxide not necessarily being that with the most negative free energy.

More than one layer can develop in a scale. Thus:

$$(p_{O_2})^{1/2}_{(A, AO)} = [\exp(\Delta G_{AO}^O/RT)]/a_A,$$



$$a_A/a_B = \exp[(\Delta G_{AO}^O - \Delta G_{BO}^O)/RT], \text{ where,}$$

p_{O_2} = the oxygen potential, A and B are the two metals with the oxide of A reacting with B to form the oxide of B, and a = the activity of A or B as subscripted.

Ideally, all the metal oxides which are thermodynamically stable at the prevailing temperature and oxygen pressure should form in the same relative proportions as their activities at the coating-

/environment interface (not necessarily their activity in the alloy). A single oxide which is the most stable and can grow with lateral coverage predominates, or more than one oxide species which are more stable than the rest can form to produce mixed oxides. However, with time, diffusion, displacement as well as dissociation reactions interfere; and, the oxidation kinetics of just one or two of the constituents can predominate. There is very little basic thermodynamic data on spinel formation but spinels have been reported (Pettit & Goward 1982; Wood et al 1965, 1966, 1967, 1969, 1970a,b). Under isothermal conditions with protective scale growth, but for an initial depletion in the alloy constituents, particularly that of the predominant oxide, stable conditions will prevail. Under all conditions which lead to spalling or unlimited scale growth, there will be progressive element/s depletion at the alloy/scale interface to some depth into the alloy, with the alloy showing a deficit in the most predominant element that forms the oxide.

The operating temperature has a strong influence on oxide predominance. Thus a Ni-20Cr alloy at 700°C is predominant in NiO while at 900°C it is Cr₂O₃-rich. Ni-Cr-Al alloys can be NiO-, Cr₂O₃- or Al₂O₃- formers as the %Cr and %Al in the alloy are increased. This mode of selective oxidation is manipulated for the benefit of achieving protective coating. The transient oxidation period over which selective oxidation occurs varies from alloy to alloy. Coating alloys are developed to have very short transient periods of oxidation of the order of seconds while structural alloys have an extended transient oxidation stage extending to a number of hours and days.

In service, thermally induced stresses are primarily responsible for the cracking and spalling of scales. Apart from the oxide thermodynamic stability, its plasticity becomes important. The most stable oxide again predominates during selective oxidation and with each subsequent scale repair step the transient oxidation period becomes longer. Eventually the alloy becomes severely depleted in the element that is selectively oxidised and a continuous scale growth of that oxide will cease. Degradation steps up as less stable oxides start forming incoherently, leading to eventual failure. Cr as an additive is an ideal example of this situation. Chromia, alpha-alumina and silica are used as effective barriers and coating alloys are designed for their selective formation. Chromia and silica however, are not stable as they can form gaseous products like CrO above 1000°C, and SiO at low pO₂ as reaction products.

Four aspects are important in selective scale growth, retention and re-growth:

- (i) The selective oxide must be capable of good lateral growth,
- (ii) Diffusion processes must be slow once the 'barrier is up',
- (iii) The alloy must have adequate activity of the metal for replenishment of the selective oxide which needs to re-form when damaged. [Coatings unlike substrate alloys are bound to

COATINGS: CHEMICAL PROPERTIES

fail in this aspect, because of their limited 'resources'],
(iv) Perhaps the most important - the oxide must have excellent thermal fatigue resistance.

Alpha-alumina formed on CoCrAlY offers an excellent example although there is much controversy about the actual mechanism by which rare earth additions influence scale retention. Some workers argue on mechanical keying and pegging effects, i.e. influence on scale nucleation, development and morphology (Whittle & Boone 1980; Whittle & Stringer 1980). Others argue on the rare earth influence on oxide stresses, the effect related to the cationic mobility of Y in Al_2O_3 (Delarnay & Huntz 1982; Delarnay et al 1980). Oxidized samples of CoCrAl and CoCrAlY were shown to bend at room temperature (Giggins & Pettit 1975). Scale spalling was far more pronounced in CoCrAl. The adherence of oxide on CoCrAlY is argued not to be due to stress relief but because of pegging. FeCrAl and FeCrAlY oxidation were compared, and found that Y incorporated in alumina changed the growth mechanism, reducing compressive stresses and the convoluted morphology (Wood et al 1980; 1976).

The feature of prime importance for a coating is to guard against thermal fatigue by good adherence. Prevention of void formation or loss of contact between developed scale and the coating must be ensured on one hand, while other means of maintaining scale plasticity have to be exercised. Voids can manifest either by diffusion and coalescence of Kirkendall voids and/or by gaps created by mechanical lifting trapped by subsequent oxidation. Additives are known to improve scale plasticity. Controversies apart, a coating needs to develop an adherent scale which can withstand thermal shock and not be incident to void coalescence at either of the interfaces - its protective scale and itself, or the interface at the substrate.

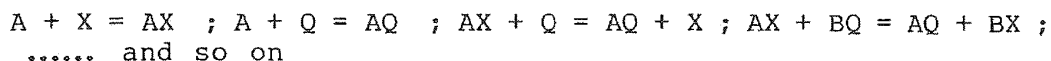
8.4.4. CASE 3:

Multiple Element + Multiple Reactants = Multiple Products

This is the most complex situation for coating degradation which exposes Case 2 conditions to a variety of permutations and combinations.

- (i) Each gas reactant can compete for the same element to form its own reaction product;
- (ii) Several elements can react with the same reactant;
- (iii) Two different compounds can react on an interchange basis;
- (iv) One compound and another element can react; and,
- (v) The most dangerous situation of all - Reactant deposition - /incorporation. Product formation and/or element distribution can occur in a drastic change of phase of the reactant and/or the reaction products to result in catastrophic degradation.

Looking at the reactions:



$$aX/aQ = \exp[(\Delta G_{AX}^{\circ} - \Delta G_{AQ}^{\circ})/RT]$$

The development of a single product layer, an oxide in particular, is still the best way to prevent further corrosion. And this product must be the one through which diffusion is slow. The case of thermal barrier ceramics is not considered in this context, since that introduces an aspect of inertness to the environment rather than the situation of a protective reactant product.

Oxygen-containing species such as CO, CO₂, SO₂, SO₃, and H₂O may be involved; or others such as H₂, H₂S, CH₄, He etc. with no oxygen radical may appear as reactants in a mixture or as impurities. Subscales of other products will form and can not be altogether prevented, as diffusional reactions occur with time. These products are stable although they cannot occur at the scale/gas interface. Repair of the stable scale subsequent to thermal fatigue for instance, will become a problem as the selective element has to diffuse through the partially damaged subscale-outerscale complex. Chromia former alloys with Cr₂N subscale or NiO top scale with Ni-sulphide subscale are good examples of this type of degradation. Although oxide barrier layers can be first formed at pO₂ < 10⁻¹⁰, their repair and re-growth is not easy under reducing conditions with prevailing low pO₂ environments. Rapid degradation will then follow, e.g. in carburizing and sulphidizing environments. Diffusional growth of multiphase scales and subscales on binary alloys has been reviewed (Smeltzer 1987).

8.4.5. CASE 4: CYCLIC OXIDATION:

The ultimate test of a substrate/coating configuration is its response to the operating environment under cyclic temperature conditions. The physical, mechanical and chemical properties of the coating, the substrate and the scale become decisive factors, and the effect of cyclic conditions on the substrate/coating interface as well as the coating/scale interface indicate the survival capability of the system. Thermal and mechanical stress, fatigue, creep, thermal expansion effects, and the stability of the chemical reactants and products exercise a combined control on the coating performance and its protective oxidation characteristics.

The processes which lead to spalling of the oxide scale may be considered in terms of the relative strengths of the surface oxide and the oxide-metal interface. If the major source of stress is assumed to be due to the differential contraction strains produced during the temperature decrease, a critical temperature may be predicted. Oxide scale cracking or adhesion

COATINGS: CHEMICAL PROPERTIES

loss will result when the strain energy, W^* , per unit volume of oxide contained in the layer thickness, z , equates to the work required either for internal cracking, g_o , or for decohesion at the oxide-metal interface, g_f . The critical condition for oxide cracking is not explicitly dependent on its thickness, but the critical value of the temperature difference for interfacial decohesion decreases with increasing oxide thickness. Expressions for a strong or weak oxide/metal interface have been tested with 20Cr-25Ni-Nb-stabilized stainless steel (Evans & Lobb 1984a). Alloy depletion profiles predicted by selective oxidation under non-protective, i.e. spalling conditions, have also been presented (Evans & Lobb 1984b).

Cyclic oxidation histograms in Fig.8-11 - 8-13 give a qualitative assessment of coating/substrate combinations. Behaviour for 20 hour cycles may be quite different from that for 1 hour cycles, for the same material. Behaviour after 1000 hours of cycling may be quite different from that after 500 hours. Adhesion to the substrate is a decisive factor. Aerospace re-entry alloys (Ta-10W) are good for short times and higher temperatures. Different test conditions used by different investigators make it very difficult to draw up even a semi-quantitative histogram like those displayed in Fig.8-11 - 8-13. Fig.8-14 illustrates cyclic oxidation and corrosion effects (Giggins & Pettit 1980). The effect of cyclic oxidation on CoCrAl and NiCrAl alloys is shown in Fig.8-15 (Nicoll 1984). Additive effect on oxidation is illustrated in Fig.8-16, where Hf and Y added to CoCrAl show the more beneficial effect of Y and the critical level effect of Hf.

Alloy existence diagrams are of great value in interpreting the fundamentals of hot corrosion phenomena. The standard free energy change for the formation of compounds is plotted as a function of temperature, and isothermal diagrams are drawn for the compound stability in mixed atmospheres. All the compounds are plotted for the normalized gas pressures and reactant activities, so that the hierarchy of stability remains constant w.r.t. temperature. Superposed data indicate the shifts expected due to the activity changes of a particular species. However, it must be emphasised that equilibrium conditions mandatory in these diagrams expose them to the criticism that they cannot clarify practical situations which are not always in equilibrium. Superposed existence diagrams have shown their utility which may not be ignored. Two simple illustrations of reactions of Ni and Cr are included here (Fig.8-17a,b; Hocking & Vasantasree 1976). Many other complex diagrams showing variations due to changing activities and partial pressures are available in the literature (e.g. Perkins & Vonk 1979; Natesan 1983; Jacob et al 1979; Rapp 1987).

Cyclic Oxidation Resistance: 1000°C in Air, 500 h

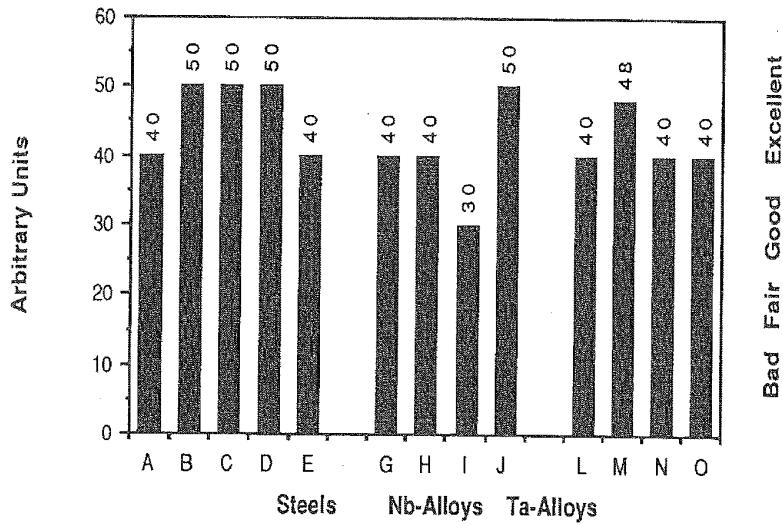


Fig.8-11

Legend	Substrate	Coating & Conditions
A	Steel	PSR1, 800°C, 6000 h
B	20Cr25NiNb stainless steel	CeO ₂ or SiO ₂ , CO ₂ , 825°C, 15 000h
C	Cr5W0.1Y	Cr5Al8
D	Cr5W0.1Y	(Fe-Cr) _x Al _y
E	Cr5W0.1Y	Ni30Cr20W4Al+Barrier (barrier is W-1ThO ₂ , W25Re or W)
G	Nb	VSi ₂
H	Nb-alloy	Si20Cr20Fe
I	Nb-alloy	Si20Cr20Fe
J	Nb-alloy	Cr-Si-Ti
L	Ta10W	VSi ₂
M	Ta10W	Sn23Al5Mo
N	Ta10W	MoSi ₂ /ZrO ₂ (duplex coat)
O	Ta10W	WSi ₂ /ZrO ₂

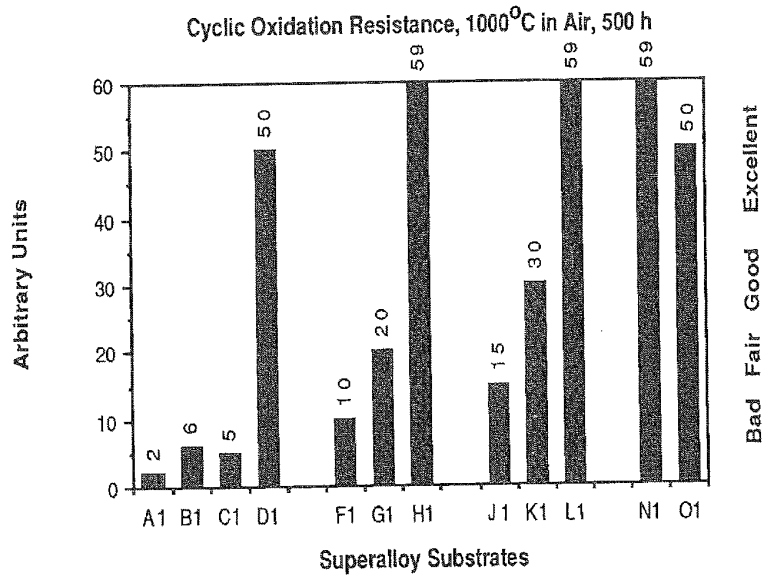


Fig.8-12

Legend	Substrate	Coating & Conditions
A1	MAR-M200	none
B1	MAR-M200	Al
C1	B1900	none
D1	B1900	Al
F1	IN939	none
G1	IN939	Si
H1	IN939	SiB
J1	IN738	+Si (solution)
K1	IN738	Si
L1	IN738	SiB
N1	Superalloy	ZrO ₂ .12Y ₂ O ₃ /NiCrAl0.6Y (duplex coat)
O1	Réne80	Ni20Cr5Al0.1Y0.1C